University of Zurich

Institute of Mathematics

Master Thesis

A Comprehensive Study on Fractal Sets and Dimensions

Author:
Michele Solari

Supervisor:
Prof. Dr. Alexander Gorodnik

June 27, 2024

University of Zurich[UZH]

Abstract

This thesis explores fractals and their dimensions, delving into fundamental properties and dimensionality measures. Beginning with foundational mathematics concepts, it progresses to examine fractals, detailing different dimension measures like topological, similarity, Hausdorff, and box-counting dimensions. Iterated Function Systems (IFS) are investigated for generating self-similar sets and their fractal dimensions. Lastly, within complex dynamics, the thesis analyzes Julia sets and the Mandelbrot set as prominent fractal examples. Through this analysis, the thesis enhances understanding of fractals significance across mathematical domains.

Acknowledgements

I wish to express my sincere gratitude to my Professor and Supervisor, Dr. Alexander Gorodnik, for his dedicated guidance and attention throughout the thesis, as well as for his inspiration during my academic endeavors. Without his valuable contributions and trust in me, I would not have reached this point.

A heartfelt thank you goes to my university friends, who have shared joys, challenges, and precious moments of personal growth with me. Special mention goes to those with whom I began the university together, in particular Carolina, Giulia, Guido, Kata, Piattini, Ramsa, Thomas and Vale, as well as the friends with whom I studied together at the Lernzentrum Strickhof, especially Christian, Dada, Kim, Sabri and Timo. Their friendship and support have made this experience even more meaningful and memorable.

I cannot overlook expressing my gratitude to my roommate, Axel, for his invaluable assistance with LaTeX and for always being there to lend a hand when needed. His patience and expertise have greatly facilitated the thesis writing process.

Lastly, I would like to express my deepest appreciation to my family, who have unconditionally supported me at every stage of my academic journey. Their encouragement, support, and constant presence have been my pillars of strength and motivation.

I am profoundly grateful to all the individuals who have contributed to my academic success and who have played a role in achieving this significant milestone in my life.

Contents

Abstract **iii**

Acknowledgements **v**

1 Introduction **1**
1.1 Outline 3

2 Preliminaries **5**
2.1 Sets and Functions 5
2.2 Measure Theory 10

3 Fractals **16**
3.1 First Properties 16
3.2 Basic Examples 17

4 Fractal Dimension **33**
4.1 Topological Dimension 34
4.2 Similiarity Dimension 36
4.3 Hausdorff Dimension 42
4.4 Box-counting Dimension 62

5 Iterated Function Systems **79**
5.1 Introduction to IFS 79
5.2 Fractal Dimension of Self-Similar Sets 90

6 Complex Dynamics **98**
6.1 Julia Sets 98
6.2 Mandelbrot Set 107

A Python Scripts **119**
A.1 Visualizing the Construction of the Cantor Set 119
A.2 Visualizing the Construction of the Koch Curve 120
A.3 Visualizing the Construction of the Sierpinski Triangle 121
A.4 Visualizing Julia Sets 123
A.5 Visualizing the Mandelbrot Set 125

Bibliography **130**

Chapter 1

Introduction

Contemporary scientific discussions have seen a significant rise in the importance of fractal sets, a subset within fractal geometry and measure theory. These mathematical concepts, originating in pure mathematics, have found diverse applications across various scientific fields. Benoit Mandelbrot (1924–2010), often regarded as the 'Father of Fractals', played a pivotal role in integrating fractals into scientific modeling during the 1970s and 1980s, as demonstrated in his influential works [32] and [34]. These applications span phenomena ranging from molecular dynamics to astronomical structures, including fluid turbulence, plant growth, geographical features, galactic distributions, and financial market fluctuations [18]. Furthermore, fractal sets extend into branches of pure mathematics, such as number theory and dynamical systems [20, chap. 10 and 13].

Although mathematicians have been aware of the existence of 'pathological set' highly irregular for centuries, it was only in 1975 that Mandelbrot introduced the term *fractal* [32], deriving it from the Latin 'fractus' meaning 'broken' or 'fractured'. Initially, he tentatively defined a fractal as a set with its Hausdorff dimension surpassing its topological dimension. However, Mandelbrot acknowledged the inadequacy of this definition, particularly in excluding highly irregular sets that undoubtedly deserve consideration as fractals. In the second edition of [34], he proposed *... to use fractal without a pedantic definition and to employ fractal dimension as a generic term for all variants.* Before Mandelbrot's nomenclature, mathematicians used various designations for such irregular sets, including 'sets of fractional dimension', 'sets of Hausdorff measure', 'sets with a fine structure', or simply 'irregular sets' [18].

The formal, original definition of a fractal, as articulated by Mandelbrot, encounters limitations due to the inherent complexity and irregularity of fractals, defying precise categorization. An alternative proposal suggests characterizing fractals by a set of defining properties, acknowledging their intricate structures, irregularities, and potential self-similarity. This flexible approach aims to encapsulate the essence of fractals without rigidly circumscribing them within a narrowly delineated definition. A detailed list of properties shared by

fractal will be given in section 3.1.

Roughly speaking when we refer to a figure as self-similar we mean that it is composed of parts that are small replicas of the whole. We use the term strictly self-similar set when the figure can be decomposed into parts that are exact replicas of the whole [38].

Historically, phenomena characterized by irregularity or complexity eluded comprehensive description or analysis through traditional mathematics. Classical geometry primarily focused on regular and smooth objects, relegating irregularities to the periphery of mathematical discourse. The advent of calculus in the 17th century further entrenched the preference for smooth objects, marginalizing considerations of irregularities in natural phenomena. It was only in the late 1960s that the study of irregular figures gained systematic traction [21]. In his seminal work, *The Fractal Geometry of Nature* [34], Mandelbrot asserted that irregular objects should be perceived as commonplace across physics, biology, finance, and mathematics. *Clouds are not spheres, mountains are not cones, coastlines are not circles, and bark is not smooth, nor does lightning travel in a straight line.* He posited that these irregularities share a kinship, necessitating the development of fractal mathematics, a concept that has since burgeoned in interest.

Since the 1980s, fractals have not only infiltrated every scientific domain but have also captured public imagination. Fractal geometry, now a major area of mathematics, serves as both a subject of intrinsic interest and a practical tool for diverse applications. Fractals have found their way into art exhibitions, literature, and even science fiction films, captivating audiences with visually striking representations [21].

In the realm of fractals, a confluence of natural and mathematical considerations arises. Natural objects, often described as fractals in physics literature, exhibit fractal-like features over certain scales, although they deviate from true fractals when viewed at sufficiently small scales. The distinction between 'natural fractals' and the idealized 'fractal sets' employed in mathematical descriptions, as emphasized by Mandelbrot, has somewhat blurred over time. Notwithstanding the absence of true fractals in nature, the viability of fractal geometry hinges on its applicability to physical scenarios.

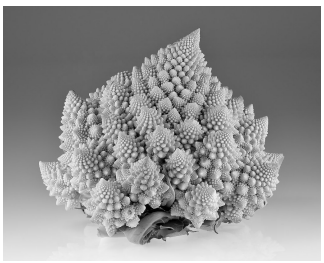

Figure 1.1: Romanesco, showing its self-similar form.
Source: [54]

1.1 Outline

This thesis is structured as follows:

- **Chapter 1: Introduction**

  This chapter provides an overview of the research topic and its significance.

- **Chapter 2: Preliminaries**

  This chapter discusses fundamental concepts in mathematics, including sets, functions, and measure theory (section 2.2), laying the groundwork for understanding fractals and their dimensions.

- **Chapter 3: Fractals**

  This chapter explores the basics of fractals, starting with their initial properties (section 3.1) and presenting various examples to illustrate their characteristics. Among others, this chapter introduces three iconic examples of fractals: the Cantor set (Example 2), the Koch curve (Example 3), and the Sierpinski triangle (Example 6). These will recur throughout the thesis and serve as main examples for the study of fractal dimension in the subsequent Chapter 4.

- **Chapter 4: Fractal Dimension**

  This core chapter focuses on different measures of fractal dimension, including topological (Definition 34), similarity (Definition 35), Hausdorff (Definition 38), and box-counting (Definition 41) dimensions. Particular emphasis is given to the Hausdorff and box-counting dimensions, with numerous examples provided to aid in understanding how to calculate dimensionality across various cases. Here, we mention just some of the most important results: Theorem 6 establishes a connection between Hausdorff measure and Lebesgue measure. Proposition 27 relates the topological and the Hausdoorff dimension. Proposition 23 (scaling property), and Proposition 38 (Mass distribution principle) are helpful for computing the Hausdorff dimension. Proposition 37 offers a topological perspective on a set's structure through the Hausdorff dimension. Additionally, Remark 11 presents a couple of alternative and equivalent ways to define the Hausdorff dimension. Proposition 41 relates the box-counting dimension with the Lebesgue measure. Proposition 43 presents a useful way to compute the box-counting dimension, and finally, Proposition 42 relates Hausdorff and box-counting dimensions.

- **Chapter 5: Iterated Function Systems**

  This chapter introduces the theory of IFS (Definition 44) and delves into the fractal dimension of self-similar sets generated by such systems.

Important new concepts of this chapter include the definition of an attractor (Definition 45), the Hausdorff distance (Definition 46), and the uniqueness of an attractor for an IFS (Theorem 11). The most relevant theorem of the chapter, and indeed of the entire thesis, assures that under certain conditions, the fractal dimensions discussed in Chapter 4, specifically, similarity, Hausdorff, and box-counting dimensions, are all equal. Furthermore, it provides a computational method to determine this value (Theorem 13). Propositions 56 and 57 offer useful upper and lower bounds for the Hausdorff dimension.

- **Chapter 6: Complex Dynamics**

  This chapter explores the intricate shapes known as Julia sets (Definition 57 and equivalent formulations in Propositions 63 and 66, along with Theorem 15), as well as the renowned Mandelbrot set (Definition 61 and Theorem 18), within the context of complex dynamics. It seeks to understand the dimension of these fascinating mathematical sets through Theorems 16, 19, Example 69, and Theorems 20 and 21.

Chapter 2

Preliminaries

In this section, we provide an introductory overview of key mathematical concepts that can help facilitate the understanding of the material presented in this thesis.

2.1 Sets and Functions

All the definitions of this section are fundamental concepts in set theory and calculus; therefore, a precise citation of sources has been omitted for almost all definitions, as the entire content of this section can be found in any standard mathematics textbook.

Through this thesis we work in the Euclidean space $\mathbb{R}^n$ with the usual Euclidean distance. Sets will be denoted with capital letters and elements of sets are denoted with lower letters.

Definition 1 (basic operations for sets)**.** *Given two sets A and B, we define the following:*

- *The union of A and B:* $A \cup B = \{x : x \in A \vee x \in B\}$
- *The intersection of A and B:* $A \cap B = \{x : x \in A \wedge x \in B\}$
- *The difference of A and B:* $A \backslash B = \{x : x \in A \wedge x \notin B\}$
- *The complement of A:* $A^c = \mathbb{R}^n \backslash A$

Definition 2 (metric)**.** *A metric on a set X is a function $d : X \times X \to [0, \infty)$ such that for all $x, y, z \in X$*

- $d(x, y) > 0$ *if* $x \neq y$
- $d(x, y) = 0$ *if and only if* $x = y$
- $d(x, y) = d(y, x)$

- $d(x,z) \leq d(x,y) + d(y,z)$ *(triangle inequality)*

The pair (X,d) is called a metric space.

Definition 3 (Euclidean distance on $\mathbb{R}^n$)**.** *For x, y two points of $\mathbb{R}^n$, the Euclidean distance or metric is the distance between them.*

$$|x-y| = \left(\sum_{i=1}^{n} |x_i - y_i|^2 \right)^{1/2}$$

Definition 4 (diameter of a set)**.** *The diameter $|A|$ of a (non-empty) subset of $\mathbb{R}^n$ is the greatest distance apart of pairs of points in A.*

$$|A| = \sup\{|x-y| : x, y \in A\}$$

In $\mathbb{R}^n$ a ball of radius r has diameter $2r$, and a cube of side length δ has diameter $\delta\sqrt{n}$.

Definition 5 (δ-neighbourhood)**.** *The δ-neighbourhood (also called δ-parallel body), F_δ, of a set $F \subset \mathbb{R}^n$, is the set of points within distance δ of F.*

$$F_\delta = \{x : |x-y| \leq \delta \text{ for some } y \text{ in } F\}$$

Definition 6 (supremum and infimum of a set)**.** *If A is a non-empty set of $\mathbb{R}$ then the supremum $\sup A$ is the least number y such that $x \leq y$ for every x in A, or is ∞ if no such number exists. Similarly, the infimum $\inf A$ is the greatest number y such that $y \leq x$ for all x in A, or is $-\infty$ if no such number exists. We use the notation $\sup_{x \in B}()$ for the supremum of the quantity in brackets, which may depend on x, as x ranges over some set B.*

Definition 7 (open and closed ball)**.** *The closed ball of center x and radius r is defined by*

$$B(x,r) = \{y : |y-x| \leq r\}$$

Similarly the open ball is defined as

$$B^\circ(x,r) = \{y : |y-x| < r\}$$

Definition 8 (neighbourhood of a set)**.** *A set $A \subset \mathbb{R}^n$ is termed a neighborhood of a point x if there exists a ball $B(x,r)$ centered at x and contained within A.*

Definition 9 (open and closed subset on $\mathbb{R}^n$)**.** *A subset U of the Euclidean space $\mathbb{R}^n$ is open if, for every point x in U, there exists a positive real number ε (depending on x) such that any point in $\mathbb{R}^n$ whose Euclidean distance from x is smaller than ε, belongs to U. Equivalently, a subset U of $\mathbb{R}^n$ is open if every point in U is the center of an open ball contained in U. The complement of an open set is a closed set.*

Definition 10 (cover of a set)**.** *A countable collection $\{U_i\}$ of subsets of $\mathbb{R}^n$ is a cover of $A \subset \mathbb{R}^n$ if $A \subseteq \bigcup U_i$. If each of the sets U_i has diameter at most δ for some $\delta > 0$, then the collection is said to be a δ-cover of A. Furthermore, if each of the sets U_i is an open set, then we call the collection an open cover of A.*

Definition 11 (connected set)**.** *Let $F \subset \mathbb{R}^n$. Then F is called connected if there are no two open, disjoint subsets $\mathcal{O}_1, \mathcal{O}_2 \subset F$ with $\mathcal{O}_1 \cup \mathcal{O}_2 = F$ beside F and $\emptyset$.*

Definition 12 (totally disconnected set)**.** *A set $F \subset \mathbb{R}^n$ is said to be totally disconnected if the connected component of each point of F consists of just that point. The connected component of a point x in F is the union of all connected subsets of F that contain x.*

Definition 13 (closure and interior of a set)**.** *The intersection of all the closed sets containing a set $F \subset \mathbb{R}^n$ is called the closure of F, and denoted by $\bar{F}$. The union of all the open sets contained in F is the called the interior of F and is denoted by $\text{int}(F)$. The closure of F is seen of as the smallest closed set containing F, and the interior as the largest open set contained in F.*

Definition 14 (compact set)**.** *A set $F \subset \mathbb{R}^n$ is compact if for every family of open sets which covers F, there exists a finite subfamily which also covers F. Equivalenty, every open cover of F has a finite subcover.*

Theorem 1 (Heine-Borel Theorem, [1, Thm 3.12])**.** *Given a subset F of the Euclidean space $\mathbb{R}^n$, the following are equivalent:*

- *F is closed and bounded*
- *F is compact*

Proof. Omitted. See [1, Thm 3.12]. □

Definition 15 (Borel sets, [18])**.** *The sets belonging to the σ-algebra (see Def. 24) generated by the closed subsets of $\mathbb{R}^n$ are called the Borel sets of $\mathbb{R}^n$.*

In particular, the class of Borel sets is the smallest collection of subsets of $\mathbb{R}^n$ with the following properties [20]:

- every open set and every closed set is a Borel set.
- the union of every finite or countable collection of Borel sets is a Borel set, and the intersection of every finite or countable collection of Borel sets is a Borel set.

In this thesis, we will operate under the assumption that the sets encountered belong to the class of Borel sets.

We introduce now some more definitions regarding functions.

Definition 16 (similarity). *A function $S : \mathbb{R}^n \to \mathbb{R}^n$ is a similarity of ratio or scale $c > 0$ if $|S(x) - S(y)| = c|x - y|$ for all x, y in $\mathbb{R}^n$. A similarity transforms sets into geometrically similar ones with all lengths multiplied by the factor c.*

Definition 17 (isometry). *A function $S : \mathbb{R}^n \to \mathbb{R}^n$ is called an isometry (or congruence) if $|S(x) - S(y)| = |x - y|$ for all x, y in $\mathbb{R}^n$. An isometry preserves distances (and therefore also angles). It is therefore a special case of similarity.*

Definition 18 (linear function). *A function $f : \mathbb{R}^n \to \mathbb{R}^n$ is a linear transformation if $f(x + y) = f(x) + f(y)$ and $f(\lambda x) = \lambda f(x)$ for all $x, y \in \mathbb{R}^n$ and $\lambda \in \mathbb{R}$. Linear transformations $f : \mathbb{R}^n \to \mathbb{R}^n$ may be represented by $n \times n$ matrices in the usual way.*

Definition 19 (affine transformation, [20, chap. 9.4]). *An affine transformation $S : \mathbb{R}^n \to \mathbb{R}^n$ is a transformation of the form*

$$S(x) = f(x) + b$$

where f is a linear transformation on $\mathbb{R}^n$ and b is a vector in $\mathbb{R}^n$. Thus an affine transformation S is a combination of a translation, rotation, dilation and reflection. In particular, S maps spheres to ellipsoids, squares to parallelograms, etc. Unlike similarities, affine transformations contract with differing ratios in different directions.

Definition 20 (homeomorphism). *A function $f : X \to Y$ is considered a homeomorphism if it is a continuous bijection with a continuous inverse $f^{-1} : Y \to X$. When such a relationship holds, X and Y are said to be homeomorphic sets. Examples of homeomorphisms include congruences, similarities, and affine transformations on $\mathbb{R}^n$.*

Definition 21 (Hölder function). *Let $X, Y \subset \mathbb{R}^n$. A function $f : X \to Y$ is called a Hölder function of exponent $\alpha > 0$ if*

$$|f(x) - f(y)| \leq c|x - y|^\alpha \quad (x, y \in X) \tag{2.1}$$

for some constant $c \geq 0$.

Condition (2.1) is known as Hölder condition of exponent α.

Definition 22 (Lipschitz and bi-Lipschitz function). *The function f from Definition 21 is called a Lipschitz function if α may be taken to be equal to 1, that is if*

$$|f(x) - f(y)| \leq c|x - y| \quad (x, y \in X)$$

and a bi-Lipschitz function if

$$c_1|x - y| \leq |f(x) - f(y)| \leq c_2|x - y| \quad (x, y \in X)$$

for $0 < c_1 \leq c_2 < \infty$.

Proposition 1. *Assume $f : X \to Y$ is a bi-Lipschitz function, then f is injective.*

Proof. Assume $f(x) = f(y)$ then $|x - y| \leq \frac{1}{c_1}|f(x) - f(y)| = 0$. Therefore $|x - y| = 0$ implies $x = y$. □

Proposition 2. *Assume $f : X \to Y$ is a Lipschitz function, then $f^{-1} : f(X) \to X$ is Lipschitz if and only if f is bi-Lipschitz.*

Proof. Assume f is bi-Lipschitz. f is well-defined because of the previous proposition. Let now $a = f(x)$ and $b = f(y) \in f(X)$. Then

$$\begin{aligned} &\left|f^{-1}(a) - f^{-1}(b)\right| = \left|f^{-1}(f(x)) - f^{-1}(f(x))\right| = |x - y| \\ &\leq \frac{1}{c_1}|f(x) - f(y)| = \frac{1}{c_1}|a - b|. \end{aligned} \tag{2.2}$$

The other implication follows in an analogous way. □

Example 1 ([20, Exercise 1.16])**.** *$f(x) = x^2$ is Lipschitz on $[0, 2]$, bi-Lipschitz on $[1, 2]$ and not Lipschitz on $\mathbb{R}$.*

Proof. For $x, y \in [0, 2]$,

$$|f(x) - f(y)| = \left|x^2 - y^2\right| = |x + y||x - y| \leq 4|x - y|$$

thus f is Lipschitz on $[0, 2]$ and in particular Lipschitz on $[1, 2]$, with $f([1, 2]) = [1, 4]$. For $x, y \in [1, 4]$,

$$\left|f^{-1}(x) - f^{-1}(y)\right| = |\sqrt{x} - \sqrt{y}| = \left|\frac{x - y}{\sqrt{x} + \sqrt{y}}\right| \leq \frac{1}{2}|x - y|$$

therefore f^{-1} is Lipschitz on $[1, 4]$, and thus f is bi-Lipschitz on $[1, 2]$. For $x > 0$,

$$\frac{|f(2x) - f(x)|}{|2x - x|} = \frac{4x^2 - x^2}{x} = 3x.$$

Therfore $|f(x) - f(y)|/|x - y|$ is not bounded on $\mathbb{R}$ and as a consequence f can not be Lipschitz on $\mathbb{R}$. □

Definition 23 (upper and lower limit)**.** *The upper limit of a function $f : \mathbb{R}^+ \to \mathbb{R}$ is defined as*

$$\overline{\lim_{x \to 0}} f(x) = \lim_{r \to 0}(\sup\{f(x) : 0 < x < r\})$$

Similarly, the lower limit is defined as

$$\underline{\lim_{x \to 0}} f(x) = \lim_{r \to 0}(\inf\{f(x) : 0 < x < r\})$$

If the upper limit and the lower limit agree, we say that the limit exists and write: $\lim_{x \to 0} f(x)$.

2.2 Measure Theory

This section serves as a concise introduction to the fundamental concepts of measure theory, a crucial foundation for comprehending Hausdorff dimension (introduced in section 4.3) in the context of fractal geometry. In essence, our focus is on measures applied to subsets of Euclidean spaces $\mathbb{R}^n$, where a measure serves as a systematic approach to numerically quantifying the 'size' of sets with the request that when a set is divided into disjoint subsets and these subsets are summed together, the total measure equals that of the entire original set, represented by the union of these subsets. In this section we will mainly follow [18, chap. 1], [15, chap. 5] and [42, chap. 1] More general and broad references in measure theory can be found in [10] and [23].

Let X be any set. In our setting we will usually take X to be the n-dimensional Euclidean space $\mathbb{R}^n$.

Definition 24 (σ-algebra, [10])**.** *A collection $\mathcal{A}$ of subsets of X is a σ-algebra (sometimes also called σ-field) on X if*

1. *$X \in \mathcal{A}$.*
2. *for each set A that belongs to $\mathcal{A}$, the complement set A^c belongs to $\mathcal{A}$.*
3. *for each countable sequence $\{A_i\}$ of sets that belong to $\mathcal{A}$, the set $\bigcup_{j=1}^{\infty} A_j$ belongs to $\mathcal{A}$.*

From the definition it follows that the σ-algebra is also closed under countable intersection and, further, that the empty set $\emptyset$ is in $\mathcal{A}$.

Let $\mathcal{C}$ be any collection of subsets of X. Then the σ-algebra generated by $\mathcal{C}$, written $\sigma(\mathcal{C})$, is the intersection of all σ-algebras containing $\mathcal{C}$. A straightforward proof shows that $\sigma(\mathcal{C})$ is itself a σ-algebra which may be seen of as the 'smallest' σ-algebra containing $\mathcal{C}$.

Definition 25 (measure, [10])**.** *A measure μ is a function defined on some σ-algebra $\mathcal{A}$ of subsets of X and taking values in the range $[0, \infty]$ such that*

$$\mu(\emptyset) = 0 \tag{2.3}$$

and

$$\mu\left(\bigcup_{j=1}^{\infty} A_j\right) = \sum_{j=1}^{\infty} \mu\left(A_j\right) \tag{2.4}$$

for every countable sequence of disjoint sets $\{A_j\}$ in $\mathcal{A}$.

Property (2.4) is called σ-additivity or countable additivity. Also, from (2.4) it follows that μ is an increasing function, that is, if $A \subset A'$ and $A, A' \in \mathcal{A}$, then

$$\mu(A) \leq \mu\left(A'\right)$$

If X is a set, if $\mathcal{A}$ is a σ-algebra on X, and if μ is a measure on $\mathcal{A}$, then the triplet $(X, \mathcal{A}, \mu)$ is often called a measure space. Likewise, if X is a set and if A is a σ-algebra on X, then the pair $(X, \mathcal{A})$ is often called a measurable space. A measure μ on a measurable space $(X, \mathcal{A})$ is called a finite measure if it satisfies

$$\mu(X) < \infty.$$

Theorem 2 (continuity of measures, [18, Thm 1.1])**.** *Let μ be a measure on a σ-algebra $\mathcal{A}$ of subsets of X.*

(a) If $A_1 \subset A_2 \subset \ldots$ is an increasing sequence of sets in $\mathcal{A}$, then

$$\mu\left(\lim_{j\to\infty} A_j\right) = \lim_{j\to\infty} \mu\left(A_j\right)$$

(b) If $F_1 \supset F_2 \supset \ldots$ is a decreasing sequence of sets in $\mathcal{A}$ and $\mu\left(F_1\right) < \infty$, then

$$\mu\left(\lim_{j\to\infty} F_j\right) = \lim_{j\to\infty} \mu\left(F_j\right)$$

(c) For any sequence of sets $\{F_j\}$ in $\mathcal{A}$,

$$\mu\left(\varliminf_{j\to\infty} F_j\right) \leq \varliminf_{j\to\infty} \mu\left(F_j\right)$$

Proof. (a) We can write $\bigcup_{j=1}^{\infty} A_j$ as the disjoint union $A_1 \cup \bigcup_{j=2}^{\infty} \left(A_j \backslash A_{j-1}\right)$. Then by (2.4),

$$\begin{aligned}
\mu\left(\lim_{j\to\infty} A_j\right) &= \mu\left(\bigcup_{j=1}^{\infty} A_j\right) \\
&= \mu\left(A_1\right) + \sum_{j=2}^{\infty} \mu\left(A_j \backslash A_{j-1}\right) \\
&= \lim_{k\to\infty} \left[\mu\left(A_1\right) + \sum_{j=2}^{k} \mu\left(A_j \backslash A_{j-1}\right)\right] \\
&= \lim_{k\to\infty} \mu\left(A_1 \cup \bigcup_{j=2}^{k} \left(A_j \backslash A_{j-1}\right)\right) \\
&= \lim_{k\to\infty} \mu\left(A_k\right).
\end{aligned}$$

(b) If $A_j = F_1 \backslash F_j$, then $\{A_j\}$ is as in (a). Since $\bigcap_j F_j = F_1 \backslash \bigcup_j A_j$,

$$\begin{aligned}\mu\left(\lim_{j\to\infty} F_j\right) &= \mu\left(\bigcap_{j=1}^{\infty} F_j\right)\\ &= \mu\left(F_1\right) - \mu\left(\bigcup_j A_j\right)\\ &= \mu\left(F_1\right) - \lim_{j\to\infty}\mu\left(A_j\right)\\ &= \lim_{j\to\infty}\left(\mu\left(F_1\right) - \mu\left(A_j\right)\right)\\ &= \lim_{j\to\infty}\mu\left(F_j\right).\end{aligned}$$

(c) Now let $A_k = \bigcap_{j=k}^{\infty} F_j$. Then $\{A_k\}$ is an increasing sequence of sets in $\mathcal{A}$, so by (a),

$$\mu\left(\underline{\lim}_{j\to\infty} F_j\right) = \mu\left(\bigcup_{k=1}^{\infty} A_k\right) = \lim_{k\to\infty}\mu\left(A_k\right) \leq \underline{\lim}_{j\to\infty}\mu\left(F_j\right)$$

□

We introduce now the concept of outer measure.

Definition 26 (outer measure, [10])**.** *An outer measure v on a set X is a function defined on all subsets of X taking values in $[0,\infty]$ such that*

$$v(\emptyset) = 0, \tag{2.5}$$

$$v(A) \leq v\left(A'\right) \text{ if } A \subset A' \tag{2.6}$$

and

$$v\left(\bigcup_{j=1}^{\infty} A_j\right) \leq \sum_{j=1}^{\infty} v\left(A_j\right) \quad \text{for any subsets } \{A_j\} \text{ of } X. \tag{2.7}$$

Property 2.7 is called σ-subadditivity. Thus an outer measure on X is a monotone and countably subadditive function from $\mathcal{P}(X)$ to $[0,+\infty]$ whose value at $\emptyset$ is 0.

Definition 27 (measurable set, [10])**.** *A subset E of X is called v-measurable or measurable with respect to the outer measure v if*

$$v(A) = v(A\cap E) + v(A\backslash E) \tag{1.6}$$

for every subset $A \subset X$.

To show that a set E is v-measurable, it is enough to check that

$$v(A) \geq v(A \cap E) + v(A \backslash E) \tag{2.8}$$

since the opposite inequality is included in (2.7).

Theorem 3 ([18, Thm 1.2])**.** *Let v be an outer measure. The collection $\mathcal{M}$ of v-measurable sets forms a σ-algebra, and the restriction of v to $\mathcal{M}$ is a measure.*

Proof. Omitted. See [18, Thm 1.2]. □

Outer measures are therefore very useful since there is always a σ-algebra of subsets on which they behave as measures.

Definition 28 (regular outer measure, [42])**.** *An outer measure v is called outer regular if for every set A in X there is a v-measurable set E with*

$$A \subset E, \quad \mu(E) = \mu(A)$$

Lemma 1 ([18, Lemma 1.3])**.** *If v is a regular outer measure and $\{A_j\}$ is any increasing sequence of sets, then*

$$\lim_{j \to \infty} v\left(A_j\right) = v\left(\lim_{j \to \infty} A_j\right)$$

Proof. Take a v-measurable E_j such that $E_j \supset A_j$ and $v\left(E_j\right) = v\left(A_j\right)$ for each j. Then, using (2.6) and Theorem 2(c),

$$v\left(\lim A_j\right) = v\left(\underline{\lim}\, A_j\right) \leq v\left(\underline{\lim}\, E_j\right) \leq \underline{\lim}\, v\left(E_j\right) = \lim v\left(A_j\right)$$

The opposite inequality follows directly from (2.6).

□

Let now (X, d) be a metric space (recall that in this thesis X will be the n-dimensional Euclidean space, $\mathbb{R}^n$, with d the usual Euclidean distance).

Definition 29 (metric outer measure, [42])**.** *An outer measure v on X is called a metric outer measure if*

$$v(E \cup F) = v(E) + v(F) \tag{2.9}$$

whenever E and F are positively separated, that is, whenever

$$d(E, F) = \inf\{d(x, y) : x \in E, y \in F\} > 0.$$

In order to prove that if v is a metric outer measure, then the collection of v-measurable sets includes the Borel sets, we first state the following lemma.

Lemma 2 ([18, Lemma 1.4])**.** *Let v be a metric outer measure on (X, d). Let $\{A_j\}_1^\infty$ be an increasing sequence of subsets of X with $A = \lim_{j\to\infty} A_j$, and suppose that $d(A_j, A\backslash A_{j+1}) > 0$ for each j. Then $v(A) = \lim_{j\to\infty} v(A_j)$.*

Proof. Omitted. See [18, Lemma 1.4]. □

Theorem 4 ([18, Thm. 1.5])**.** *If v is a metric outer measure on (X, d), then all Borel subsets of X are v-measurable.*

Proof. The v-measurable sets form a σ-algebra, and the Borel sets form the smallest σ-algebra containing the closed subsets of X, therefore it is enough to show that (2.8) holds when E is closed and A is arbitrary.

Let A_j be the set of points in $A\backslash E$ at a distance at least $1/j$ from E. Then $d(A \cap E, A_j) \geq 1/j$, so

$$v(A \cap E) + v(A_j) = v((A \cap E) \cup A_j) \leq v(A) \tag{2.10}$$

for each j, as v is a metric outer measure. The sequence of sets $\{A_j\}$ is increasing and, since E is closed, $A\backslash E = \bigcup_{j=1}^\infty A_j$. Hence, provided that $d(A_j, A\backslash E\backslash A_{j+1}) > 0$ for all j, previous Lemma gives $v(A\backslash E) \leq \lim_{j\to\infty} v(A_j)$ and (2.8) follows from (2.10). But if $x \in A\backslash E\backslash A_{j+1}$ there exists $z \in E$ with $d(x, z) < 1/(j+1)$, so if $y \in A_j$ then $d(x, y) \geq d(y, z) - d(x, z) > 1/j - 1/(j+1) > 0$. Thus $d(A_j, A\backslash E\backslash A_{j+1}) > 0$, as needed. □

To conclude the review on measure theory, let's highlight the example of the Lebesgue measure. As we will see, it is merely a particular case of the Hausdorff measure.

The Lebesgue measure

Lebesgue measure $\mathcal{L}^1$ extends the idea of 'length' to a large collection of subsets of $\mathbb{R}$, 'the Lebesgue measurable sets', that includes the Borel sets, and sometimes we just write length(A) for $\mathcal{L}^1(A)$. For open and closed intervals, we take $\mathcal{L}^1(a, b) = \mathcal{L}^1[a, b] = b - a$. If $A = \bigcup_i [a_i, b_i]$ is a finite or countable union of disjoint intervals, we let $\mathcal{L}^1(A) = \sum (b_i - a_i)$ be the length of A thought of as the sum of the length of the intervals. This gives the definition of the Lebesgue outer measure $\mathcal{L}^1(A)$ of an arbitrary set A.

Definition 30 (Lebesgue outer measure on $\mathbb{R}$, [20, Ex. 1.3])**.**

$$\mathcal{L}^1(A) = \inf\left\{\sum_{i=1}^\infty (b_i - a_i) : A \subset \bigcup_{i=1}^\infty [a_i, b_i]\right\},$$

where the infimum is taken over all coverings of A by countable collections of intervals.

If $A = \{(x_1, \ldots, x_n) \in \mathbb{R}^n : a_i \leq x_i \leq b_i\}$ is a 'coordinate parallelepiped' on $\mathbb{R}^n$, the n-dimensional volume of A is given by

$$\mathrm{vol}^n(A) = (b_1 - a_1)(b_2 - a_2) \cdots (b_n - a_n).$$

where vol^1 is the length, vol^2 is the area and vol^3 is the usual 3-dimensional volume.

Then the n-dimensional Lebesgue outer measure $\mathcal{L}^n$ may be seen as an extension of the n-dimensional volume.

Definition 31 (Lebesgue outer measure on $\mathbb{R}^n$, [20, Ex. 1.4])**.**

$$\mathcal{L}^n(A) = \inf\left\{\sum_{i=1}^{\infty} \mathrm{vol}^n(A_i) : A \subset \bigcup_{i=1}^{\infty} A_i\right\}$$

where the infimum is taken over all coverings of A by coordinate parallelepipeds A_i. We get that $\mathcal{L}^n(A) = \mathrm{vol}^n(A)$ if A is a coordinate parallelepiped or more generally any set for which the volume can be determined by the usual rules of mensuration. Sometimes it is more common to write $\mathrm{area}(A)$ instead of $\mathcal{L}^2(A)$, and similarly $\mathrm{vol}(A)$ for $\mathcal{L}^3(A)$ and $\mathrm{vol}^n(A)$ for $\mathcal{L}^n(A)$.

One can prove that $\mathcal{L}^n$ is a metric outer measure on $\mathbb{R}^n$ [15, Thm. 5.1.5 and Thm. 5.1.6], therefore the restriction of $\mathcal{L}^n$ to the $\mathcal{L}^n$-measurable sets or Lebesgue measurable sets, which, by Theorem 4, include the Borel sets, is a measure (Thm. 3), called Lebesgue n-dimensional measure or volume.

Chapter 3

Fractals

In this chapter, we initiate the exploration of fractal geometry by initially introducing the key features shared by fractals (section 3.1). Subsequently, we delve into some of the most well-known examples of fractals and discuss their construction methods (section 3.2). The main sources for this chapter are the introductory part of [20], [39, chap. 2] and [15, chap. 1].

3.1 First Properties

As already seen in the introduction, fractals, captivating mathematical constructs, defy precise definition due to their inherent complexity and diversity in form. At a basic level, a fractal is often described as a self-similar image, a structure that repeats itself at diminishing scales, it has parts that look like the whole structure in some way. Zooming into a specific section of a fractal reveals replicated patterns, a process that can be iterated indefinitely. Fractals that truly deserve the name have detailed patterns at every level.

Sometimes, though, this similarity isn't exactly geometric; it might be more of an approximation or a statistical resemblance.

However, the broad concept of self-similarity is insufficient to encompass all entities deemed fractals. A simple line segment, while self-similar, does not qualify as a fractal. Consequently, the challenge of establishing a universal definition persists, leading to the absence of a standardized description for fractals. Despite this definitional difficulty, certain properties commonly associated with fractals can be outlined [20]:

1. **Fine Structure:** Fractals exhibit intricate details at arbitrarily small scales, allowing for an endless exploration of patterns within patterns.

2. **Irregular Geometry:** Their shapes elude classical geometric categorization due to their irregularity, both locally and globally.

3. **Self-Similarity:** While not mandatory, many fractals possess some degree of self-similarity, where parts resemble the whole.

4. **Fractal Dimension:** The fractal dimension, typically exceeding the topological dimension, serves as a crucial characteristic. This dimensionality discrepancy contributes to the unique nature of fractals.

5. **Recursive Definition:** Fractals often lend themselves to recursive or simple formulations, enabling a systematic understanding of their structure.

Mandelbrot's initial definition included the condition that the fractal dimension should be strictly greater than the topological dimension [34], but subsequent studies revealed exceptions. Consequently, a consensus has emerged in the scientific community to identify a fractal based on the presence of most of the aforementioned properties. This pragmatic approach acknowledges the inherent difficulty in precisely defining fractals and draws parallels with the challenge of defining life in biology based on a set of characteristic features [21]. As a result, the definition of a fractal remains more a set of guiding principles than a rigid, universally applicable definition.

To precisely elucidate the nature of a fractal, we will illustrate its characteristics through specific examples and constructions in the following section.

3.2 Basic Examples

Research on the distinctive category of sets now known as fractals initially commenced during the 19th century. However, this interest waned until experiencing a resurgence, consisting of a systematic exploration of irregular shapes, in the 1970s, primarily attributable to Mandelbrot's seminal contributions and advancements in computer technology. Hence, although the formal investigation of fractals officially commenced only in recent times, individuals had previously encountered some of these fractals without recognizing them [21].

The Weierstrass function, named after the German mathematician Karl Weierstrass (1815-1897), stands as a pioneering example of what we now understand as a fractal. It is an example of a real-valued function that is continuous everywhere (Proposition 3) but differentiable nowhere [51]. The function was firstly described in 1872 [51]. Its original definition is as follows:

$$f(x) = \sum_{n=0}^{\infty} a^n \cos\left(b^n \pi x\right) \tag{3.1}$$

where $0 < a < 1, b$ is a positive odd integer, and

$$ab > 1 + \frac{3}{2}\pi.$$

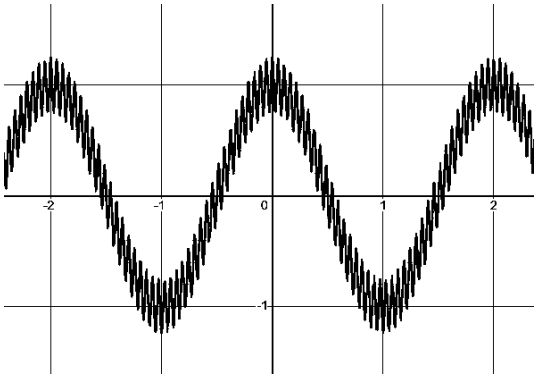

Figure 3.1: The Weierstrass function with parameters $a = 0.25$ and $b = 29$.

Proposition 3. *The Weierstrass function (3.1) is continuous everywhere.*

Proof. For all $n \in \mathbb{N}_0$ and $x \in \mathbb{R}$, we have $|a^n \cos(b^n \pi x)| \leq a^n$. Furthermore, since $0 < a < 1$, the series $\sum_{n=0}^{\infty} a^n$ is convergent. Then, by the Weierstrass M-test [1, Thm 1.6], the series $\sum_{n=0}^{\infty} a^n \cos(b^n \pi x)$ converges uniformly with respect to $x \in \mathbb{R}$. Since the individual partial sums of the series are continuous functions (as finite sums of continuous functions), and the limit function of a uniformly convergent sequence of continuous functions must also be continuous [1, Thm 2.1], the claim follows. □

Proposition 4 ([55, Exercise 1.10])**.** *The Weierstrass function (3.1) is a Hölder function (see Definition 21) with exponent* $\frac{log 1/a}{log b}$.

Proof. Omitted. See [55, Exercise 1.10]. □

The Weierstrass function encapsulates two fundamental properties often associated with fractals: intricate fine structure and a form of (approximate) self-symmetry. These characteristics will reappear consistently in subsequent examples, emphasizing their importance in the study and understanding of fractals.

In the creation of most fractal, the typical approach involves initiating the process with a base set and applying transformations to that set. The initial set, denoted as E_0, serves as the initiator. The first transformation applied to the set, labeled E_1, is known as the generator, and the transformation at the k-th step is denoted as E_k. The ultimate fractal, represented as F, is obtained as the limiting set when the number of transformations approaches infinity, i.e.

$$F = \lim_{k \to \infty} E_k$$

One famous example, considered as the prototype of a fractal is the Cantor set. It was explored by Georg Cantor (1845–1918) in the late 1800s, before anyone even used the word 'fractal'. Cantor published his findings about the Cantor set in 1883 [8].

Example 2 (Cantor set)**.** *The Cantor set is given by iteratively removing the open middle third from a set of line segments. We begin with the unit interval* $E_0 = [0, 1]$*. We get* E_1 *by removing the open middle third interval from* E_0*, so that* $E_1 = [0, \frac{1}{3}] \cup [\frac{2}{3}, 1]$*, thus* E_1 *is given by 2 line segments each of length* $\frac{1}{3}$*. In the same way, we get* E_2 *by removing the middle third of each of the two line segments of* E_1*, so that* $E_2 = [0, \frac{1}{9}] \cup [\frac{2}{9}, \frac{1}{3}] \cup [\frac{2}{3}, \frac{7}{9}] \cup [\frac{8}{9}, 1]$ *is given by 4 line segments each of length* $\frac{1}{9}$*. Therefore* E_k *is given by* 2^k *disjoint intervals each of length* 3^{-k} *and the Cantor set comprises all the points within the interval* $[0, 1]$ *that persist throughout each step in this infinite process of iterative deletion. The Cantor set* F *is then given by*

$$F = \lim_{k\to\infty} E_k = \bigcap_{k=0}^{\infty} E_k$$

Remark 1. *Some authors refer to the term 'tremas' for the parts that are deleted through the iteration process for the construction of a fractal F [15]. Mandelbrot derived this term from a Latin word signifying 'hole' [34].*

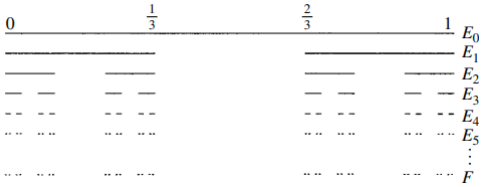

Figure 3.2: The Cantor set.
Source: [20, p. xviii]

For an animation of the construction of F, see Appendix A.1.

Note that this set present the most common properties presented above. In particular F exhibits self-similarity, evident in the observation that the segment of F within the interval $[0, \frac{1}{3}]$ and the segment within $[\frac{2}{3}, 1]$ both share geometric similarity to the entire set F, scaled by a factor of $\frac{1}{3}$. This pattern extends further, as sections of F within each of the four sub-intervals of E_2 also mirror F but on a smaller scale, scaled by a factor of $\frac{1}{9}$, and so forth. Moreover, as we zoom in, we notice more gaps, showing that the Cantor set as a fine structure.

It is easy to see that E_k is of length $\left(\frac{2}{3}\right)^k$. The total length of the Cantor set F tends to zero as $k \to \infty$, i.e.

$$\lim_{k\to\infty} \left(\frac{2}{3}\right)^k = 0$$

Thus F has zero length (more formally this is analogous to say that the Lebesgue measure is 0, see section 2.2). In particular this is related to the

fact that the fractal dimension of F is strictly less than 1, as we will discuss later in Chapter 4.

Conversely, F is an infinte set, to see this notice that the endpoints of the intervals are members of F and that in each iteration, there are 2^k new endpoints. It follows that when $k \to \infty$, the number of points in the Cantor set tends to infinity. The set of endpoints of F is a countable set, but note that in F there are points other than these endpoints (see Proposition 6) and that in fact F is uncountable.

Proposition 5 ([15, Prop 1.1.5])**.** *The Cantor set F is uncountable.*

Proof. Let $x \in [0,1]$. We claim that x belongs to F if and only if x has a base 3 expansion using only the digits 0 and 2.

The first place to the right of the ternary point is a 1 if and only if x is between

$$(0.1000000\cdots)_3 = 1/3 \quad \text{and} \quad (0.1222222\cdots)_3 = 2/3.$$

The first trema is the interval $(1/3, 2/3)$. After removing this trema, we obtain E_1. Note that the numbers $1/3$ and $2/3$ each have two expansions: one with a 1 in the first place, and one without. Therefore, they should not be removed. Consequently, E_1 contains exactly the numbers in $[0,1]$ that have a base 3 expansion not using 1 in the first place. The second place of a number x in E_1 is 1 if and only if x belongs to one of the second-level tremas $(1/9, 2/9)$ or $(7/9, 8/9)$. After removing these tremas, we obtain E_2. Therefore, E_2 contains precisely the numbers in $[0,1]$ that have a base 3 expansion using 1 neither in the first place nor the second place. By continuing this process iteratively, we conclude that the points left in $F = \bigcap_{k\in\mathbb{N}} E_k$ are exactly the numbers in $[0,1]$ that have a base 3 expansion not using 1 at all.

We now establish a surjective function $f : F \to [0,1]$, implying that the cardinality of F is at least that of $[0,1]$. Since F is a subset of $[0,1]$, its cardinality is also less than or equal to that of $[0,1]$. Hence, we conclude that the two sets have equal cardinality.

To define $f : F \to [0,1]$, consider constructing f by taking a number composed entirely of the digits $\{0,2\}$ and replacing each occurrence of $\{2\}$ with $\{1\}$ in its representation.

To demonstrate the surjectivity of f, let $x \in [0,1]$ be any element. Represent x in its binary form, and then replace each occurrence of a $\{1\}$ digit with a $\{2\}$. Denote this new number as y. It follows that $f(y) = x$. Therefore, f is surjective. By our previous observation, we assert that the cardinality of F is equal to that of $[0,1]$, which is uncountable. □

Proposition 6. *The point $1/4$ is not an endpoint of any interval of any set E_k. But the point $1/4 \in F$.*

Proof. Consider the point $\frac{1}{4}$. While it doesn't belong to the endpoints of the Cantor set (which all have denominators as powers of three), $\frac{1}{4}$ does indeed reside within the Cantor set. Specifically, it's in the lower third, then in the upper third of that lower third, and so forth, infinitely subdividing.

Furthermore, we can express $\frac{1}{4}$ as the sum of an infinite geometric series

$$\frac{2}{9} + \frac{2}{9^2} + \frac{2}{9^3} + \cdots = \frac{1}{4}.$$

This representation illustrates that the base-3 expansion of $\frac{1}{4}$ is $0.02020202\ldots$. Since this expansion consists only of digits 0 and 2, it confirms that $\frac{1}{4}$ lies within the Cantor set. □

Proposition 7. *The Cantor set F is compact.*

Proof. $F = \bigcap_{k=0}^{\infty} E_k$, where E_k consists of the union of 2^k disjoint closed intervals in $[0, 1]$, each of length 3^{-k}. For every k, E_k is closed since it is the union of finitely many closed sets. Since the intersection of any collection of closed sets is closed, F is closed. F is a subset of $[0, 1]$ so it is bounded, and therefore F is compact. □

Proposition 8. *The Cantor set F is nowhere dense.*

Proof. Since F is closed, $\bar{F} = F$. Since F contains no open interval, $\operatorname{int} F = \varnothing$. Hence, F is nowhere dense, i.e, its closure has empty interior. To claim that F contains no open interval, one can notice that this follows from the fact that the Lebesgue measure of F is zero together with the monotonicity of the measure. □

Proposition 9. *The Cantor set F is perfect (F is a closed set and every point of F is a limit point of F).*

Proof. We already know that F is closed. We have to show that every point of F is a limit point. Let $x \in F$ and let U be any open interval such that $x \in U$.

Let I_k be the interval of E_k which contains x (recall from the definition that $x \in \bigcap_{k=1}^{\infty} E_k$). For k large enough, $I_k \subset U$. Thus $(U \backslash \{x\}) \cap F \neq \varnothing$, and therefore x is a limit point of F. Since $x \in F$ was arbitrary we conclude that F is perfect. □

Proposition 10 ([20, Exercise 1.5])**.** *The Cantor set F is totally disconnected.*

Proof. Assume $x, y \in F$ with $x < y$. Consequently, there exists an E_k such that x and y lie in different intervals $[a, b]$ and $[c, d]$ of E_k, where $b < c$. Suppose $b < p < c$. Consequently, F is contained within the union of disjoint open intervals $(-1, p)$ and $(p, 2)$, where $x \in (-1, p)$ and $y \in (p, 2)$. Hence, F is indeed totally disconnected. □

The next example we illustrate is the Koch curve, introduced by Helge von Koch (1870-1924), a Swedish mathematician, in 1904 [29]. Similar to the Weierstrass function, the Koch curve is an example of a continuous non-differentiable curve and thus does not have a tangent at any of its points [50].

Example 3 (Koch curve)**.** *We start from a straight line segment of unit length E_0. We divide the line segment into three equal parts and replace the middle segment with an equilateral triangle by removing the middle portion of the line and add an outward-facing equilateral triangle. In this way we get E_1. In order to get E_2 we apply the same steps to each of the four segments created in the previous iteration. The Koch curve F is given as the limit of E_k when k tends to infinity, by applying iteratively the same steps to each of the four segments created in the previous iteration E_{k-1}. In particular for each iteration there are 4^k line segments of length 3^{-k}.*

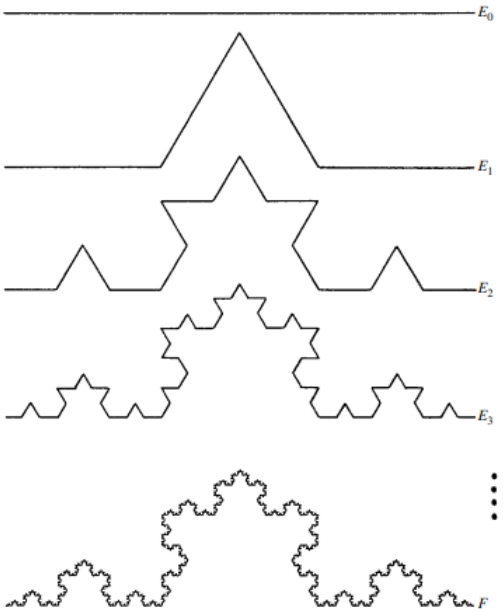

Figure 3.3: The Koch curve.
Source: [20, p. xix]

For an an animation of the construction of F, see Appendix A.2.

It is easy to see that E_k is of length $\left(\frac{4}{3}\right)^k$. The length of the Koch curve tends to infinity as $k \to \infty$, i.e.

$$\lim_{k\to\infty} \left(\frac{4}{3}\right)^k = \infty$$

Thus F has infinite length. Conversely, the set F takes up no area within the plane, rendering both length and area as insufficient descriptors of its size.

In particular, the curve spans a much larger space than conventional curves, due to its infinite length, thus designating it as a one-dimensional shape appears inadequate. Conversely, characterizing the curve as two-dimensional is also imprecise, given its negligible area, amounting to zero. We thus need a more flexible definition of dimension. The formal discussion about fractal dimension has to be found in Chapter 4.

The Koch curve exhibits characteristics typical of fractals. It demonstrates self-similarity, composed of four sections, each resembling the entire set but scaled down by a factor of $\frac{1}{3}$. The intricate details, observable at various scales, reflect a fine structure. Interestingly, this complex structure originates from a fundamentally straightforward construction process. As for the Cantor set, also the Koch curve is given by a recursive procedure.

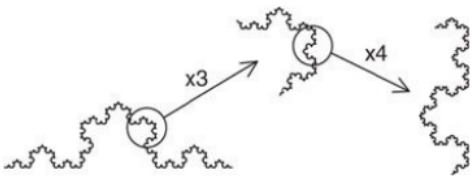

Figure 3.4: Repeated magnification reveals more irregularity.
Source: [21, p. 28]

Proposition 11 ([41])**.** *The area bounded between the Koch curve F and the initial horizontal unit line segment is $\frac{\sqrt{3}}{20}$.*

Proof. The area, A, enclosed by the Koch curve and the initial segment can be calculated as follows. First, we find the area of the equilateral triangle inside the bounded region. Since its side length is $1/3$, its area is given by $\frac{\sqrt{3}}{4} \cdot \left(\frac{1}{3}\right)^2 = \frac{\sqrt{3}}{36}$. Then, there are four smaller regions outside this equilateral triangle, each bounded by a copy of F that has been scaled by a factor of by $1/3$. Thus, each of these regions has an area of $A/9$. Therefore

$$A = \frac{\sqrt{3}}{36} + 4 \cdot \frac{A}{9} \Rightarrow \frac{5}{9}A = \frac{\sqrt{3}}{36} \Rightarrow A = \frac{\sqrt{3}}{36} \cdot \frac{9}{5} = \frac{\sqrt{3}}{20}.$$

□

The next proposition explains why the Koch curve is actually called a 'curve', i.e. the continuous image of the unit interval.

Consider the construction of the Koch curve (Figure 3.3). We have a sequence (E_k) of polygonal curves intended to 'converge' to the Koch curve F. However, since E_{k+1} is not a subset of E_k, it's not appropriate to simply take the intersection. Here's one approach to produce a reasonable limit.

The curve E_k consists of 4^k line segments. We partition the interval $[0, 1]$ into 4^k subintervals of equal length. We define a function $g_k : [0, 1] \to \mathbb{R}^2$ to

be affine on each of these subintervals (a continuous curve $f : [0,1] \to \mathbb{R}^d$ is piecewise affine if there exist 'division points' $0 = a_0 < a_1 < \cdots < a_n = 1$, such that f is affine on each subinterval $[a_{j-1}, a_j]$. The range of such a function is called a polygonal curve [15, p. 68]). This function is continuous on all of $[0,1]$, so that the subintervals are mapped to the line segments of E_k. Therefore, we have $g_k[[0,1]] = E_k$.

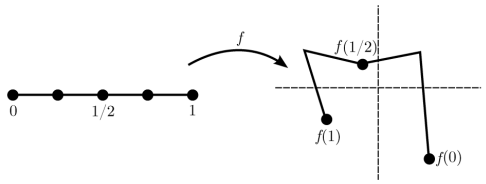

Figure 3.5: A piecewise affine curve.
Source: [15, p. 69]

Proposition 12 ([15, Prop. 2.4.10])**.** *The sequence (g_k), in the construction of the Koch curve F, converges uniformly.*

Proof. First, note that every point of E_1 is within a distance of 1 from every point of E_0. Let's define the uniform metric as follows:

$$\rho(f,g) = \sup_{t\in[0,1]} \{|f(t) - g(t)|\} \text{ where } f \text{ and } g \text{ are functions on } [0,1].$$

So, certainly, $\rho(g_0, g_1) \leq 1$. Now, let's estimate $\rho(g_k, g_{k+1})$. Take $t \in [0,1]$. Then t lies in one of the 4^k subintervals J on which g_k is affine. Its image $g_k[J]$ is a line segment of length 3^{-k}. When g_{k+1} is constructed, the interval J is subdivided into 4 equal intervals, and a scaled, translated, and rotated copy of g_1 is used there, with the scaling factor of $.3^{-k}$. Hence, $\rho(g_k, g_{k+1}) \leq 3^{-k}\rho(g_0, g_1)$. Therefore, $\rho(g_k(t), g_{k+1}(t)) \leq 3^{-k}$. Now, for $m > k$, we have

$$\rho(g_k, g_m) \leq \sum_{j=k}^{m-1} \rho(g_j, g_{j+1}) \leq \sum_{j=k}^{m-1} 3^{-j} < 3^{-k+1}/2.$$

This shows that (g_k) is a Cauchy sequence for the uniform metric, so by the Cauchy criterion for uniform convergence [1, Prop. 1.4], it converges uniformly. □

Write $g(t) = \lim_{k\to\infty} g_k(t)$ for all $t \in [0,1]$. Then, using the result that the limit function of a uniformly convergent sequence of continuous functions is continuous [1, Thm 2.1], we conclude that the function g is continuous. The limit set, the Koch curve, is then $F = g[[0,1]]$. This result explains therefore the use of the word 'curve'.

Example 4 (Cesàro fractal)**.** *The Cesàro fractal is one of the variations of the Koch curve. The construction method closely resembles that of the Koch curve, with one significant difference: the angle between the base of the triangles and the other sides varies. During each iteration step of constructing the Cesàro fractal, an isosceles triangle is formed with the angle ranging from* 60° *(matching the Koch curve) to* 90°*.*

Figure 3.6: The Cesàro fractal with an angle of 85°.
Source: [21, p. 64]

Example 5 (Koch snowflake)**.** *The Koch snowflake's boundary, is composed of three identical parts, each of which is a Koch curve (see Figure 3.7). This fractal is created by starting with a filled equilateral triangle of unit side length and iteratively transforming each line segment. Applying the same transformations of the Koch curve to each side of the triangle yields the snowflake. Despite having an infinite perimeter, the figure maintains a finite area.*

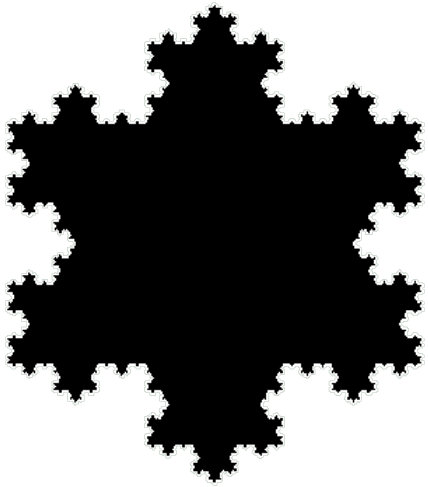

Figure 3.7: The Koch snowflake.
Source: [39, p. 88]

While von Koch is widely recognized for introducing the Koch curve in 1904, his original articles lack any depiction of the snowflake associated with

his name. A fascinating investigation into the history of the fractal snowflake, explored in [12], sheds light on its true origins.

Proposition 13 ([41])**.** *The area of the Koch snowflake F is $\frac{2\sqrt{3}}{5}$.*

Proof. The area of the original equilateral triangle with unit side length is $\frac{\sqrt{3}}{4}$. For the subsequent iteration, the area of the snowflake is expanded by incorporating three new smaller triangles, each having a side length of $1/3$. Consequently, the area after the first iteration becomes

$$A_1 = \frac{\sqrt{3}}{4} + 3 \cdot \frac{\sqrt{3}}{4} \left(\frac{1}{3}\right)^2 = \frac{\sqrt{3}}{4} \left(1 + \frac{3}{9}\right)$$

Moving on to the next iteration, we introduce an additional 12 smaller triangles. The area of each new triangle contributes to the total area. Hence, after the second iteration, the area becomes

$$A_2 = \frac{\sqrt{3}}{4} \left(1 + \frac{3}{9}\right) + 3 \cdot 4 \cdot \frac{\sqrt{3}}{4} \left(\frac{1}{9}\right)^2 = \frac{\sqrt{3}}{4} \left(1 + \frac{3}{9} + \frac{3 \cdot 4}{9^2}\right)$$

Continuing this pattern, after the third iteration, we have:

$$A_3 = \frac{\sqrt{3}}{4} \left(1 + \frac{3}{9} + \frac{3 \cdot 4}{9^2}\right) + 3 \cdot 4 \cdot 4 \cdot \frac{\sqrt{3}}{4} \left(\frac{1}{3^3}\right) = \frac{\sqrt{3}}{4} \left(1 + \frac{3}{9} + \frac{3 \cdot 4}{9^2} + \frac{3 \cdot 4^2}{9^3}\right)$$

The recurring pattern becomes evident by now. At the k-th iteration, we include $3 \cdot 4^{k-1}$ additional triangles, each with an area of $\frac{\sqrt{3}}{4} \left(\frac{1}{3^k}\right)^2$. This yields an added total area of

$$3 \cdot 4^{k-1} \cdot \frac{\sqrt{3}}{4} \left(\frac{1}{3^k}\right)^2 = \frac{\sqrt{3}}{4} \left(\frac{3 \cdot 4^{k-1}}{9^k}\right)$$

to the area A_{k-1}, resulting in the area of A_k. Thus, after n iterations, we express the area A_n as

$$A_n = \frac{\sqrt{3}}{4} \left(1 + \sum_{k=1}^{n} \frac{3 \cdot 4^{k-1}}{9^k}\right)$$

The summation within the parentheses represents the partial sum of a geometric series with a ratio of $r = 4/9$. Consequently, the sum converges as n approaches infinity. Therefore, the area of the Koch snowflake is determined to be

$$\begin{aligned} \frac{\sqrt{3}}{4} \left(1 + \sum_{k=1}^{\infty} \frac{3 \cdot 4^{k-1}}{9^k}\right) &= \frac{\sqrt{3}}{4} \left(1 + \frac{3/9}{1 - 4/9}\right) \\ &= \frac{\sqrt{3}}{4} \left(\frac{8}{5}\right) \\ &= \frac{2\sqrt{3}}{5} \end{aligned}$$

Upon closer examination of the formulas, one can discern that the limiting area of the Koch snowflake corresponds precisely to 8/5 of the area of the initial triangle. □

Let's see now a shorter way to compute the area of F using the self-similarity property.

Proposition 14 ([44])**.** *Using the self-similarity property of F, the area of the Koch snowflake F is $\frac{8}{5}$ times the area of the original equilateral triangle.*

Proof. Let's start by considering the area of the center equilateral triangle within the Koch snowflake F as 1 unit. Let A be the area outside the central equilateral triangle but within the region of the snowflake located on the right side (see Figure 3.7). Within this region, the area of the equilateral triangle is a scaled-down version of the central one by $\frac{1}{3}$, thus its area is $\frac{1}{9}$. Each of the four smaller copies of this region is $\frac{1}{3}$-scaled versions of the entire region, so each has an area of $\frac{A}{9}$. This gives us the equation:

$$A = \frac{1}{9} + 4\frac{A}{9}$$

Solving this equation, we find $A = \frac{1}{5}$. The areas of the left and bottom sections outside the central equilateral triangle but inside the snowflake mirror the right section, so their combined area is also $\frac{1}{5}$. Consequently, the total area of the Koch snowflake is $1 + 3\frac{1}{5} = \frac{8}{5}$.

Now, to generalize this, let's consider the area of the snowflake concerning the original equilateral triangle with a side length s. We know that the area of an equilateral triangle is $\frac{\sqrt{3}}{4}s^2$, so the area of the snowflake would be:

$$\frac{\sqrt{3}}{4}\left(\frac{8}{5}\right)s^2$$

□

The next classical fractal proposed is the Sierpinski triangle (also known as Sierpinski gasket), introduced in 1916 by the Polish mathematician Wacław Sierpiński (1882–1969) [47]. Again it consists of a strict self-similar set, each part of the fractal is a miniature version of the entire fractal scaled by some constant factor.

Example 6 (Sierpinski triangle)**.** *The process for the construction of the Sierpinski triangle starts with a filled equilateral triangle E_0 of side length 1. We connect the midpoints of its sides to form 4 congruent smaller triangles. Removing the middle triangle, leaves three triangles of sides $\frac{1}{2}$, each with $\frac{1}{4}$ the area of the original. Call the remaining set E_1 and by following the same process for each of the three remaining triangles, we get E_2 with 9 triangles of side length $\frac{1}{4}$. Proceeding in this way, E_k consists of 3^k triangles of side length*

2^{-k}. *The Sierpinski triangle, denoted as* F*, is the set of points that remain when this process is iterated infinitely often.*

$$F = \bigcap_{k=0}^{\infty} E_k$$

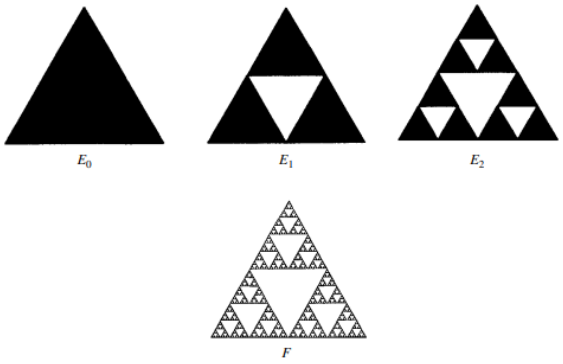

Figure 3.8: The Sierpinski triangle.
Source: [20, p. xx]

For an animation of the construction of F, see Appendix A.3.

The area of the Sierpinski triangle at stage E_k is given by $3^k \cdot \left(2^{-k}\right)^2 \cdot \frac{\sqrt{3}}{4}$, and by taking the limit when $k \to \infty$, we get that the total area converges to zero, i.e.

$$\lim_{k\to\infty} \frac{\sqrt{3}}{4} \left(\frac{3}{4}\right)^k = 0.$$

Let's see an alternative way to measure the area of F using the self-similarity property.

Proposition 15 ([41])**.** *The area of* F *is* 0*.*

Proof. Assume that the triangle covering F has area 1. Let A be the total area of the tremas in F (see Remark 1). We can express this as follows: $A = \frac{1}{4} + 3\left(\frac{1}{4}A\right)$. This equation represents the area of the center hole plus the combined areas of the holes in the three scaled copies of the Sierpinski triangle surrounding the center hole, each of which is a scaled-down version of the original by a factor of $\frac{1}{2}$, thus scaling the area of those holes by $\frac{1}{4}$.

Now, simplifying this equation:

$$A = \frac{1}{4} + \frac{3}{4}A \Rightarrow \frac{1}{4}A = \frac{1}{4} \Rightarrow A = 1.$$

This result shows that the total area of the tremas is 1, which is equal to the area of the covering triangle. Therefore, the Sierpinski triangle F has an area of 0.

□

Intuitively, area is used to measure the size of a set of dimension 2. Therefore, we would expect the Sierpinski triangle to have a dimension less than 2. At the same time we notice that in each step, we always keep the line segments that constitute the boundary of the triangles from the iteration before, and simultaneously we get new line segments from the new triangles that have been created, meaning that the total perimeter of E_k is $3^k \cdot 3 \cdot 2^{-k}$. As $k \to \infty$ the total perimeter of F diverges to ∞. We conclude that the length of the Sierpinski triangle is infinite. Intuitively, length is used to measure the size of a set of dimension 1. Therefore, we would expect the Sierpinski triangle to have a dimension greater than 1.

So, while it's expected that the dimension of the Sierpinski triangle is greater than 1 but less than 2, we encounter a challenge as the traditional dimension is given by integers, and there is no integer between 1 and 2. To address this, we must formalize the concept of dimension and introduce innovative methods for defining dimension, which would permit a set to have a fraction as its dimension, a concept known as fractal dimension, as discussed in the next chapter.

Remark 2. *Pascal's Triangle is a triangular array of numbers where each entry is determined by the sum of the two numbers directly above it. These numbers are binomial coefficients, representing the number of different ways to choose k objects out of n. Specifically, the binomial coefficient $\binom{n}{k}$ in row n and column k is calculated using Pascal's rule:*

$$\begin{pmatrix} n \\ k \end{pmatrix} = \begin{pmatrix} n-1 \\ k-1 \end{pmatrix} + \begin{pmatrix} n-1 \\ k \end{pmatrix}$$

Here, n is a non-negative integer, and k is an integer such that $0 \leq k \leq n$. The pattern begins with each row starting and ending with 1. Investigating the numbers' parity in Pascal's Triangle uncovers an intriguing pattern: the odd binomial coefficients closely resemble a discrete Sierpinski triangle [49]. While basic diagrams can show the odd entries, a more detailed representation is needed to fully appreciate the pattern. Computational analysis confirms that the odd coefficients align with the Sierpinski triangle's intricate structure. In 1890, Lucas provided a mathematical explanation for this intriguing correlation, which relies on the binary notation system for numbers (Lucas's theorem) [30]. A complete proof is available in [41].

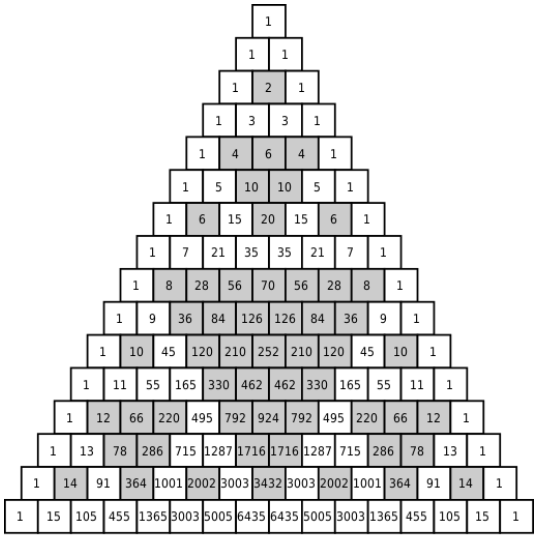

Figure 3.9: Approximation of the Sierpinski triangle obtained by shading the even entries of the Pascal's triangle.
Source: [52]

To conclude this chapter, let's provide additional illustrations of common fractal examples without delving too much into their discussion.

Example 7 (Cantor dust)**.** *At every iteration of the construction process, the squares are subdivided into 16 smaller squares, each having a quarter of the side length of the original square. In each of these smaller squares, the identical pattern of four squares is preserved.*

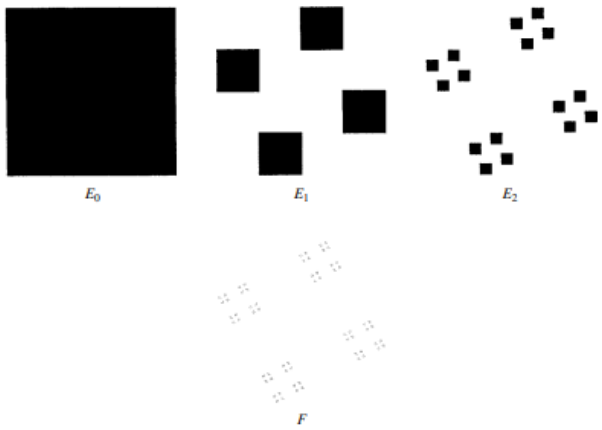

Figure 3.10: The Cantor dust.
Source: [20, p. xxi]

The next example introduces a random component in the construction process of a fractal. Clearly, the set will no longer be a strictly self-similar set; in this case, we refer to it as a statistically self-similar set. This implies that enlargements of small parts exhibit the same statistical distribution as the whole set [20, chap. 15]. In facts, objects in the real world, like coastlines, often exhibit statistical self-similarity, meaning that their statistical properties remain consistent across various scales [31].

Example 8 (random Koch curve)**.** *The iteration steps the same principles as those in the original Koch curve, except for one key difference: the orientation of the triangle is randomly selected (by tossing a coin) during each step.*

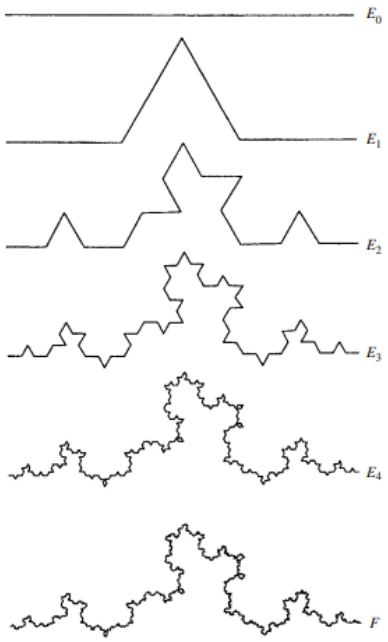

Figure 3.11: A random Koch curve.
Source: [20, p. 245]

The last example illustrates a self-affine set, where the scaling factor is different in different directions.

Example 9 (self-affine fractal)**.** *Consider the set F, constructed iteratively as follows: At each stage k, every rectangle in E_k is substituted with an affine copy of the rectangles in E_1. In this process, the contraction is more pronounced along the y direction than the x direction. Notably, the width-to-height ratio of the rectangles in E_k tends to infinity as k approaches infinity.*

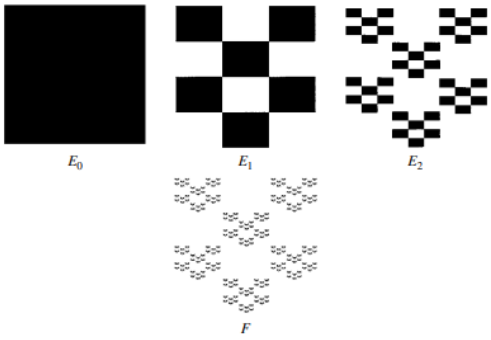

Figure 3.12: A self-affine fractal.
Source: [20, p. 107]

Chapter 4

Fractal Dimension

A crucial aspect of fractal geometry lies in its capacity to describe irregularity across various scales, a capability not afforded by classical Euclidean geometry. Consequently, numerous distinctive fractal characteristics have been recognized, with the fractal dimension standing out as particularly significant.

Roughly, a dimension describes of how much space a set fills. It is a measure of the prominence of the irregularities of a set when viewed at very small scales and encompasses a wealth of detail about the geometrical properties of a set [20].

Mathematicians have formulated a comprehensive concept of dimension to aid in the examination of such sets. In reality, they have devised multiple approaches; a specific definition of dimension may serve one purpose effectively but not necessarily another. For this reason, it is important, while speaking about dimension, to always refer to the one considered, as the dimension of a set may vary according to the definition used.

Determining whether a quantity can be considered a dimension doesn't adhere to strict rules. The acceptability of a dimension definition is often guided by experience and intuition. Typically, one seeks for some scaling behavior and a sense of natural fit within the specific context [19].

We will explore more than one of these definitions, categorizing them into two main groups: topological dimension (section 4.1) and fractal dimension (sections 4.2, 4.3, 4.4). The topological dimension is the one that meet our intuitive feeling of dimension, while the others are needed to capture the complexity of fractal sets, and should ideally evaluate the proportion of the variation in detail to the variation in scale [34].

Basic properties of dimensions

In general to qualify something as a dimension, it is advisable for the majority of the specified criteria to be fulfilled [19, pp. 23-24].

1. **Monotonicity:** $E \subset A \Rightarrow \dim E \leq \dim A$.

2. **Countable sets:** If E is finite or countable, then $\dim E = 0$.

3. **Open sets:** If $E \subset \mathbb{R}^n$ open set, then $\dim E = n$.

4. **Smooth manifolds:** If E is any smooth, m-dimensional submanifold of $\mathbb{R}^n$, then $\dim E = m$.

5. **Countable stability:** If E_1, E_2, ... is a countable sequence of sets then $\dim\left(\bigcup_{i=1}^{\infty} E_i\right) = \sup_i \{\dim E_i\}$.

6. **Lipschitz Mappings:** If $f : E \to \mathbb{R}^m$ is Lipschitz, then $\dim f(E) \leq \dim(E)$.

7. **Bi-Lipschitz Mappings:** If $f : E \to \mathbb{R}^m$ is bi-Lipschitz, then $\dim f(E) = \dim(E)$.

8. **Geometric invariance:** $\dim f(E) = \dim E$ when f is a similarity or an affine transformation (special case of bi-Lipschitz invariance).

The properties of 'open sets' and 'smooth manifolds' guarantee that the dimension is an extension of the classical topological definition [20, p. 41].

4.1 Topological Dimension

We are familiar with linking dimension 1 to a curve, dimension 2 to a square, and dimension 3 to a cube. The concept of topological dimension serves as a method to articulate this intuition more accurately. In this section we formalise this notion, more precisely we present the covering dimension, also known as Lebesgue covering dimension or simply topological dimension. It is important to say that the covering dimension is only one of the several ones in the field of topological dimensions, other common definitions include the small inductive dimension and the large inductive dimension, however these three topological dimensions coincide for any separable metric space [16, Thm 1.7.7], so in particular this holds for the Euclidean space $\mathbb{R}^n$ where we focus on. All of these are also integer valued: no 'fractional' dimensions at all. More details about topological dimension can be found in [15, chap. 5], which is the main reference for this section.

Definition 32 (refinement of a cover, [15, p. 86])**.** *If $\mathcal{A}$ and $\mathcal{B}$ are two collections of sets, we say that $\mathcal{B}$ is subordinate to $\mathcal{A}$ if and only if for every $B \in \mathcal{B}$ there is $A \in \mathcal{A}$ with $B \subset A$. Let $\mathcal{A}$ be an open cover of $F \subset \mathbb{R}^n$. A refinement of $\mathcal{A}$ is an open cover $\mathcal{B}$ of F that is subordinate to $\mathcal{A}$. We also say say $\mathcal{B}$ refines $\mathcal{A}$.*

Definition 33 (order, [15, p. 91]). *Let $n \geq -1$ be an integer. The order of a family $\mathcal{A}$ of sets is $\leq n$ if and only if any $n+2$ of the sets have empty intersection. If $n \geq 0$, then we say $\mathcal{A}$ has order n if and only if it has order $\leq n$ but does not have order $\leq n-1$.*

Example 10. *A collection $\mathcal{A}$ of non-empty sets is disjoint if and only if its order is 0. A collection of sets $\mathcal{A}$ has order -1 if and only if it is empty or is the singleton $\{\emptyset\}$.*

Definition 34 (topological dimension, [15, p. 92]). *Let $n \geq -1$ be an integer and $F \subset \mathbb{R}^n$ be a set. We say that F has topological dimension (or covering dimension or Lebesgue topological dimension) $\leq n$ if and only if every finite open cover of F has a refinement with order $\leq n$. The topological dimension is n if and only if the topological dimension is $\leq n$ but not $\leq n-1$. We will write $\dim F = n$ in that case. If the topological dimension is $\leq n$ for no integer n, then we say $\dim F = \infty$.*

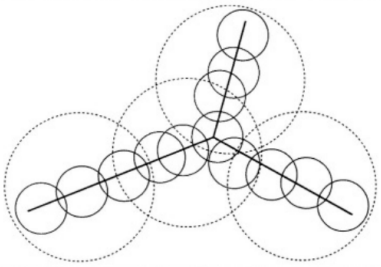

Figure 4.1: The covering at a branching point and a refinement.
Source: [39, p. 109]

Figure 4.1 highlights the significance of the concept of refinement. The large cover, represented by dotted circles, covers the y-shaped object, resulting in three intersecting disks in one case. However, a refinement with smaller disks (solid circles) ensures that at most two disks intersect.

Example 11. *When $\dim F = -1$, the open cover $\{F\}$ is refined by a cover of order -1, which is either $\emptyset$ or $\{\emptyset\}$. This constitutes a cover only if $F = \emptyset$. Thus, the dimension of F is -1 if and only if $F = \emptyset$.*

Remark 3. *A non-empty set $F \subset \mathbb{R}^n$ should be considered zero-dimensional, if every finite open cover of F has a refinement which is a cover by disjoint open sets.*

Example 12. *An open cover of the unit circle can always be refined to consist of a collection of open arcs. According to the definition of topological dimension, the circle has a dimension of 1 because any such cover can be refined so that any given point on the circle is within at most two open arcs. This means*

that regardless of the initial collection of arcs, it is always possible to discard or shrink some of them so that the remaining ones still cover the circle with simple overlaps.

The intuitive understanding is that a finite set of points can be covered without any intersections. For curves, we can find a cover with an order of 1, and there is no cover with order 0 using sufficiently small disks or balls. Similarly, surfaces can be covered with an order of 2, and there is no cover with order 1 using sufficiently small disks or balls. This implies that the topological dimension is 0 for points, 1 for curves, and 2 for surfaces. These principles extend to higher dimensions. Furthermore, the method of covering a curve, whether it is embedded in a plane or in space, using disks or balls, remains the same [39].

Proposition 16 ([11, Thm. A.4.13])**.** *If $F \subset \mathbb{R}^n$ is a compact set, then $\dim F = 0$ if and only if F is totally disconnected.*

Proof. Omitted. See [11, Thm. A.4.13]. □

Proposition 17 ([11, Thm. A.4.14])**.** $\dim \mathbb{R}^n = n$.

Proof. Omitted. See [11, Thm. A.4.14]. □

Proposition 18 ([11, Thm. A.4.15])**.** *Topological dimension is a topological invariant.*

Proof. Omitted. See [11, Thm. A.4.15]. □

This last proposition implies, for example, that a curve, being a homeomorphic image of an interval, possesses a topological dimension of 1.

To conclude this section, note that while these sets may exhibit fractal characteristics, such complexities are not accounted for in their topological dimension analysis.

4.2 Similiarity Dimension

Calculating the fractal dimension through the similarity dimension is considered the simplest method. However, this approach is restricted to a specific subset of strictly self-similar sets, furthermore this method assumes that we are already aware of the scaling ratio, which is not always the case. Despite its ease of computation, more versatile definitions of dimension are available and will be explored in the subsequent sections.

We start with the familiar setting of traditional geometry. Consider firstly a unit segment line, a classical 1-dimensional topological object, divided in 2 equal parts, each of length $\frac{1}{2}$.

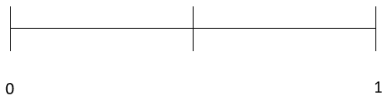

Figure 4.2: A unit line divided into 2 segments.

Then the scaling ratio c is $\frac{1}{2}$ and the number of copies N is 2 and we get the following relation:

$$N = c^{-s}$$

where $s = 1$ corresponds to the dimension of the line. Similarly, consider now a unit square, a prototype of a 2-dimensional object, with side length divided by 2.

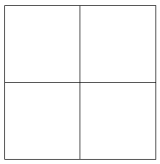

Figure 4.3: A unit square divided into 4 subsquares.

Then the number of copies N is 4, while the scaling factor is $\frac{1}{2}$. We have

$$N = c^{-s}$$

where $s = 2$ corresponds to the dimension of the square. Finally consider a 3-dimensional unit cube, with side length divided by 2.

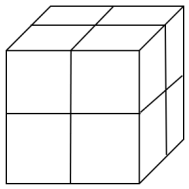

Figure 4.4: A unit cube divided into 8 subcubes.

Then the number of copies N is 8, while the scaling factor is $\frac{1}{2}$. We have

$$N = c^{-s}$$

where $s = 3$ corresponds to the dimension of the cube.

Solving for s we get the following relation:

$$\log_c N = -s = \frac{\log N}{\log c}$$

The concept extends further to a fractal set F. We denote the similarity dimension by $\dim_S F$.

$$s = \dim_{\mathrm{S}} F = \frac{\log N}{\log \frac{1}{c}}$$

Example 13. *The Cantor set F (Example 2) is made up of 2 copies of itself scaled by a scale factor of $\frac{1}{3}$. Recall that the k-iteration E_k is given by 2^k disjoint intervals each of length 3^{-k}. Thus $\dim_{\mathrm{S}} F = \frac{\log 2}{\log 3} = 0.63\ldots$. This agrees with the fact that F is more than 0-dimensional (F is uncountable) and less than 1-dimensional (the length of F is zero).*

Example 14. *The Koch curve F (Example 3) is made up of 4 copies of itself scaled by a scale factor of $\frac{1}{3}$. Recall that the k-iteration E_k is given by 4^k segments each of length 3^{-k}. Thus $\dim_{\mathrm{S}} F = \frac{\log 4}{\log 3} = 1.26\ldots$. It possesses a dimension exceeding one but falls short of being two-dimensional. This aligns with the concept that the curve cannot be adequately characterized by either length (the length of F is infinite) or area alone (F has area zero).*

Example 15. *The Sierpinski triangle F (Example 6) is made up of 3 copies of itself scaled by a scale factor of $\frac{1}{2}$. Recall that the k-iteration E_k consists of 3^k triangles of side length 2^{-k}. Thus $\dim_{\mathrm{S}} F = \frac{\log 3}{\log 2} = 1.58\ldots$. The Sierpinski triangle possesses a higher dimension compared to the Koch curve. Consequently, we describe intuitively the Sierpinski triangle as filling the plane more extensively than the Koch curve.*

Example 16. *The construction of the Sierpinski Carpet F (Figure 4.5) initiates with a solid unit square E_0, subsequently partitioned into 9 congruent smaller squares. The first step E_1 involves excising the central square from this arrangement. This recursive procedure is systematically reproduced for each residual square. At the k-iteration stage, denoted as E_k, the construct comprises 8^k squares, with each square with an area of 9^{-k}. In particular the Sierpinski carpet is made up of 8 copies of itself scaled by a scale factor of $\frac{1}{3}$. Thus $\dim_{\mathrm{S}} F = \frac{\log 8}{\log 3} = 1.89\ldots$.*

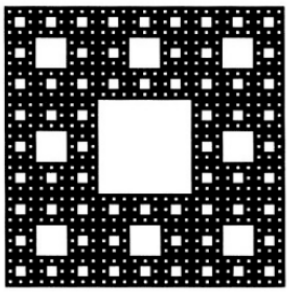

Figure 4.5: The Sierpinski carpet.
Source: [39, p. 194]

Example 17. *A simple trigonometric argument shows that the Cesàro fractal F (Example 4) is made up of 4 copies of itself scaled by a scale factor of $\frac{1}{2(1+\cos\alpha)}$. In the specific case of Figure 3.6 we get*

$$\dim_{\mathrm{S}} F = \frac{\log 4}{\log(2(1+\cos 85°))} = 1.78\ldots.$$

Note that for $0° < \alpha < 90°$, $\dim_{\mathrm{S}} F \in (1,2)$.

However, numerous self-similar fractals consist of components scaled by various proportions. In this context, we aim to understand the computation of the similarity dimension for these more complex self-similar fractal structures.

Definition 35 (similarity dimension, [15, chap. 4])**.** *Let F be a self-similar compact set such that*

$$F = T_1(F) \cup T_2(F) \cup \cdots \cup T_N(F),$$

where $T_i, i = 1,\ldots,N$, are similarities with contraction ratios $c_i \in (0,1)$. The similarity dimension of F, $\dim_{\mathrm{S}} F$, is the unique solution s to the Moran equation

$$c_1^s + c_2^s + \cdots + c_N^s = \sum_{i=1}^{N} c_i^s = 1. \tag{4.1}$$

In the special case when

$$c_1 = c_2 = \cdots = c_N = c$$

we have that

$$Nc^s = 1 \text{ and therefore } \log N + s\log c = 0.$$

Thus

$$\dim_{\mathrm{S}} F = s = \frac{\log N}{\log(1/c)}.$$

which is exactly the previous definition as expected.

Proposition 19 ([15, Thm. 4.1.1])**.** *There is a unique non-negative number s satisfying equation (4.1). The number s is 0 if and only if $N = 1$.*

Proof. Consider the function $\Phi : [0,\infty) \to [0,\infty)$ given by

$$\Phi(s) = \sum_{i=1}^{N} c_i^s.$$

This function is continuous, with $\Phi(0) = N \geq 1$, and $\lim_{s\to\infty} \Phi(s) = 0 < 1$. Thus, by the intermediate value theorem, there exists at least one value s such that $\Phi(s) = 1$. The derivative of Φ is

$$\sum_{i=1}^{N} r_i^s \log c_i.$$

Since this expression is negative, Φ is strictly decreasing. Hence, there exists only one solution s to $\Phi(s) = 1$. If $N > 1$, then $\Phi(0) > 1$, implying $s \neq 0$. □

Example 18 ([41])**.** *Consider the Koch snowflake F (see Figure 3.7). Then* $\dim_{\mathrm{S}} F = 2$.

Proof. The Koch snowflake, exhibits self-similarity with six components scaled by $1/3$ and one component scaled by $1/\sqrt{3}$ (see Figure 4.6 and Example 55 for more details). According to Moran's equation, the similarity dimension s needs to satisfy the equation:

$$1 = 6\left(\frac{1}{3}\right)^s + \left(\frac{1}{\sqrt{3}}\right)^s$$

The solution to this equation is uniquely $s = 2$. However, note that the boundary of the Koch snowflake comprises multiple iterations of the Koch curve, which possesses a fractal dimension of approximately 1.26186. □

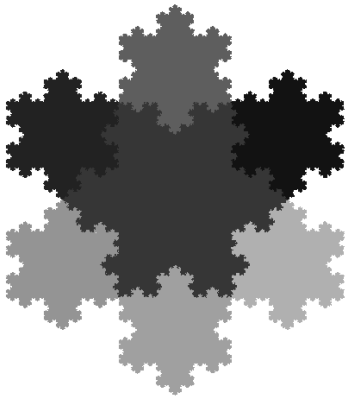

Figure 4.6: The Koch snowflake is made up of 7 smaller copies of itself.
Source: [41]

Remark 4 ([7])**.** *Figure 4.6 suggests that it is possible to have a tiling of the plane with Koch snowflakes in two different sizes, their diameters being in ratio $\sqrt{3} : 1$ and one copy rotated by $30°$ with respect to the first size (see Figure 4.7). However using snowflakes of only one size will not achieve this*

tessellation. Moreover, since each snowflake can be split into seven smaller ones of two sizes, it's possible to achieve tessellations with more than two sizes simultaneously.

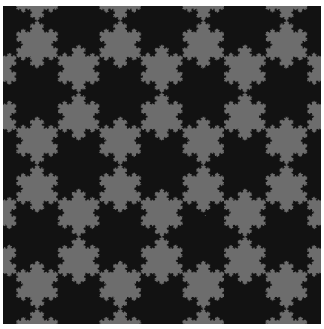

Figure 4.7: Tessellation of the plane using two sizes of the Koch snowflake.
Source: [41]

While named similarity dimension, it generally doesn't satisfy the dimension conditions outlined at the beginning of the section.

In particular it is possible for a specific set F to have two distinct decompositions, leading to two different similarity dimensions. Therefore, it is more accurate to view the value s as a characteristic of the decomposition rather than solely as a characteristic of the set F.

Example 19. *Consider $F = [a, b] \subset \mathbb{R}$ where $a < b$. F is given by the union of two smaller intervals, $[a, (a + b)/2]$ and $[(a + b)/2, b]$. Each subinterval is similar to the whole set F with scaling ratio $c = \frac{1}{2}$. The similarity dimension of F is the solution s of the equation*

$$2\left(\frac{1}{2}\right)^s = 1,$$

Thus $s = 1$. In the same way $F = [0, 1] = [0, 2/3] \cup [1/3, 1]$, where both intervals are scaled by a factor of $c = \frac{2}{3}$. This yields a value of the dimension $s > 1$.

In the previous example, we observed that for the similarity dimension to characterize the set, it is essential to limit and control the overlap in some way. Specifically, in certain situations and under the right circumstances, it aligns with other dimension definitions, such as the Hausdorff dimension, justifying its classification as a dimension. A rigorous approach and further details will be provided in section 5.2.

4.3 Hausdorff Dimension

This section delves into the exploration of Hausdorff dimension, a widely adopted and crucial concept in fractal geometry. Regarded as the most general and powerful notion of fractal dimension [20], Hausdorff dimension holds the advantage of being applicable to any set and is mathematically convenient due to its reliance on measure theory, specifically through the utilization of the outer Hausdorff measure, resulting in a well-defined and well-behaved fractal dimension concept. However, the determination of a fractal's Hausdorff dimension poses a greater complexity compared to dimensions like box-counting or similarity dimension.

The introduction of measures using covers of sets was initially proposed by Carathéodory in 1914 [9], with Hausdorff adopting this method in 1919 [24], leading to the formulation of the measure that now bears his name. Ongoing developments in the properties of Hausdorff measures, notably by Besicovitch [see for example 4], have contributed to the occasional reference to the Hausdorff dimension as the Besicovitch-Hausdorff dimension.

Following the introduction of the measure and the primary definitions, this section further explores essential properties and examples of Hausdorff dimension. The main source for this section is [20, chap. 2].

The Hausdorff measure

Assume that $F \subset \mathbb{R}^n$ and $s \geq 0$ a real number. For any $\delta > 0$ we define

$$\mathcal{H}^s_\delta(F) = \inf \left\{ \sum_{i=1}^{\infty} |U_i|^s : \{U_i\} \text{ is a } \delta\text{-cover of } F \right\} \tag{4.2}$$

We examine all covers of the set F, considering sets with a diameter no larger than δ. The objective is to minimize the sum of the s-th powers of these diameters. As the value of δ decreases, the range of allowable covers for F diminishes. Consequently, the infimum $\mathcal{H}^s_\delta(F)$ increases, approaching a limit as δ approaches zero. This limit exists for any subset F of $\mathbb{R}^n$, though the limiting value can be ∞.

Definition 36 (Hausdorff s-dimensional outer measure, [20, p. 27])**.** *We define the s-dimension Hausdorff outer measure by*

$$\mathcal{H}^s(F) = \lim_{\delta \to 0} \mathcal{H}^s_\delta(F) \tag{4.3}$$

Proposition 20 ([20, Exercise 2.3])**.** *$\mathcal{H}^s(F)$ is an outer measure on $\mathbb{R}^n$.*

Proof. 1. For each $0 < \epsilon \leq \delta$, we can cover the empty set with a single set of diameter ϵ, so $0 \leq \mathcal{H}^s_\delta(\emptyset) \leq \epsilon^s$ for all $\epsilon > 0$, so that $\mathcal{H}^s_\delta(\emptyset) = 0$. Therefore $\mathcal{H}^s(\emptyset) = \lim_{\delta \to 0} \mathcal{H}^s_\delta(\emptyset) = 0$.

2. If $E \subset F$, every δ-cover of F is also a δ-cover of E, then taking the infimum over all δ-covers gives $\mathcal{H}^s_\delta(E) \leq \mathcal{H}^s_\delta(F)$ for all $\delta > 0$. By letting $\delta \to 0$ we get $\mathcal{H}^s(E) \leq \mathcal{H}^s(F)$.

3. Let $F_1, F_2, \ldots$ be a countable sequence of subsets of $\mathbb{R}^n$. Without loss of generality, we may assume that $\sum_{i=1}^{\infty} \mathcal{H}^s_\delta(F_i) < \infty$. For $\epsilon > 0$ let $\{U_{i,j} : j = 1, 2, \ldots\}$ be a δ-cover of F_i such that $\sum_{j=1}^{\infty} |U_{i,j}|^s \leq \mathcal{H}^s_\delta(F_i) + 2^{-i}\epsilon$. Then $\{U_{i,j} : i = 1, 2, \ldots, j = 1, 2, \ldots\}$ is a δ-cover of $\bigcup_{i=1}^{\infty} F_i$ and

$$\begin{aligned}\mathcal{H}^s_\delta\left(\bigcup_{i=1}^{\infty} F_i\right) &\leq \sum_{i=1}^{\infty}\sum_{j=1}^{\infty} |U_{i,j}|^s \leq \sum_{i=1}^{\infty}\left(\mathcal{H}^s_\delta(F_i) + \frac{\epsilon}{2^i}\right) = \epsilon + \sum_{i=1}^{\infty}\mathcal{H}^s_\delta(F_i) \\ &\leq \epsilon + \sum_{i=1}^{\infty}\mathcal{H}^s(F_i)\end{aligned}$$

Since this is true for every $\epsilon > 0$, it follows that

$$\mathcal{H}^s\left(\bigcup_{i=1}^{\infty} F_i\right) = \lim_{\delta\to 0}\mathcal{H}^s_\delta\left(\bigcup_{i=1}^{\infty} F_i\right) \leq \sum_{i=1}^{\infty}\mathcal{H}^s(F_i)$$

as required.

□

Proposition 21 ([18])**.** *$\mathcal{H}^s(F)$ is a metric outer measure on $\mathbb{R}^n$.*

Proof. One inequality is already given from the subadditivity property. To show the opposite inequality, take $\delta > 0$ with $\delta < d(A, B)$, where A and B are positively separated. For any δ-cover $\{U_i\}$ of $A \cup B$, define $U'_i = A \cap U_i$ and $U''_i = B \cap U_i$. Then clearly $\{U'_i\}_i$ and $\{U''_i\}_i$ are disjoint covers of A and B, respectively. We deduce the following inequality:

$$\sum_{i=1}^{\infty}|U'_i|^s + \sum_{j=1}^{\infty}\left|U''_j\right|^s \leq \sum_{k=1}^{\infty}|U_k|^s.$$

Taking the infimum over the covers in the equality above gives

$$\mathcal{H}^s_\delta(A) + \mathcal{H}^s_\delta(B) \leq \mathcal{H}^s_\delta(A \cup B).$$

Letting $\delta \to 0$ yields the inequality. □

Definition 37 (Hausdorff s-dimensional measure)**.** *The restriction of $\mathcal{H}^s$ to the σ-algebra of $\mathcal{H}^s$-measurable sets, which by Theorem 4 includes the Borel sets gives a measure (Thm. 3) that is called Hausdorff s-dimensional measure.*

Proposition 22 ([18, Thm. 1.6.a])**.** *$\mathcal{H}^s(F)$ is a regular outer measure on $\mathbb{R}^n$.*

Proof. Let E be any subset of $\mathbb{R}^n$. We have to show that there exists a $\mathcal{H}^s$-measurable set G containing E with $\mathcal{H}^s(G) = \mathcal{H}^s(E)$.

If $\mathcal{H}^s(E) = \infty$, then $\mathbb{R}^n$ is an open set of equal measure, so suppose that $\mathcal{H}^s(E) < \infty$.

For each $i = 1, 2 \ldots$ choose an open $2/i$-cover of E, $\{U_{ij}\}_j$, such that

$$\sum_{j=1}^{\infty} |U_{ij}|^s < \mathcal{H}^s_{1/i}(E) + 1/i$$

Then $E \subset G$, where $G = \bigcap_{i=1}^{\infty} \bigcup_{j=1}^{\infty} U_{ij}$ is by construction a Borel set. Since $\{U_{ij}\}_j$ is a $2/i$ cover of $G, \mathcal{H}^s_{2/i}(G) \leq \mathcal{H}^s_{1/i}(E) + 1/i$, and it follows on letting $i \to \infty$ that $\mathcal{H}^s(E) = \mathcal{H}^s(G)$. Since G is $\mathcal{H}^s$-measurable by Theorem 4, $\mathcal{H}^s$ is a regular outer measure. □

Example 20 ([20, Exercise 2.4])**.** *Let $F = [0, 1]$. Then $\mathcal{H}^s(F) = \infty$ if $0 \leq s < 1$, $\mathcal{H}^s(F) = 0$ if $s > 1$, and $0 < \mathcal{H}^1(F) < \infty$.*

Proof. First we observe that when computing $\mathcal{H}^s_\delta([0, 1])$, it suffices to examine coverings comprised of intervals.

Let first $0 \leq s < 1$ and consider $\{U_i\}$ a δ-cover of $[0, 1]$ given by intervals. Then

$$1 \leq \sum_i |U_i| = \sum_i |U_i|^{1-s} |U_i|^s \leq \delta^{1-s} \sum_i |U_i|^s .$$

By taking the infimum we get $\mathcal{H}^s_\delta([0, 1]) \geq \delta^{s-1}$, and by letting $\delta \to 0$ we conclude $\mathcal{H}^s([0, 1]) = \infty$.

Let now $s > 1$, we may cover $[0, 1]$ by at most $(1 + 1/\delta)$ intervals of length δ, then

$$\mathcal{H}^s_\delta([0, 1]) \leq (1 + 1/\delta)\delta^s$$

by taking the limit $\delta \to 0$, we conclude $\mathcal{H}^s([0, 1]) = 0$.

Consider finally the case $s = 1$. If $\{U_i\}$ is a δ-cover of [0,1] by intervals, then

$$1 \leq \sum_i |U_i| \text{ thus } \mathcal{H}^1_\delta([0, 1]) \geq 1$$

By taking the limit $\delta \to 0$ we get $\mathcal{H}^1([0, 1]) \geq 1$.

By taking a cover $[0, 1]$ of at most $(1 + 1/\delta)$ intervals of length δ,

$$\mathcal{H}^1_\delta([0, 1]) \leq (1 + 1/\delta)\delta \to 1$$

as $\delta \to 0$, and so $\mathcal{H}^1([0, 1]) \leq 1$. Thus we can conclude that $\mathcal{H}^1([0, 1]) = 1$.

□

We look now at some interesting properties of Hausdorff measure and how it is related to the Lebesgue measure.

Proposition 23 (scaling property, [20, p. 29])**.** *Let S be a similarity transformation of scale factor $\lambda > 0$ (see Def. 16). If $F \subset \mathbb{R}^n$, then*

$$\mathcal{H}^s(S(F)) = \lambda^s \mathcal{H}^s(F).$$

Proof. If $\{U_i\}$ is a δ-cover of F then $\{S(U_i)\}$ is a $\lambda\delta$-cover of $S(F)$, so

$$\Sigma |S(U_i)|^s = \lambda^s \Sigma |U_i|^s$$

therefore

$$\mathcal{H}^s_{\lambda\delta}(S(F)) \leq \lambda^s \mathcal{H}^s_\delta(F)$$

by taking the infimum. Letting $\delta \to 0$ gives that $\mathcal{H}^s(S(F)) \leq \lambda^s \mathcal{H}^s(F)$. To get the reverse inequality we replace S by the inverse function S^{-1}, so we get $1/\lambda$ instead of λ and $S(F)$ instead of F. □

Proposition 24 ([20, Prop. 2.2])**.** *Let $F \subset \mathbb{R}^n$ and $f : F \to \mathbb{R}^m$ be a Hölder function (see Def. 21) with constants $c > 0$ and $\alpha > 0$. Then for each $s > 0$*

$$\mathcal{H}^{s/\alpha}(f(F)) \leq c^{s/\alpha} \mathcal{H}^s(F).$$

Proof. If $\{U_i\}$ is a δ-cover of F, then, as $|f(F \cap U_i)| \leq c\,|F \cap U_i|^\alpha \leq c\,|U_i|^\alpha$, it follows that $\{f(F \cap U_i)\}$ is an ε-cover of $f(F)$, where $\varepsilon = c\delta^\alpha$. Therefore $\sum_i |f(F \cap U_i)|^{s/\alpha} \leq c^{s/\alpha} \sum_i |U_i|^s$, and then $\mathcal{H}^{s/\alpha}_\varepsilon(f(F)) \leq c^{s/\alpha} \mathcal{H}^s_\delta(F)$. As $\delta \to 0$, $\varepsilon \to 0$, and we get the required result. □

Remark 5. *From the previous proposition, if we take $\alpha = 1$, then f is called a Lipschitz mapping (see Def. 22), and*

$$\mathcal{H}^s(f(F)) \leq c^s \mathcal{H}^s(F).$$

Remark 6. *From Proposition 23, if we take $\lambda = 1$, then f is called an isometry (see Def. 17), and*

$$\mathcal{H}^s(f(F)) = \mathcal{H}^s(F).$$

Therefore, Hausdorff measures are translation invariant, i.e. $\mathcal{H}^s(F + y) = \mathcal{H}^s(F)$, where $F + y = \{x + y : x \in F\}$ and rotation invariant.

Proposition 25. *If F is a countable or finite set, then $\mathcal{H}^s(F) = 0$ for all $s > 0$.*

Proof. It follows directly from the definition of Hausdorff s-dimensional measure. □

Proposition 26 ([15, Exercise 2.2])**.** *Given $F \subset \mathbb{R}^n$, $\mathcal{H}^0(F)$ is a counting measure. So $\mathcal{H}^0(F) = \#F$ if F is finite and $\mathcal{H}^0(F) = \infty$ if F is infinite.*

Proof. Assume that $\{U_i\}$ is a δ-cover of F. Then for any set U_i in the cover we have $|U_i|^0 = 1$ and therefore $\sum_i |U_i|^0$ is equal to the number of sets in the cover, so that $\mathcal{H}^0_\delta(F)$ is the smallest number of sets that form a δ-cover of F.

Assume now that F has n points, $x_1, x_2, \ldots, x_n$, then the n balls of radius $\delta/2$ with centers at $x_1, x_2, \ldots, x_n$ form a δ-cover of F and so $\mathcal{H}^0_\delta(F) \leq n$. Also, if $\delta > 0$ is so small so that $|x_i - x_j| > \delta$ for every $i \neq j$, then any δ-cover of F must contain at least n sets and so $\mathcal{H}^0_\delta(F) \geq n$. To conclude, for δ small enough, we have $\mathcal{H}^0_\delta(F) = n$ and hence $\mathcal{H}^0(F) = \lim_{\delta \to 0} \mathcal{H}^0_\delta(F) = n$.

Assume now that F has infinitely many points, then for each positive integer n, we can take a set $F_n \subset F$ such that F_n has n points. Therefore $\mathcal{H}^0(F) \geq \mathcal{H}^0(F_n) = n$ for all n, so $\mathcal{H}^0(F) = \infty$. □

Hausdorff measures extend the conventional concepts of length, area, volume, and so on. It can be demonstrated that, when considering subsets of $\mathbb{R}^n$, the n-dimensional Hausdorff measure is essentially proportional to the n-dimensional Lebesgue measure, which corresponds to the standard n-dimensional volume.

Theorem 5 ([17, Thm 2.2])**.** *Let $A \subset \mathbb{R}$, then $\mathcal{H}^1(A) = \mathcal{L}^1(A)$*

Proof. Take $A \subset \mathbb{R}$ and consider $\delta > 0$.

$$\begin{aligned}
\mathcal{L}^1(A) &= \inf\left\{\sum_{i=1}^{\infty}(|U_i|) \mid A \subset \bigcup_{i=1}^{\infty} U_i\right\} \\
&\leq \inf\left\{\sum_{i=1}^{\infty}(|U_i|) \mid \{U_i\}_{i=1}^{\infty} \text{ is a } \delta\text{-covering of } A\right\} \\
&= \mathcal{H}^1_\delta(A).
\end{aligned}$$

Let now $I_k = [k\delta, (k+1)\delta], k \in \mathbb{Z}$. We note that that $(|U_i \cap I_k|) \leq |U_i| \leq \delta$ Therefore $\{U_i \cap I_k\}_{i,k}$ is a δ-covering of A and

$$|U_i| = \left(|\bigcup_{k\in\mathbb{Z}}(U_i \cap I_k)|\right) \geq \sum_{k\in\mathbb{Z}} |(U_i \cap I_j)|$$

Hence

$$\begin{aligned}
\mathcal{L}^1(A) &= \inf\left\{\sum_{i=1}^{\infty}(|U_i|) \mid A \subset \bigcup_{i=1}^{\infty} U_i\right\} \\
&\geq \inf\left\{\sum_{i=1}^{\infty}\sum_{k\in\mathbb{Z}}(|U_i \cap I_k|) \mid A \subset \bigcup_{i=1}^{\infty} U_i\right\} \\
&\geq \mathcal{H}^1_\delta(A)
\end{aligned}$$

The last inequality comes from the fact that $\{U_i \cap I_k\}_{i,k}$ is a δ-covering of A. We have $\mathcal{H}^1_\delta = \mathcal{L}^1$ and by letting $\delta \to 0$ we conclude the proof as $\mathcal{H}^1 = \mathcal{L}^1$. □

Theorem 6 ([42, Thm. 30])**.** *Let $A \subset \mathbb{R}^n$, then $\mathcal{L}^n(A) = \alpha(n) \cdot \mathcal{H}^n(A)$, where $\alpha(n) = \frac{\pi^{n/2}}{2^n \Gamma(n/2+1)}$ and $\Gamma(z) = \int_0^\infty t^{z-1} e^{-t}\, dt$ is the usual Gamma function.*

Proof. Omitted. See [42, Thm. 30]. □

So for example if F is a smooth curve $\mathcal{H}^1(F)$ gives the length of F (already seen from previous Theorem for the case n=1), $\mathcal{H}^2(F) = (4/\pi) \cdot \text{area}(F)$ when F is a smooth surface, $\mathcal{H}^3(F) = (6/\pi) \cdot \text{vol}(F)$; and $\mathcal{H}^m(F) = \alpha(n)^{-1} \cdot \text{vol}^m(F)$ when F is a smooth m-dimensional submanifold of $\mathbb{R}^n$.

Remark 7. *Certain authors adjust the definition of Hausdorff measure by scaling the value $\mathcal{H}^n$ by the factor $\alpha(n)$, to align the n-dimensional Hausdorff measure exactly with the n-dimensional Lebesgue measure in Euclidean space [see for example 17, Thm. 2.2].*

Example 21 (Pythagorean Theorem, [3, p. 97])**.** *It's easy to see that a right triangle T in $\mathbb{R}^2$ comprises two smaller copies of itself (refer to Figure 4.8). Clearly, both transformations are similarities. The scaling factors are b/c and a/c. Hence, the Hausdorff measure of T, is given by $\mathcal{H}^2(T) = (b/c)^2\mathcal{H}^2(T) + (a/c)^2\mathcal{H}^2(T)$, utilizing the σ-additivity and the scaling property (Proposition 23). Multiplying both sides by c^2 and dividing by $\mathcal{H}^2(T)$ (noting that $0 < \mathcal{H}^2(T) < \infty$ since the area $\mathcal{L}^2(T)$ is finite and non-zero) yields the well-known equation:*

$$a^2 + b^2 = c^2.$$

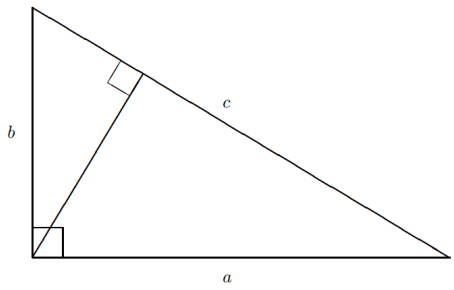

Figure 4.8: A right triangle comprises two smaller copies of itself.

The Hausdorff dimension

Theorem 7 ([15, Thm 6.1.6]). *Let $F \subset \mathbb{R}^n$. Let $0 < s < t$. If $\mathcal{H}^s(F) < \infty$, then $\mathcal{H}^t(F) = 0$. If $\mathcal{H}^t(F) > 0$, then $\mathcal{H}^s(F) = \infty$.*

Proof. From equation (4.2) for every set $F \subset \mathbb{R}^n$ and $\delta < 1$, $\mathcal{H}^s_\delta(F)$ is non-increasing with s, so by equation (4.3) $\mathcal{H}^s(F)$ is also non-increasing. More generally, if $t > s$ and $\{U_i\}$ is a δ-cover of F we have

$$\sum_i |U_i|^t \leq \sum_i |U_i|^{t-s} |U_i|^s \leq \delta^{t-s} \sum_i |U_i|^s$$

Then taking the infimum, we have $\mathcal{H}^t_\delta(F) \leq \delta^{t-s}\mathcal{H}^s_\delta(F)$. Letting $\delta \to 0$ we see that if $\mathcal{H}^s(F) < \infty$ then $\mathcal{H}^t(F) = 0$ for $t > s$. The second assertion is the contrapositive. □

The interpretation of this Theorem is that there exists a critical value s at which $\mathcal{H}^s(F)$ jumps from $+\infty$ to 0. This value is called the Hausdorff dimension of F and denoted by $\dim_{\mathrm{H}}(F)$.

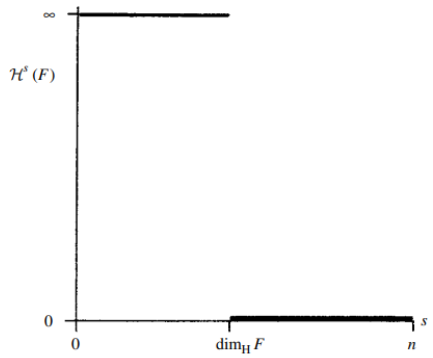

Figure 4.9: The plot of $\mathcal{H}^s(F)$ against s for a given set F.
Source: [20, p. 31]

Definition 38 (Hausdorff dimension, [20, p. 31]). *The Hausdorff dimension of a set $F \subset \mathbb{R}^n$ is defined as*

$$\dim_{\mathrm{H}} F = \inf\{s \geq 0 : \mathcal{H}^s(F) = 0\} = \sup\{s : \mathcal{H}^s(F) = \infty\}$$

The above definition can also be written as

$$\mathcal{H}^s(F) = \begin{cases} \infty & \text{if } 0 \leq s < \dim_{\mathrm{H}} F \\ 0 & \text{if } s > \dim_{\mathrm{H}} F \end{cases}$$

We observe that the definition does not involve the actual value of $\mathcal{H}^s(F)$ when $s = \dim_{\mathrm{H}} F$. In fact in that case $\mathcal{H}^s(F)$ can possibly take on the value 0, ∞ or any non-zero finite value.

Definition 39 (s-set)**.** *A set $F \subset \mathbb{R}^n$ such that $s = \dim_{\mathrm{H}} F$ and $0 < \mathcal{H}^s(F) < \infty$ is called an s-set.*

Remark 8. *The Hausdorff dimension of a set F is not necessarily an integer number, we will see later some examples.*

Remark 9. *From Theorem 7 we have that $\dim_{\mathrm{H}} F$ is well defined and if $0 < \mathcal{H}^s(F) < \infty$ then $s = \dim_{\mathrm{H}} F$. Thus s-sets have Hausdorff dimension s. The other implication may be false, for example $\dim_{\mathrm{H}}(\mathbb{R}^n) = n$ (see Prop. 32) but $\mathcal{H}^n(\mathbb{R}^n) = \alpha(n)^{-1} \cdot \mathcal{L}^n(\mathbb{R}^n) = \infty$.*

Intuitively we can think about Hausdorff dimension in the following way: when measuring objects, such as lengths of lines, areas of squares, or volumes of cubes, the concept of dimension enhances our understanding. We can place an endless number of points on a line, but the area of that line is essentially zero. A square can accommodate countless lines or a very long curve, yet its volume remains zero. Although a cube has an infinite area, capable of accommodating many planes or a curvy surface with infinite area, it still possesses a finite volume. If we use a dimension that's too low for measuring something, it may appear as if there's an endless amount of it. On the flip side, if we use a dimension that's too big, it may seem as if there's nothing there. The Hausdorff dimension offers a more flexible approach to comprehending the size and complexity of sets, especially when they don't neatly fit into regular geometric categories.

Example 22. *Let F be the unit flat disk in the xy-plane in $\mathbb{R}^3$.*

$$F = \left\{(x, y, z) \in \mathbb{R}^3 \mid x^2 + y^2 \leq 1 \text{ and } z = 0\right\}$$

Then $\mathcal{H}^1(F) = \mathcal{L}^1(F) = \infty$ as F can be covered by infinitely many lines. By Theorem 6, $\mathcal{H}^2(F) = \frac{4}{\pi} \cdot$ Area $(F) = \frac{4}{\pi} \cdot \pi = 4$ and $\mathcal{H}^3(F) = \frac{6}{\pi} \cdot \mathrm{vol}(F) = \frac{6}{\pi} \cdot 0 = 0$. By Theorem 7, we get

$$\mathcal{H}^s(F) = \begin{cases} \infty & \text{if } s < 2 \\ 4 & \text{if } s = 2 \\ 0 & \text{if } s > 2 \end{cases}$$

Therefore $\dim_{\mathrm{H}}(F) = 2$.

The Hausdorff dimension and the topological dimension (see section 4.1) are related through the following proposition:

Proposition 27 ([15, Thm. 6.3.10])**.** *Let $F \subset \mathbb{R}^n$. Then* $\dim F \leq \dim_{\mathrm{H}} F$

Proof. Omitted. See [14, section 3.1]. □

The Hausdorff dimension $\dim_{\mathrm{H}} F$, fulfills the proprieties for dimensions outlined in the beginning of the section. Most of them are a straightforward consequence of the definition of Hausdorff measure.

Proposition 28. *Let $E \subset A \subset \mathbb{R}^n$, then $\dim_{\mathrm{H}} E \leq \dim_{\mathrm{H}} A$.*

Proof. This is a consequence of the monotonicity of the Hausdorff measure. In particular $\mathcal{H}^s(E) \leq \mathcal{H}^s(A)$ for each s. □

Example 23 ([15, Prop. 6.3.5])**.** $\dim_{\mathrm{H}} \mathbb{R}^2 = 2$.

Proof. Consider the half-open unit square $Q = [0,1) \times [0,1)$. It is covered by n^2 small squares with side $1/n$, so if $\delta \geq \sqrt{2}/n$, we have $\mathcal{H}^2_\delta(Q) \leq n^2(\sqrt{2}/n)^2 = 2$. Hence $\mathcal{H}^2(Q) \leq 2$, thus $\dim_{\mathrm{H}} Q \leq 2$.

Conversely, if $\mathcal{A}$ is any cover of Q by closed sets, then, since any set A of diameter r is contained in a closed square Q_A with side $\leq r$,

$$\begin{aligned}\sum_{A\in\mathcal{A}} (|A|)^2 &\geq \sum_{A\in\mathcal{A}} \mathcal{L}^2\left(Q_A\right) \\ &\geq \mathcal{L}^2\left(\bigcup_{A\in\mathcal{A}} Q_A\right) \\ &\geq \mathcal{L}^2(Q) = 1.\end{aligned}$$

Thus $\mathcal{H}^2(Q) \geq 1$, so $\dim_{\mathrm{H}} Q \geq 2$. For $\mathbb{R}^2$, since $Q \subseteq \mathbb{R}^2$, by Prop. 28 we have $\dim_{\mathrm{H}} \mathbb{R}^2 \geq \dim_{\mathrm{H}} Q = 2$ (note that this inequality can be directly deduced from Theorem 6). If $s > 2$, then $\mathcal{H}^s(Q) = 0$ (by Thm. 7); but $\mathbb{R}^2$ can be covered by a countable collection $\{Q_n : n \in \mathbb{N}\}$ of squares of side 1 , so $\mathcal{H}^s\left(\mathbb{R}^2\right) \leq \sum_n \mathcal{H}^s\left(Q_n\right) = 0$. This proves that $\dim_{\mathrm{H}} \mathbb{R}^2 \leq s$. Hence $\dim_{\mathrm{H}} \mathbb{R}^2 \leq 2$. □

Proposition 29. *If E_1, E_2, ... is a countable sequence of sets then*

$$\dim_{\mathrm{H}}\left(\bigcup_{i=1}^{\infty} E_i\right) = \sup_i \left\{\dim_{\mathrm{H}} E_i\right\}.$$

Proof. From the monotonicity property we have for each j,

$$\dim_{\mathrm{H}}\left(\bigcup_{i=1}^{\infty} E_i\right) \geq \dim_{\mathrm{H}} E_j$$

and by taking supremum over all j,

$$\dim_{\mathrm{H}}\left(\bigcup_{i=1}^{\infty} E_i\right) \geq \sup_i \left\{\dim_{\mathrm{H}} E_i\right\}.$$

For the opposite inequality we note that if $s > \dim_{\mathrm{H}} E_i$ for all i, then $\mathcal{H}^s(E_i) = 0$ for all i, which gives $\mathcal{H}^s\left(\bigcup_{i=1}^{\infty} E_i\right) = 0$ so

$$\dim_{\mathrm{H}}\left(\bigcup_{i=1}^{\infty} E_i\right) \leq s.$$

□

Proposition 30. *If E is finite or countable, then $\dim_{\mathrm{H}} E = 0$.*

Proof. It follows directly from Proposition 25. Another way of proving the proposition is noticing that for a singleton E_i we have

$$\mathcal{H}^0(E_i) = 1$$

and so $\dim_{\mathrm{H}} E_i = 0$ and conclude by countable stability (Proposition 29). □

Example 24. *Consider the set $F = \left\{0, 1, \frac{1}{2}, \frac{1}{3}, \frac{1}{4}, \ldots\right\}$. Then $\dim_{\mathrm{H}} F = 0$ since F is a countable set.*

Proposition 31. *Let $F \subset \mathbb{R}^n$, then $\dim_{\mathrm{H}} F \leq n$.*

Proof. We check that $\mathcal{H}^{n+s}(A) = 0$ for all $s > 0$ and then we conclude by applying the definition of Hausdorff dimension.

$$\mathcal{H}^{n+s}(A) = \mathcal{H}^{n+s}\left(\bigcup_{k=1}^{\infty} A \cap B_k(0)\right) \leq \sum_{k=1}^{\infty} \mathcal{H}^{n+s}\left(A \cap B_k(0)\right)$$

where $B_k(0)$ denotes a ball of radius k centered in 0. At the same time we have

$$\mathcal{H}^n\left(A \cap B_k(0)\right) \leq \mathcal{H}^n\left(B_k(0)\right) = \alpha(n)^{-1} \cdot \mathcal{L}^n\left(B_k(0)\right) < \infty.$$

By Theorem 7 we conclude that $\mathcal{H}^{n+s}\left(A \cap B_k(0)\right) = 0$ for all k. Finally,

$$\mathcal{H}^{n+s}(A) \leq \sum_{k=1}^{\infty} \mathcal{H}^{n+s}\left(A \cap B_k(0)\right) = \sum_{k=1}^{\infty} 0 = 0.$$

□

Proposition 32. *If $F \subset \mathbb{R}^n$ is an open set, then $\dim_{\mathrm{H}} F = n$.*

Proof. If F is an open set, then it contains a ball of positive volume, say B, and therefore

$$\mathcal{H}^n(F) \geq \mathcal{H}^n(B) = \alpha(n)^{-1} \cdot \mathcal{L}^n(B) > 0$$

and $\dim_{\mathrm{H}} F \geq n$. To get the opposite inequality, we use Proposition 31. □

Proposition 33 ([20, p. 32])**.** *If* E *is a smooth, m-dimensional submanifold of $\mathbb{R}^n$, then $\dim_{\mathrm{H}} E = m$.*

Proof. The conclusion can be inferred by examining the connection between Hausdorff and Lebesgue measures. The detailed proof is not provided here, but additional information can be found in reference [20, p. 32]. □

Corollary 1. *Let $F \subset \mathbb{R}^n$ and assume that $f : F \to \mathbb{R}^n$ is a similarity function (see Def. 16). Then*

$$\dim_{\mathrm{H}} f(F) = \dim_{\mathrm{H}} F.$$

Proof. From Proposition 23, we have

$$\mathcal{H}^s(f(F)) = \lambda^s \mathcal{H}^s(F).$$

and thus $\dim_{\mathrm{H}} f(F) = \dim_{\mathrm{H}} F$. □

Proposition 34 ([20, Prop. 2.3])**.** *Let $F \subset \mathbb{R}^n$ and assume that $f : F \to \mathbb{R}^m$ satisfies the Hölder condition of exponent α (see Def. 21).*

Then

$$\dim_{\mathrm{H}} f(F) \leq \frac{1}{\alpha} \dim_{\mathrm{H}} F.$$

Proof. By Proposition 24 we have

$$\mathcal{H}^{s/\alpha}(f(F)) \leq c^{s/\alpha} \mathcal{H}^s(F).$$

We know that if $s > \dim_{\mathrm{H}} F$ then $\mathcal{H}^s(F) = 0$.

Therefore $\mathcal{H}^{s/\alpha}(f(F)) = 0$, which implies that $\dim_{\mathrm{H}} f(F) \leq s/\alpha$ for every $s > \dim_{\mathrm{H}} F$. By letting $s \to \dim_{\mathrm{H}}(F)$ we obtain the desired inequality. □

Corollary 2 ([20, Cor. 2.4.a])**.** *Let $F \subset \mathbb{R}^n$ and assume that $f : F \to \mathbb{R}^m$ is a Lipschitz function (see Def. 22). Then*

$$\dim_{\mathrm{H}} f(F) \leq \dim_{\mathrm{H}} F.$$

Proof. The inequality follows by Proposition 34, by taking $\alpha = 1$. □

Corollary 3 ([20, Cor. 2.4.b])**.** *Let $F \subset \mathbb{R}^n$ and assume that $f : F \to \mathbb{R}^m$ is a bi-Lipschitz function (see Def. 22). Then*

$$\dim_{\mathrm{H}} f(F) = \dim_{\mathrm{H}} F.$$

Proof. One inequality is already given by the previous corollary. By Proposition 2 we know that f^{-1} is Lipschitz, therefore by previous corollary

$$\dim_{\mathrm{H}} F = \dim_{\mathrm{H}} f^{-1}(f(F)) \leq \dim_{\mathrm{H}} f(F).$$

□

Proposition 35 ([20, Exercise 2.5])**.** *Let $f : \mathbb{R} \to \mathbb{R}$ be a differentiable function with continuous derivative. Assume $F \subset \mathbb{R}$, then* $\dim_{\mathrm{H}} f(F) \leq \dim_{\mathrm{H}} F$.

Proof. Assume first that F is bounded, so that $F \subset [-m, m]$. By Mean value Theorem, there exists some $z \in [-m, m]$ such that

$$|f(x) - f(y)| = |f'(z)|\,|x - y| \leq \left(\sup_{z \in [-m,m]} |f'(z)| \right) |x - y|$$

By the continuity of $f'(z)$ it follows that $f'(z)$ is bounded on the compact set $[-m, m]$. So f is Lipschitz on F, and by Corollary 2 $\dim_{\mathrm{H}} f(F) \leq \dim_{\mathrm{H}}(F)$.

For a general $F \subset \mathbb{R}$, $f(F) = \bigcup_{m=1}^{\infty} f(F_n \cap [-m, m])$, so by Proposition 29

$$\begin{aligned} \dim_{\mathrm{H}} f(F) &= \sup_m \dim_{\mathrm{H}} f(F_n \cap [-m, m]) \leq \sup_m \dim_{\mathrm{H}} (F_n \cap [-m, m]) \\ &\leq \dim_{\mathrm{H}} F, \end{aligned}$$

by the bounded case. □

Example 25 ([20, Exercise 2.6])**.** *Let $f : \mathbb{R} \to \mathbb{R}$ be the function $f(x) = x^2$. Then $\dim_{\mathrm{H}} f(F) = \dim_{\mathrm{H}}(F)$ for every $F \subset \mathbb{R}$.*

Proof. Define $F_k = F \cap [1/k, k]$. Then if $x, y \in F_k$,

$$|f(x) - f(y)| = \left|x^2 - y^2\right| = |x - y||x + y|$$

and thus

$$\frac{2}{k}|x - y| \leq |f(x) - f(y)| \leq 2k|x - y|.$$

Therefore f is bi-Lipschitz on F_k and thus, by Corollary 3, $\dim_{\mathrm{H}} f(F_k) = \dim_{\mathrm{H}} F_k$. In the same way, if $G_k = F \cap [-k, -1/k]$, then $\dim_{\mathrm{H}} f(G_k) = \dim_{\mathrm{H}} G_k$.

Moreover, $F = (F \cap \{0\}) \cup \bigcup_{k=1}^{\infty} (F_k \cup G_k)$ and $f(F) = f(F \cap \{0\}) \cup \bigcup_{k=1}^{\infty} (f(F_k) \cup f(G_k))$. Since $F \cap \{0\}$ and $f(F \cap \{0\})$ contain at most one point, they both must have zero dimension. Then, by countable stability (see Proposition 29),

$$\begin{aligned} \dim_{\mathrm{H}} F &= \sup \{\dim_{\mathrm{H}} F_k, \dim_{\mathrm{H}} G_k : k = 1, 2, \ldots\} \\ &= \sup \{\dim_{\mathrm{H}} f(F_k), \dim_{\mathrm{H}} f(G_k) : k = 1, 2, \ldots\} = \dim_{\mathrm{H}} f(F). \end{aligned}$$

□

Proposition 36 ([20, Exercise 2.7])**.** *Let $f : [0, 1] \to \mathbb{R}$ be a Lipschitz function. Let $\mathrm{graph} f = \{(x, f(x)) : 0 \leq x \leq 1\}$, then $\dim_{\mathrm{H}} \mathrm{graph} f = 1$.*

Proof. Define $g : [0, 1] \to \mathrm{graph} f$ by $g(x) = (x, f(x))$. We assert that g is bi-Lipschitz. Then

$$|g(x) - g(y)|^2 = |x - y|^2 + |f(x) - f(y)|^2$$

thus

$$|x - y|^2 \leq |g(x) - g(y)|^2 \leq |x - y|^2 + c^2|x - y|^2 = \left(1 + c^2\right)|x - y|^2$$

since $|f(x) - f(y)| \leq c|x - y|$ for some $c > 0$. Consequently g is bi-Lipschitz, therefore by Corollary 3, $1 = \dim_{\mathrm{H}}([0, 1]) = \dim_{\mathrm{H}} g([0, 1]) = \dim_{\mathrm{H}} \mathrm{graph} f$. □

Remark 10. *Corollary 3 reveals that Hausdorff dimension remains unchanged under bi-Lipschitz transformations, implying that sets with different dimensions lack a bi-Lipschitz mapping between them. This concept in fractal geometry parallels topological invariants distinguishing non-homeomorphic sets. While Hausdorff dimension alone may not reveal much about a set's topology, it proves useful in differentiating between sets and asserting the impossibility of specific dimensions through bi-Lipschitz invariance. The next proposition discussed highlights an exception where Hausdorff dimension offers insights into the topological structure.*

Before the next proposition, we have to state the following lemma.

Lemma 3. *Let $C \subset \mathbb{R}$ with $\mathcal{L}^1(C) = 0$. Then $[0,1]\backslash C$ is dense in $[0,1]$.*

Proof. By contraposition, if $[0,1]\backslash C$ is not dense in $[0,1]$, then we could find a non-empty open subset of $[0,1]$ that is disjoint from $[0,1]\backslash C$. Simultaneously, this implies that the open subset is a subset of C. Since any non-empty open subset of $[0,1]$ does not have measure zero, it follows that C does not have measure zero. □

Proposition 37 ([20, Prop. 2.5])**.** *Let $F \subset \mathbb{R}^n$ with $\dim_{\mathrm{H}} F < 1$, then F is totally disconnected.*

Proof. Let $x, y \in F$ be any two different points. Define the map

$$\begin{aligned} f : \mathbb{R}^n &\to [0, +\infty) \\ z &\mapsto f(z) = |z - x| \end{aligned}$$

By the reverse triangular inequality we have that $|f(z) - f(w)| \leq |z - w|$. So in particular f is a Lipschitz mapping with Lipschitz constant 1 and from Corollary 2 we deduce that $\dim_{\mathrm{H}}(f(A)) \leq \dim_{\mathrm{H}}(A) < 1$. and then $f(F) \subset \mathbb{R}$ with $0 = \mathcal{H}^1(f(F)) = \mathcal{L}^1(f(F))$. By the previous Lemma $f(F)$ has a dense complement in $[0,1]$. let now $r \notin f(A)$ and $0 < r < f(y)$. It follows that

$$F = \{z \in F : |z - x| < r\} \cup \{z \in F : |z - x| > r\}.$$

Therefore F is contained in two disjoint open sets with x in the first set and y in the second one, so that x and y lie in different connected components of F. □

The following last theorem estimates the Hausdorff dimension of the graph of a continuous Hölder function (see Definition 21).

Theorem 8 ([55, Thm 1.3])**.** *Let*

$$\mathrm{graph} f = \{(x, f(x)) \mid x \in [a, b]\},$$

denote the graph of a continuous function. Assume f satisfies the Hölder condition with exponent $\alpha \in (0, 1]$ for every $x, y \in [a, b]$. Then $\mathcal{H}^{2-\alpha}(\mathrm{graph} f) < \infty$, and thus $\dim_{\mathrm{H}}(\mathrm{graph} f) \leq 2 - \alpha$.

Proof. The interval $[a, b]$ is divided into k equal parts, denoted as $I_1, I_2, \ldots, I_k$. Each subinterval has a length of $|I_i| = (b-a)/k$. When y is moved within I_i while the left endpoint x of I_i is fixed, it follows that

$$|f(x) - f(y)| \leq c|x-y|^\alpha \leq c\,|I_i|^\alpha = c(b-a)^\alpha k^{-\alpha},$$

Thus, starting at the point $(x, f(x))$, if we stack $[c(b-a)^{\alpha-1}k^{1-\alpha}] + 1$ squares of width $(b-a)/k$ upwards and downwards, the point $(y, f(y))$ will fall within one of them. The squares, considered over the entire interval $[a, b]$, form a δ-covering of graph$f$, where $\delta = \sqrt{2}(b-a)/k$ is the diameter of any square under consideration. Consequently,

$$\begin{aligned}\mathcal{H}_\delta^{2-\alpha}\left(\text{graph}f\right) &\leq 2k\left(\frac{\sqrt{2}(b-a)}{k}\right)^{2-\alpha}\left\{1 + c(b-a)^{\alpha-1}k^{1-\alpha}\right\} \\ &\leq 2(\sqrt{2}(b-a))^{2-\alpha}\left\{1 + c(b-a)^{\alpha-1}\right\},\end{aligned}$$

where the right-hand side is a constant independent of k. Furthermore, we can make δ arbitrarily small, implying that $\mathcal{H}^{2-\alpha}\left(\text{graph}f\right) < \infty$. □

Remark 11 ([20, section 2.4])**.** *There exist alternative types of covering sets that can be utilized to establish measures resulting in Hausdorff dimension. One such example involves employing coverings comprised of spherical balls.*

$$\mathcal{B}_\delta^s(F) = \inf\left\{\Sigma\,|B_i|^s : \{B_i\} \;\; \textit{is a } \delta\textit{-cover of } F \textit{ by balls}\right\}$$

Then $\mathcal{B}^s(F) = \lim_{\delta\to 0}\mathcal{B}_\delta^s(F)$ gives a measure and a dimension given by the jump of $\mathcal{B}^s(F)$ from ∞ to 0.

Proof. $\mathcal{H}_\delta^s(F) \leq \mathcal{B}_\delta^s(F)$ follows by the definition. If the collection $\{U_i\}$ forms a δ-cover of F, then selecting balls $\{B_i\}$ such that each B_i contains U_i with a radius $|U_i| \leq \delta$ results in a 2δ-cover. Consequently, the sum of the sizes of these balls, denoted by $\Sigma\,|B_i|^s$, is bounded by $\Sigma\,(2\,|U_i|)^s = 2^s\Sigma\,|U_i|^s$. Taking the infimum yields $\mathcal{B}_{2\delta}^s(F) \leq 2^s\mathcal{H}_\delta^s(F)$. As δ tends to 0, it implies $\mathcal{H}^s(F) \leq \mathcal{B}^s(F) \leq 2^s\mathcal{H}^s(F)$. Notably, this indicates that the values where $\mathcal{H}^s$ and $\mathcal{B}^s$ transition from ∞ to 0 are identical, ensuring equality in the dimensions defined by both measures. □

Another example involves employing covering comprised of closed sets (see [20, Exercise 2.1]). Define

$$\overline{\mathcal{H}}_\delta^s(F) = \inf\left\{\sum_i |U_i|^s : \{U_i\} \;\; \textit{is a } \delta\textit{-cover of } F \textit{ by closed sets}\right\}.$$

We claim that $\mathcal{H}^s(F) = \overline{\mathcal{H}}^s(F)$. Hence in this case we get the same values not only for the Hausdorff dimension but also for the Hausdorff measure.

Proof. Since we have restricted our attention to covers by closed sets, the class of allowed covers has narrowed, indicating that $\overline{\mathcal{H}}^s_\delta(F) \geq \mathcal{H}^s_\delta(F)$. Let us assume $\{U_i\}$ forms a δ-cover for F. Given that the closure $\bar{U}_i$ of each U_i maintains $\left|\bar{U}_i\right| = |U_i|$, we deduce that $\left\{\bar{U}_i\right\}$ serves as a δ-cover for F using closed sets, with $\sum_i \left|\bar{U}_i\right|^s = \sum_i |U_i|^s$. This holds true for any δ-cover of F, leading to $\overline{\mathcal{H}}^s_\delta(F) \leq \mathcal{H}^s_\delta(F)$. Consequently, $\overline{\mathcal{H}}^s_\delta(F) = \mathcal{H}^s_\delta(F)$ for all $\delta > 0$, ensuring that the value of $\mathcal{H}^s(F) = \lim_{\delta\to 0} \mathcal{H}^s_\delta(F)$ remains unchanged when exclusively considering δ-covers by closed sets. □

Computing the Hausdorff dimension

In this subsection, we provide some examples of fractals, accompanied by their respective Hausdorff dimensions. It is crucial to emphasize that the computation of dimensions often requires both an upper and a lower estimate of the s-dimensional Hausdorff measure, for a given $s > 0$. In this regard, we propose some useful techniques and results to facilitate this purpose. This dual estimation approach facilitates the subsequent application of Remark 9. It becomes evident that determining Hausdorff dimensions, even for seemingly straightforward sets, can be intricate, particularly due to the challenging nature of obtaining the lower estimate. In the upcoming section, we will explore a new dimension definition that generally proves more computationally efficient.

Example 26 ([20, Ex. 2.7])**.** *The Cantor set F (see Figure 3.2) satisfies* $\dim_{\mathrm{H}} F = \frac{\log 2}{\log 3}$.

Proof. First note that from Example 2 we know that the length of F is zero. Thus $\mathcal{L}^1(F) = \mathcal{H}^1(F) = 0$ and therefore $\dim_{\mathrm{H}} F \leq 1$.

We claim that $\frac{1}{2} \leq \mathcal{H}^s(F) \leq 1$ for $s = \frac{\log 2}{\log 3}$.

Recall from Example 2 that the k-level intervals E_k consists of 2^k disjoint intervals each of length 3^{-k}.

To construct an upper bound for F we take the intervals of E_k as a 3^{-k}-cover. Then

$$\mathcal{H}^s_{3^{-k}}(F) \leq 2^k 3^{-ks} = 1 \text{ if } s = \frac{\log 2}{\log 3}$$

Letting $k \to \infty$ gives $\mathcal{H}^s(F) \leq 1$.

To prove the opposite inequality we prove that

$$\sum |U_i|^s \geq \frac{1}{2} = 3^{-s} \tag{4.4}$$

for any cover $\{U_i\}$ of F. We can assume that the $\{U_i\}$ are intervals,

and by expanding them slightly and using the compactness of F (Proposition 7), it is enough to check (4.4) if $\{U_i\}$ is a finite collection of closed subintervals of $[0, 1]$.

For each U_i, we let k be the integer satisfying

$$\frac{1}{3^{k+1}} \leq |U_i| < \frac{1}{3^k}. \tag{4.5}$$

Then U_i can intersect at most one level-k interval (the separation of the intervals at level-k is at least 3^{-k}).

For $j \geq k$, U_i intersects at most $2^{j-k} = 2^j 3^{-sk} \leq 2^j 3^s |U_i|^s$ level- j intervals of E_j, by (4.5).

If we choose j large enough, since $\{U_i\}$ is finite, we can have $3^{-(j+1)} \leq |U_i|$ for all U_i, then, since the $\{U_i\}$ intersect all 2^j intervals of length 3^{-j} we get by counting all intervals $2^j \leq \sum_i 2^j 3^s |U_i|^s$, which proves (4.4). □

The next proposition presents a useful technique that proves helpful when determining a lower estimate of the s-dimensional Hausdorff measure, often needed when computing the Hausdorff dimension. Before stating this result, we need to introduce a new definition.

Definition 40 (mass distribution, [20, p. 60])**.** *A mass distribution μ on $F \subset \mathbb{R}^n$ is a measure with support contained in F such that $0 < \mu(F) < \infty$.*

Proposition 38 (Mass distribution principle, [20, p. 60])**.** *Consider μ be a mass distribution on F and suppose that for some $s > 0$ there are $c > 0$ and $\epsilon > 0$ such that*

$$\mu(U) \leq c|U|^s$$

for any sets U with $|U| \leq \epsilon$. Then $\mathcal{H}^s(F) \geq \frac{\mu(F)}{c}$ and $s \leq \dim_{\mathrm{H}} F$.

Proof. Let $\{U_i\}$ be any cover of F. Then

$$0 < \mu(F) \leq \mu\left(\bigcup_i U_i\right) \leq \sum_i \mu\left(U_i\right) \leq c \sum_i |U_i|^s$$

By taking the infimum, for δ small enough, $\mathcal{H}^s_\delta(F) \geq \mu(F)/c$. By letting $\delta \to 0$ we deduce $\mathcal{H}^s(F) \geq \mu(F)/c$. Finally since $\mu(F) > 0$ we also get $\dim_{\mathrm{H}} F \geq s$. □

Example 27. *Let F be the Cantor set. By the Mass distribution principle $\mathcal{H}^s(F) \geq \frac{1}{2}$ for $s = \frac{\log 2}{\log 3}$.*

Proof. We define μ to be the natural mass distribution on F such that at each level E_k, every interval of length 3^{-k} has mass 2^{-k}. Then $\mu\left(E_0\right) = 1, \mu\left(E_1\right) = \frac{1}{2} + \frac{1}{2} = 1$, and so on. Consider U be a set with $|U| < 1$ and let k be a non-negative integer such that $\frac{1}{3^{(k+1)}} \leq |U| < \frac{1}{3^k}$. Then U can intersect at most one interval of E_k, therefore

$$\mu(U) \leq 2^{-k} = \left(3^{\log_3 2}\right)^{-k} = \left(3^{-k}\right)^{\frac{\log 2}{\log 3}} \leq (3|U|)^{\frac{\log 2}{\log 3}}$$

and

$$(3|U|)^{\frac{\log 2}{\log 3}} = 3^{\frac{\log 2}{\log 3}}|U|^{\frac{\log 2}{\log 3}} = 2|U|^{\frac{\log 2}{\log 3}}.$$

By the Mass distribution principle it follows that

$$\mathcal{H}^s(F) \geq \frac{\mu(F)}{c} = \frac{1}{2} \text{ and } \dim_{\mathrm{H}} F \geq \frac{\log 2}{\log 3}.$$

□

Proposition 39 ([20, Exercise 4.5])**.** *Let F be the Cantor set. Then* $\dim_{\mathrm{H}}(F \times F) = \frac{\log 4}{\log 3}$.

Proof. Consider E'_k, which represents the collection of 2^k intervals each with a length of 3^{-k}, derived at the k-th stage during the conventional construction of the Cantor set. Consequently, $E_k = E'_k \times E'_k$ comprises 4^k squares, each with sides of length 3^{-k} and diameters of $3^{-k}\sqrt{2}$. Furthermore, $F \times F = \bigcap_{k=0}^{\infty} E_k$. Each positive integer k yields 4^k squares in E_k, constituting a $3^{-k}\sqrt{2}$-cover for F. Hence, $\mathcal{H}^{\log 4/\log 3}_{3^{-k}\sqrt{2}}(F \times F) \leq 4^k \left(3^{-k}\sqrt{2}\right)^{\log 4/\log 3} = 2^{\log 2/\log 3} 4^k 4^{-k} = 2^{\log 2/\log 3}$. As k approaches infinity, $\mathcal{H}^{\log 4/\log 3}(F \times F) \leq 2^{\log 2/\log 3}$.

Let μ denote the natural mass distribution on $F \times F$, obtained through iterative subdivision of mass into 4 equal parts, such that each of the 4^k squares in E_k carries a mass of 4^{-k}. If $3^{-(k+1)} \leq |U| < 3^{-k}$ for some $k \geq 1$, then U intersects at most one of the squares in E_k, yielding:

$$\mu(U) \leq 4^{-k} = \left(3^{-k}\right)^{\log 4/\log 3} \leq (3|U|)^{\log 4/\log 3} = 4|U|^{\log 4/\log 3}$$

According to the Mass distribution principle, $\mathcal{H}^{\log 4/\log 3}(F \times F) \geq 1/4$. From these observations, we conclude that $\mathcal{H}^{\log 4/\log 3}(F \times F)$ is both positive and finite, establishing $\dim_{\mathrm{H}}(F \times F) = \log 4/\log 3$.

□

Example 28 ([20, Exercise 2.12])**.** *Define F as the set of real numbers with base 3 expansion $b_m b_{m-1} \cdots b_1 \cdot a_1 a_2 \cdots$ with none of the digits b_i or a_i equal to 1. Then* $\dim_{\mathrm{H}} F = \frac{\log 3}{\log 2}$.

Proof. Recall from Proposition 5 that for $x \in [0, 1]$, x belongs to the Cantor set if and only if x has a base 3 expansion using only the digits 0 and 2. Therefore F is constructed by a Cantor-like process extending outwards as well as inwards. Thus F is the union of countably many shifts of the Cantor set, each with a Hausdorff dimension of $\frac{\log 3}{\log 2}$. Due to the property of countable stability (Proposition 29), $\dim_{\mathrm{H}} F = \frac{\log 3}{\log 2}$. □

Example 29 ([20, Ex. 4.3])**.** *Let $F_1 = F \times [0, 1] \subset \mathbb{R}^2$ denote the Cartesian product of the Cantor set F and the unit interval. Then, with $s = 1 + \frac{\log 2}{\log 3}$, it follows that* $\dim_{\mathrm{H}} F_1 = s$.

Proof. For every k, F can be covered by 2^k intervals of length 3^{-k}. A column of 3^k squares of side 3^{-k} with diameter $3^{-k}\sqrt{2}$, covers the portion of F_1 above each such interval. Thus, the total coverage of F_1 by squares of side 3^{-k} is $2^k \cdot 3^k$. Consequently, $\mathcal{H}^s_{3^{-k}\sqrt{2}}(F_1) \leq 3^k 2^k \left(3^{-k}\sqrt{2}\right)^s = \left(3 \cdot 2 \cdot 3^{-1-\frac{\log 2}{\log 3}}\right)^k 2^{\frac{s}{2}} = 2^{\frac{s}{2}}$, leading to $\mathcal{H}^s(F_1) \leq 2^{\frac{s}{2}}$ and $\dim_{\mathrm{H}} F_1 \leq s$.

We define a mass distribution μ on F_1 by adopting the natural mass distribution on F, where each k-th level interval of F of side 3^{-k} has mass 2^{-k} and uniformly distributing it along the intervals above F. Therefore, for a rectangle U with sides parallel to the coordinate axes and height $h \leq 1$, positioned above a k-th level interval of F, $\mu(U) = h \cdot 2^{-k}$. Any set U lies within a square of side $|U|$ with sides parallel to the coordinate axes. If $3^{-(k+1)} \leq |U| < 3^{-k}$, then U is positioned above at most one k-th level interval of F of side 3^{-k}. Then

$$\mu(U) \leq |U|2^{-k} \leq |U|3^{-k\log 2/\log 3} \leq |U|(3|U|)^{\log 2/\log 3} = 3^{\log 2/\log 3}|U|^s = 2|U|^s.$$

Hence by the Mass distribution principle (Proposition 38), $\mathcal{H}^s(F_1) > \frac{1}{2}$ and therefore $\dim_{\mathrm{H}} F_1 = s$. □

Example 30 (Cantor tartan, [20, Exercise 4.1])**.** *The Cantor tartan is given by* $F' = \{(x, y) \in \mathbb{R}^2 \ : \ \text{either } x \in F \text{ or } y \in F\}$ *where* F *is the Cantor set. Then* $\dim_{\mathrm{H}} F' = 1 + \frac{\log 2}{\log 3}$.

Proof. Let's start by recognizing that the Cantor tartan is defined as $F' = (F \times \mathbb{R}) \cup (\mathbb{R} \times F)$. In Example 29, it's demonstrated that $\dim_{\mathrm{H}}(F \times [0, 1]) = 1 + \frac{\log 2}{\log 3}$. Now, $F \times [n, n+1]$ is a translation of $F \times [0, 1]$, so for every integer n, $\dim_{\mathrm{H}}(F \times [n, n+1]) = 1 + \frac{\log 2}{\log 3}$. Thus, by countable stability, $\dim_{\mathrm{H}}(F \times \mathbb{R}) = 1 + \frac{\log 2}{\log 3}$. Since $\mathbb{R} \times F$ is congruent to $F \times \mathbb{R}$ under a 90 degree rotation, $\dim_{\mathrm{H}}(\mathbb{R} \times F) = 1 + \frac{\log 2}{\log 3}$. Ultimately,

$$\begin{aligned}&\dim_{\mathrm{H}}((F \times \mathbb{R}) \cup (\mathbb{R} \times F)) \\ &\quad = \max\{\dim_{\mathrm{H}}(F \times \mathbb{R}), \dim_{\mathrm{H}}(\mathbb{R} \times F)\} = 1 + \frac{\log 2}{\log 3}.\end{aligned}$$

□

To conclude the study of the Cantor set, we provide a final example of computing its dimension. This example is based on the similarity dimension (see Def. 35) and can be therefore compared to Example 13.

Example 31 ([20, Ex. 2.7])**.** *The Cantor set* F *(see Figure 3.2) satisfies* $\dim_{\mathrm{S}} F = \dim_{\mathrm{H}} F = \frac{\log 2}{\log 3}$.

Proof. The Cantor set F splits into two parts. Let $F_{\mathrm{L}} = F \cap \left[0, \frac{1}{3}\right]$ be the left part and $F_{\mathrm{R}} = F \cap \left[\frac{2}{3}, 1\right]$ be the right part. Both left and right parts are geometrically similar to F with scaling ratio $\frac{1}{3}$, and then

$$F = F_L \cup F_R \text{ and } F_L \cap F_R = \emptyset$$

Therefore for any s and by scaling property (Proposition 23) we have

$$\mathcal{H}^s(F) = \mathcal{H}^s\left(F_{\mathrm{L}}\right) + \mathcal{H}^s\left(F_{\mathrm{R}}\right) = \left(\frac{1}{3}\right)^s \mathcal{H}^s(F) + \left(\frac{1}{3}\right)^s \mathcal{H}^s(F)$$

By assuming that at the critical value $s = \dim_{\mathrm{H}} F$ we have $0 < \mathcal{H}^s(F) < \infty$ (otherwise the result is false) we may divide both sides by $\mathcal{H}^s(F)$. Thus

$$1 = 2\left(\frac{1}{3}\right)^s \text{ or } s = \log 2 / \log 3$$

This final equation should be compared with equation (4.1). □

In this specific case, we have $\dim_{\mathrm{S}} F = \dim_{\mathrm{H}} F$. To ensure that this result holds for any set F, we should require that if $F = \bigcup_{i=1}^m F_i$, where each F_i is geometrically similar to F but scaled by a factor c_i, then the sets F_i do not overlap 'too much'. By studying iterated function systems, we will see what the rigorous condition is for this result to be true in general.

Remark 12. *From Example 26,* $\dim_{\mathrm{H}} F < 1$. *Thus by Proposition 37 the Cantor set F (see Figure 3.2) is totally disconnected. This conlusion should be compared with Proposition 10.*

Example 32 ([20, Ex. 2.6])**.** *The Cantor dust F (see Figure 3.10) satisfies* $\dim_{\mathrm{H}} F = 1$. *It is an unusual example of a fractal since it has an integer Hausforff dimension.*

Proof. We claim that $1 \leq \mathcal{H}^1(F) \leq \sqrt{2}$.

At each iteration step E_k, there are 4^k squares with side length 4^{-k}. The diameter of each square is then $4^{-k}\sqrt{2}$.

Let $\delta = 4^{-k}\sqrt{2}$, then the squares of E_k are a δ-cover of F. So

$$\mathcal{H}^1_\delta(F) \leq \sum_{i=1}^{4^k} 4^{-k}\sqrt{2} = 4^k 4^{-k}\sqrt{2} = \sqrt{2}$$

By letting $\delta \to 0$, we obtain $\lim_{\delta\to 0} \mathcal{H}^1_\delta(F) = \mathcal{H}^1(F) \leq \sqrt{2}$. For the opposite inequality consider $\pi : \begin{cases} \mathbb{R}^2 & \to \mathbb{R} \\ (x,y) & \mapsto x \end{cases}$ the projection map into the x-axis. By construction we have that $\pi(F) = [0,1]$. Projections do not increase distances, so for any $x, y \in F$, $|\pi(x) - \pi(y)| \leq |x - y|$. π is therefore a Lipschitz map and we can apply Remark 5

$$1 = \mathcal{L}^1([0,1]) = \mathcal{H}^1([0,1]) = \mathcal{H}^1(\pi(F)) \leq \mathcal{H}^1(F)$$

This proves that $1 \leq \mathcal{H}^1(F) \leq \sqrt{2}$, so $s = \dim_{\mathrm{H}} F = 1$. □

Let's see how we can produce an upper bound for the Cantor dust using the Mass distribution principle.

Example 33. *Let F be the Cantor dust. By the Mass distribution principle $\mathcal{H}^1(F) \geq \frac{1}{4}$.*

Proof. We define μ to be the natural mass distribution on F, so that at each level E_k, every square of side 4^{-k} carries a mass of 4^{-k}.

If $4^{-(k+1)} \leq |U| < 4^{-k}$ for some $k \geq 1$, then U can intersect at most one of the squares in E_k and so

$$\mu(U) \leq 4^{-k} \leq 4|U|.$$

It follows from the Mass distribution principle (Prop. 38) that $\mathcal{H}^1(F) \geq \frac{1}{4}$ and $\dim_{\mathrm{H}} F \geq 1$. □

Example 34 ([20, Exercise 4.2])**.** *Let F be the set of numbers in $[0,1]$ containing only even digits. Then $\dim_{\mathrm{H}} F = \frac{\log 5}{\log 10}$.*

Proof. We claim that

$$\frac{1}{5} \leq \mathcal{H}^s(F) \leq 1 \text{ for } s = \frac{\log 5}{\log 10}$$

Define E_k as the set of numbers in $[0,1]$ containing only even digits in the first k decimal places. Then $F = \bigcap_{k=0}^{\infty} E_k$. For each positive integer k, the 5^k intervals in E_k of length 10^{-k} form a 10^{-k}-cover of F. Therefore

$$\mathcal{H}^{\log 5/\log 10}_{10^{-k}}(F) \leq 5^k \left(10^{-k}\right)^{\log 5/\log 10} = 5^k 5^{-k} = 1.$$

By taking $k \to \infty$ we get the upper bound $\mathcal{H}^{\log 5/\log 10}(F) \leq 1$.

Define μ as the natural mass distribution on F, derived by iteratively dividing mass into five equal portions. Consequently each of the 5^k intervals, each with a length of 10^{-k} within E_k carries a mass of 5^{-k}. If $10^{-(k+1)} \leq |U| < 10^{-k}$ for some $k \geq 1$, then U can intersect at most one of the intervals in E_k. Thus

$$\mu(U) \leq 5^{-k} = \left(10^{-k}\right)^{\log 5/\log 10} \leq (10|U|)^{\log 5/\log 10} = 5|U|^{\log 5/\log 10}$$

By the Mass distribution principle $\mathcal{H}^{\log 5/\log 10}(F) \geq 1/5$. We can now conclude that $\mathcal{H}^{\log 5/\log 10}(F)$ is positive and finite, so that F is an s-set and $\dim_{\mathrm{H}} F = \frac{\log 5}{\log 10}$.

□

Example 35 ([55, p. 14])**.** *Consider the Weierstrass function f (3.1). Then f is a Hölder function (see Definition 21) with exponent $\frac{log1/a}{logb}$ (Proposition 4). Therefore by Theorem 8 we get $\dim_{\mathrm{H}} \operatorname{graph} f \leq 2 + \frac{loga}{logb}$. Moreover, it has been shown that the inequality is in fact an equality so that $\dim_{\mathrm{H}} \operatorname{graph} f = 2 + \frac{loga}{logb}$ [45].*

The most examples we've encountered so far consist of s-sets, which allow us to determine the Hausdorff dimension by bounding the s-dimensional Hausdorff measure. s-sets are significantly advantageous to study, and fortunately, they appear quite frequently. Working with sets of infinite measure can be challenging, so converting them into sets of positive finite measure can be highly beneficial. One approach to dealing with s-dimensional sets where $\mathcal{H}^s(F) = \infty$ is to utilize the next Theorem to obtain a subset with positive finite measure. This subset can then be studied as an s-set, and the insights gained can be applied to understand the properties of the larger set, F [20].

Theorem 9 ([36, chap. 8])**.** *Let $F \subset \mathbb{R}^n$ with $0 < \mathcal{H}^s(F) \leq \infty$. Then there is a compact set $E \subset F$ such that $0 < \mathcal{H}^s(E) < \infty$.*

Proof. Omitted. See [36, chap. 8]. □

Initially, it may appear straightforward to simply remove portions from F until what remains has a positive finite measure. However, it's not quite as straightforward as this because it's possible to transition from infinite measure to zero measure without traversing any intermediate values. This means that it is possible to have a decreasing sequence of sets $E_1 \supset E_2 \supset \ldots$ with $\mathcal{H}^s(E_k) = \infty$ for all k, but with $\mathcal{H}^s\left(\bigcap_{k=1}^{\infty} E_k\right) = 0$. An easy example, is by taking $E_k = [0, 1/k] \subset \mathbb{R}$ and $0 < s < 1$ [20, section 4.2].

4.4 Box-counting Dimension

In this section, we explore the box-counting dimension, this definition goes back at least to the 1930s [20]. Essentially, this dimension provides insights into how the size of a fractal changes as it undergoes rescaling. The box-counting dimension stands out as one of the most widely utilized and favored dimensions in practical applications. It bears a resemblance to the similarity dimension, employing logarithms in a similar fashion. However, unlike the similarity dimension, it is not a requirement for the sets to be self-similar to apply the box dimension. While it is often straightforward to determine or estimate heuristically, it falls short of fulfilling certain fundamental properties, which restricts its mathematical utility. The drawbacks of the box-counting dimension are discussed towards the conclusion of this section. The main source for the section is [20, chap. 3].

To motivate the definition of the box-counting dimension, we observe that the number of line segments of length δ required to cover a line of length l is l/δ, the number of squares with side length δ needed to cover a square with area A is A/δ^2, and the number of cubes with side length δ needed to cover a cube with volume V is V/δ^3. It's apparent that the dimension of the object we aim to cover corresponds to the power of the side length δ and it aligns

with the more traditional notion of dimension. The box-counting dimension generalises this concept.

Consider a non-empty and bounded set $F \subset \mathbb{R}^n$ and let $N_\delta(F)$ be the smallest number of sets of diameter at most δ which can cover F.

By returning to the idea of measurement at scale δ, if

$$N_\delta(F) \sim c\delta^{-s}$$

for some constants $c > 0$ and $s > 0$, then we may think of F as having dimension s and having s-dimensional content c. By taking logarithms we get

$$\log N_\delta(F) \sim \log c - s \log \delta \tag{4.6}$$

and by isolating s

$$s = \lim_{\delta \to 0} \frac{\log N_\delta(F)}{-\log \delta}.$$

The formula (4.6) is attractive for computational use because s can be approximated by taking the negative of the slope of a logarithmic graph plotted over an appropriate range of δ (see Figure 4.10). It is important to note that in real-world scenarios, we're restricted to working within a finite range of δ, then before reaching extremely small scales, the alignment between theory and experimentation starts to diverge.

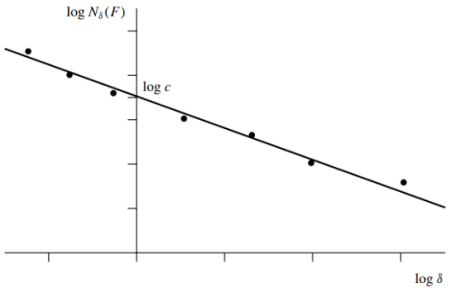

Figure 4.10: Estimating the dimension of set F via a least square fit.
Source: [20, p. 40]

This is the idea behind the box-counting dimension. Let's introduce now the formal definition.

Definition 41 (Box-counting dimension, [20, section 3.1])**.** *Let $F \subset \mathbb{R}^n$ be any non-empty bounded set and let $N_\delta(F)$ be the smallest number of sets of diameter at most δ which can cover F. The lower and upper box-counting dimensions of F respectively are defined as*

$$\underline{\dim}_{\mathrm{B}} F = \lim_{\delta \to 0} \frac{\log N_\delta(F)}{-\log \delta} \tag{4.7}$$

$$\overline{\dim}_{\mathrm{B}} F = \overline{\lim_{\delta \to 0}} \frac{\log N_\delta(F)}{-\log \delta} \tag{4.8}$$

If these are equal we refer to the shared value as the box-counting dimension (or simply box dimension) of F

$$\dim_{\mathrm{B}} F = \lim_{\delta \to 0} \frac{\log N_\delta(F)}{-\log \delta} \tag{4.9}$$

This definition provides an explanation for the significance of the box dimension. It suggests that the count of sets with diameter at most δ intersecting a set F serves as a measure of the set's spread or irregularity when observed at the scale of δ. The dimension conveys information about how quickly these irregularities emerge as δ approaches zero [20].

Remark 13. *The limit of equation (4.9) may not exists for all sets F so that the box-counting dimension may not be defined for every fractal set F.*

Remark 14. *The request for F to be bounded in Definition 41 ensures that there exists some sufficiently large set containing F which can be divided into a finite number of smaller sets, each having a diameter of at most δ. We also assume that $\delta > 0$ is sufficiently small to ensure that $-\log \delta$ and $\log N_\delta(F)$ are strictly positive. In what follows we will always assume in the context of box-counting dimension that all sets considered are non-empty and bounded.*

Various equivalent definitions of box dimension exist, and at times, alternative formulations prove to be more convenient for certain applications.

Proposition 40 ([20, p. 43])**.** *Given $F \subset \mathbb{R}^n$ the lower and upper box-counting dimensions are given respectively by (4.7) and (4.8) and the box-counting dimension, if it exists, by (4.9), where $N_\delta(F)$ is any from the following list:*

1. *the smallest number of closed balls of radius δ that cover F*
2. *the smallest number of cubes of side δ that cover F*
3. *the number of δ-mesh cubes that intersect F*
4. *the smallest number of sets of diameter at most δ that cover F*
5. *the largest number of disjoint balls of radius δ with centres in F*

Remark 15. *To recall, we define δ-mesh cubes of $\mathbb{R}^n$ as cubes of the form:*

$$Q = [m_1\delta, (m_1+1)\,\delta] \times [m_2\delta, (m_2+1)\,\delta] \times \ldots [m_n\delta, (m_n+1)\,\delta], m_i \in \mathbb{Z}$$

where a cube in $\mathbb{R}$ is just an interval and a cube in $\mathbb{R}^2$ is a square.

Remark 16. *The list could be prolonged even more but in practical terms, one typically selects the definition that is most convenient for the specific application.*

Partial proof. $3 \iff 4$

Define $N'_\delta(F)$ to be the number of δ-mesh cubes that intersect F. They are a collection of sets of diameter $\delta\sqrt{n}$ that cover F, so

$$N_{\delta\sqrt{n}}(F) \leq N'_\delta(F).$$

For $\delta\sqrt{n} < 1$ when δ is small enough, we get

$$\frac{\log N_{\delta\sqrt{n}}(F)}{-\log(\delta\sqrt{n})} \leq \frac{\log N'_\delta(F)}{-\log\sqrt{n} - \log\delta}$$

and by taking limits as $\delta \to 0$

$$\underline{\dim}_{\mathrm{B}} F \leq \underline{\lim}_{\delta\to 0} \frac{\log N'_\delta(F)}{-\log\delta}$$

and

$$\overline{\dim}_{\mathrm{B}} F \leq \overline{\lim}_{\delta\to 0} \frac{\log N'_\delta(F)}{-\log\delta}$$

To prove the opposite direction, note that any set of diameter at most δ is contained in 3^n mesh cubes of side δ. So

$$N'_\delta(F) \leq 3^n N_\delta(F)$$

The conclusion follows in a similar way by taking logarithms and limits as $\delta \to 0$.

$2 \iff 4$

We note that any cube of side δ has diameter $\delta\sqrt{n}$ and that any set of diameter of at most δ is contained in a cube of side δ. The equivalence follows then in a similar manner as above.

$1 \iff 4$

Similarly, any closed ball of radius δ has diameter δ and vice versa any set of diameter δ is contained in a closed ball of radius δ.

$5 \iff 4$

Omitted. See [20, p. 43]. □

Figure 4.11: Covering the coast of Great Britain via the largest number of disjoint balls, the smallest number of closed balls and via δ-mesh cubes.
Source: [53]

Remark 17 ([20, p. 44])**.** *In equations (4.7) and (4.8), it's noteworthy that considering limits as δ tends to 0 through any decreasing sequence δ_k suffices, where $\delta_{k+1} \geq c\delta_k$ for some constant $0 < c < 1$, particularly for $\delta_k = c^k$.*

Proof. If $\delta_{k+1} \leq \delta < \delta_k$, then, with $N_\delta(F)$ denoting the least number of sets in a δ-cover of F,

$$\frac{\log N_\delta(F)}{-\log \delta} \leq \frac{\log N_{\delta_{k+1}}(F)}{-\log \delta_k} = \frac{\log N_{\delta_{k+1}}(F)}{-\log \delta_{k+1} + \log\left(\delta_{k+1}/\delta_k\right)} \leq \frac{\log N_{\delta_{k+1}}(F)}{-\log \delta_{k+1} + \log c}$$

and thus

$$\varlimsup_{\delta \to 0} \frac{\log N_\delta(F)}{-\log \delta} \leq \varlimsup_{k \to \infty} \frac{\log N_{\delta_k}(F)}{-\log \delta_k}.$$

The reverse inequality is straightforward and similar treatment applies to the scenario involving lower limits. □

We study now the connection between the box dimension and the Lebesgue measure.

Proposition 41 ([20, Prop. 2.3])**.** *Let $F \subset \mathbb{R}^n$, then*

$$\underline{\dim}_{\mathrm{B}} F = n - \varlimsup_{\delta \to 0} \frac{\log \mathcal{L}^n\left(F_\delta\right)}{\log \delta}$$

$$\overline{\dim}_{\mathrm{B}} F = n - \varliminf_{\delta \to 0} \frac{\log \mathcal{L}^n\left(F_\delta\right)}{\log \delta}$$

where F_δ is the δ-neighbourhood of F (see Def. 5).

In the setting of Proposition 41 box dimension is also referred as Minkowsi dimension or Minkowski-Bouligand dimension [20].

Proof. If F can be covered by $N_\delta(F)$ balls of radius δ, then F_δ can be covered by concentric balls of radius 2δ. By denoting the volume of the unit ball in $\mathbb{R}^n$ by c_n, we get by taking logarithms,

$$\begin{aligned}
\mathcal{L}^n(F_\delta) &\leq N_\delta(F) c_n (2\delta)^n \\
\frac{\log \mathcal{L}^n(F_\delta)}{-\log \delta} &\leq \frac{\log 2^n c_n + n \log \delta + \log N_\delta(F)}{-\log \delta} \\
\varliminf_{\delta \to 0} \frac{\log \mathcal{L}^n(F_\delta)}{-\log \delta} &\leq -n + \underline{\dim}_{\mathrm{B}} F
\end{aligned}$$

Similarly for the upper limit. To prove the opposite inequality, we take $N_\delta(F)$ to be the largest number of disjoint balls of radius δ, using one of the equivalent definitions of $N_\delta(F)$. If there are $N_\delta(F)$ disjoint balls of radius δ with centres in F, then

$$N_\delta(F) c_n \delta^n \leq \mathcal{L}^n(F_\delta).$$

By taking logarithms and letting $\delta \to 0$ analogously as in the first part, one can prove the opposite inequality. □

The next proposition establishes a connection between the Hausdorff dimension and the box-counting dimension.

Proposition 42 ([20, p. 46])**.** *Let $F \subset \mathbb{R}^n$. Then*

$$\dim_{\mathrm{H}} F \leq \underline{\dim}_{\mathrm{B}} F \leq \overline{\dim}_{\mathrm{B}} F$$

Proof. We always have $\underline{\dim}_{\mathrm{B}} F \leq \overline{\dim}_{\mathrm{B}} F$, so it suffices to show $\dim_{\mathrm{H}} F \leq \underline{\dim}_{\mathrm{B}} F$.

Let F be covered by $N_\delta(F)$ sets of diameter δ. Then, by (4.2)

$$\mathcal{H}^s_\delta(F) \leq N_\delta(F) \delta^s.$$

Consider those s for which $1 < \mathcal{H}^s(F) = \lim_{\delta \to 0} \mathcal{H}^s_\delta(F)$

Taking logarithms gives $\log N_\delta(F) + s \log \delta > \log 1 = 0$ for δ sufficiently small.

Therefore $s \leq \varliminf_{\delta \to 0} \frac{\log N_\delta(F)}{-\log \delta}$ so

$$\dim_{\mathrm{H}} F \leq \underline{\dim}_{\mathrm{B}} F$$

□

In general, for a set $F \subset \mathbb{R}^n$ equality does not hold. While the Hausdorff and box dimensions coincide for various sets that exhibit a certain degree of regularity, there exist numerous examples where this inequality is distinctly observed [20]. Furthermore, the box-counting dimension serves as a valuable tool for establishing an upper limit on the Hausdorff dimension.

Proposition 43 ([20, Prop. 4.1])**.** *Assume F can be covered by n_k sets of diameter at most δ_k with $\delta_k \to 0$ as $k \to \infty$. Then*

$$\dim_{\mathrm{H}} F \leq \underline{\dim}_{\mathrm{B}} F \leq \lim_{k\to\infty} \frac{\log n_k}{-\log \delta_k}.$$

Furthermore, if $n_k \delta_k^s$ remains bounded as $k \to \infty$, then $\mathcal{H}^s(F) < \infty$. If $\delta_k \to 0$ but $\delta_{k+1} \geqslant c\delta_k$ for some $0 < c < 1$, then

$$\overline{\dim}_{\mathrm{B}} F \leq \overline{\lim_{k\to\infty}} \frac{\log n_k}{-\log \delta_k}.$$

Proof. The inequalities are a direct consequence of Proposition 42 and Remark 17. If $n_k \delta_k^s$ is bounded then $\mathcal{H}^s_{\delta_k}(F) \leq n_k \delta_k^s$, thus $\mathcal{H}^s_{\delta_k}(F)$ tends to a finite limit $\mathcal{H}^s(F)$ as $k \to \infty$. □

We look now at some general properties of the box dimension.

Proposition 44. $\dim_{\mathrm{B}}$ *is monotonic. If $E \subset F \subset \mathbb{R}^n$ then* $\dim_{\mathrm{B}} E \leq \dim_{\mathrm{B}} F$.

Proof. Clearly $N_\delta(E) \leq N_\delta(F)$ for all $\delta > 0$. So, for all $0 < \delta < 1$,

$$0 \leq \frac{\log N_\delta(E)}{-\log \delta} \leq \frac{\log N_\delta(F)}{-\log \delta}$$

The conclusion follows by taking the limits. □

Proposition 45. *Let $F \subset \mathbb{R}^n$* $\dim_{\mathrm{B}} F \leq n$.

Proof. Let $N_\delta(F)$ be the smallest number of δ-mesh cubes intersecting F. F is contained in some large enough cube C, so by Proposition 44, $N_\delta(F) \leq N_\delta(C) \leq c\delta^{-n}$ for a constant c. By construction, the exponent n gives $\dim_{\mathrm{B}}(F)$. So $\dim_{\mathrm{B}}(F) \leq n$. □

Proposition 46. *If $F \subset \mathbb{R}^n$ is an open set, then* $\dim_{\mathrm{B}} = n$.

Proof. F contains some cube C, so $N_\delta(F) \geq N_\delta(C) \geq c\delta^{-n}$ for some constant c. Then $\dim_{\mathrm{B}}(F) \geq n$ and the conclusion follows by Proposition 45. □

Proposition 47. *If F is a singleton, then* $\dim_{\mathrm{B}} F = 0$.

Proof. For every $\delta > 0$ we have $N_\delta(F) = 1$. So $\log N_\delta(F) = 0$ and $\dim_{\mathrm{B}} F = 0$. □

Proposition 48 ([20, Exercise 3.9])**.** *The upper box dimension is finitely stable. Let $F_i \subset \mathbb{R}^n$, for $i = 1, \ldots, k$, then*

$$\overline{\dim}_{\mathrm{B}} \bigcup_{i=1}^{k} F_i = \max_{1\leq i\leq k} \overline{\dim}_{\mathrm{B}} F_i$$

This identity does not hold for $\underline{\dim}_{\mathrm{B}}$.

Proof. It is enough to prove that

$$\overline{\dim}_{\mathrm{B}}(E \cup F) = \max\left\{\overline{\dim}_{\mathrm{B}}E, \overline{\dim}_{\mathrm{B}}F\right\}.$$

The claim follows then by iteration. Let's check both inequalities. Since $E \subset E \cup F$ and $F \subset E \cup F$, then

$$\overline{\dim}_{\mathrm{B}}E \leq \overline{\dim}_{\mathrm{B}}(E \cup F)$$

and

$$\overline{\dim}_{\mathrm{B}}E \leq \overline{\dim}_{\mathrm{B}}(E \cup F)$$

so

$$\max\left\{\overline{\dim}_{\mathrm{B}}E, \overline{\dim}_{\mathrm{B}}F\right\} \leq \overline{\dim}_{\mathrm{B}}(E \cup F)$$

For the opposite inequality let $N_\delta(F)$ denote the least number of cubes of side length δ that can cover the set F. Then $N_\delta(E \cup F) \leq N_\delta(E) + N_\delta(F) \leq 2\max\{N_\delta(E), N_\delta(F)\}$, so

$$\begin{aligned}
\overline{\dim}_{\mathrm{B}}(E \cup F) &= \overline{\lim_{\delta\to 0}} \frac{\log N_\delta(E \cup F)}{-\log\delta} \\
&\leq \overline{\lim_{\delta\to 0}} \frac{\log\left(2\max\{N_\delta(E), N_\delta(F)\}\right)}{-\log\delta} \\
&\leq \overline{\lim_{\delta\to 0}} \frac{\log 2}{-\log\delta} + \overline{\lim_{\delta\to 0}} \max\left\{\frac{\log N_\delta(E)}{-\log\delta}, \frac{\log N_\delta(F)}{-\log\delta}\right\} \\
&\leq 0 + \max\left\{\overline{\lim_{\delta\to 0}} \frac{\log N_\delta(E)}{-\log\delta}, \overline{\lim_{\delta\to 0}} \frac{\log N_\delta(F)}{-\log\delta}\right\} \\
&= \max\left\{\overline{\dim}_{\mathrm{B}}(E), \overline{\dim}_{\mathrm{B}}(F)\right\}.
\end{aligned}$$

□

Note that we cannot interchange 'max' and '$\underline{\lim}$' in the same way, so the argument fails for lower box dimension.

Corollary 4. *If F is a finite set, then* $\dim_{\mathrm{B}} F = 0$.

Proof. It follows from Proposition 47 and Proposition 48. □

Proposition 49 ([20, Exercise 3.1])**.** *Let $F \subset \mathbb{R}^n$. Assume $f : F \to \mathbb{R}^n$ satisfies the Hölder condition (see Def. 21) for some $0 < \alpha \leq 1$ and $c > 0$. Then*

$$\underline{\dim}_{\mathrm{B}} f(F) \leq \frac{1}{\alpha}\underline{\dim}_{\mathrm{B}} f(F) \quad \textit{and} \quad \overline{\dim}_{\mathrm{B}} f(F) \leq \frac{1}{\alpha}\overline{\dim}_{\mathrm{B}} f(F).$$

Proof. Assume that F can be covered by $N_\delta(F)$ sets of diameter at most δ. Then the $N_\delta(F)$ images of these sets under f form a cover of $f(F)$ by sets of diameter at most $c\delta^\alpha$. Thus considering values of δ for which $c\delta^\alpha < 1$, we have

$$\begin{aligned}\underline{\dim}_{\mathrm{B}} f(F) &= \varliminf_{c\delta^\alpha \to 0} \frac{\log N_{c\delta^\alpha}(f(F))}{-\log c\delta^\alpha} \le \varliminf_{\delta\to 0} \frac{\log N_\delta(F)}{-\alpha\log\delta - \log c} \\ &= \frac{1}{\alpha} \varliminf_{\delta\to 0} \frac{\log N_\delta(F)}{-\log\delta} = \frac{1}{\alpha}\overline{\dim}_{\mathrm{B}} F.\end{aligned}$$

An analogous argument gives the result for the lower box dimension. □

Corollary 5. *Let $F \subset \mathbb{R}^n$. Assume $f : F \to \mathbb{R}^n$ is a Lipschitz function. Then $\underline{\dim}_{\mathrm{B}} f(F) \le \underline{\dim}_{\mathrm{B}} F$ and $\overline{\dim}_{\mathrm{B}} f(F) \le \overline{\dim}_{\mathrm{B}} F$.*

Proof. It follows by Proposition 49 by taking $\alpha = 1$. □

Corollary 6. *Let $F \subset \mathbb{R}^n$. Assume $f : F \to \mathbb{R}^n$ is a bi-Lipschitz function. Then $\underline{\dim}_{\mathrm{B}} f(F) = \underline{\dim}_{\mathrm{B}} F$ and $\overline{\dim}_{\mathrm{B}} f(F) = \overline{\dim}_{\mathrm{B}} F$.*

Proof. By Proposition 2, f^{-1} is also Lipschitz. The conclusion follows then by Proposition 49. □

Corollary 7. *Let $F \subset \mathbb{R}^n$. Assume $f : F \to \mathbb{R}^n$ is a similarity function. Then $\underline{\dim}_{\mathrm{B}} f(F) = \underline{\dim}_{\mathrm{B}} F$ and $\overline{\dim}_{\mathrm{B}} f(F) = \overline{\dim}_{\mathrm{B}} F$.*

Proof. It follows directly from Corollary 6. □

Proposition 50 ([20, p. 48])**.** *A smooth m-dimensional submanifold of $\mathbb{R}^n$ has $\dim_{\mathrm{B}} F = m$.*

Proof. Omitted. See [20]. □

The next proposition illustrates a major problem for the box-counting dimension.

Proposition 51 ([20, Prop 3.4])**.** *Let $F \subset \mathbb{R}^n$. Then*

$$\underline{\dim}_{\mathrm{B}} \bar{F} = \underline{\dim}_{\mathrm{B}} F$$

and

$$\overline{\dim}_{\mathrm{B}} \bar{F} = \overline{\dim}_{\mathrm{B}} F.$$

where $\bar{F}$ denote the closure of F.

Proof. Let $B_1, B_2, \ldots, B_k$ be a finite collection of closed balls, each with radius δ. Let $N_\delta(F)$ be the smallest number of closed balls of radius δ that cover F.

If the closed set $\bigcup_{i=1}^k B_i$ contains F, it also contains $\bar{F}$. Therefore, $N_\delta(F) = N_\delta(\bar{F})$ and

$$\varliminf_{\delta\to 0} \frac{\log N_\delta(F)}{-\log\delta} = \varliminf_{\delta\to 0} \frac{\log N_\delta(\bar{F})}{-\log\delta}$$

and similarly for $\varlimsup$. □

To identify the problem of this result, consider $F = \mathbb{Q} \cap [0,1]$ the countable set of rational numbers between 0 and 1. Then

$$\bar{F} = \overline{\mathbb{Q} \cap [0,1]} = [0,1]$$

Therefore by the previous proposition

$$\underline{\dim}_{\mathrm{B}} F = \overline{\dim}_{\mathrm{B}} F = 1$$

This means that countable sets can have non-zero box dimension. In particular the example shows that box dimension does not behave well under countable unions.

$F = \mathbb{Q} \cap [0,1]$ can be written as a countable union of isolated rational points, and we know that singletons have box dimension zero. The conclusion is that $\dim_B \left(\bigcup_{i=1}^{\infty} F_i\right) = \sup_i \{\dim_B F_i\}$ does not generally hold (both for the lower and the upper box dimension). However, the countable stability property is one common property when we are referring to a certain quantity as a dimension. This suggests that in certain situations the box-counting dimension of a fractal may not accurately represent its size, as one might expect.

Corollary 8. *Let F be a dense subset of an open set $E \subset \mathbb{R}^n$ then $\underline{\dim}_{\mathrm{B}} F = \overline{\dim}_{\mathrm{B}} F = n$.*

To sum up, based on our initial criteria for a robust definition of dimension, as outlined at the beginning of this section, it becomes apparent that the upper box dimension might lack countable stability, and the lower box dimension could potentially even lack finite stability altogether. Moreover, it's conceivable that a set might yield different values for its lower and upper box dimensions, rendering the box dimension undefined. In addition to this it is also not applicable to unbounded sets. This stands in contrast to the Hausdorff dimension, which is applicable to every set and satisfy the countable stability property.

Computing the box-counting dimension

In this final part of the section we work out some concrete examples to see the box dimension in action.

Example 36 ([20, Ex. 3.3])**.** *Consider the Cantor set F (see Figure 3.2). Then $\dim_{\mathrm{B}} F = \frac{\log 2}{\log 3}$.*

Proof. Recall that the k-level E_k is given by 2^k intervals each of length 3^{-k}. Then by taking this natural cover

$$N_\delta(F) \leq 2^k \text{ if } 3^{-k} < \delta \leq 3^{-k+1}$$

From the definition of upper box dimension, we get

$$\overline{\dim}_{\mathrm{B}} F = \overline{\lim_{\delta \to 0}} \frac{\log N_\delta(F)}{-\log \delta} \leq \overline{\lim_{k \to \infty}} \frac{\log 2^k}{-\log 3^{-k+1}} = \overline{\lim_{k \to \infty}} \frac{\log 2^k}{\log 3^{k-1}} = \frac{\log 2}{\log 3}.$$

By a similar reasoning as Example 26, we have that any interval of length δ where $3^{-k-1} \leq \delta < 3^{-k}$ intersects at most one of the level-k intervals of length 3^{-k}. There are 2^k of these intervals in E_k so we require at least 2^k intervals of length δ to cover F. We get the inequality $N_\delta(F) \geq 2^k$ that brings to $\underline{\dim}_{\mathrm{B}} F \geq \frac{\log 2}{\log 3}$. Therefore $\dim_{\mathrm{H}} F = \dim_{\mathrm{B}} F = \frac{\log 2}{\log 3}$. □

Example 37 (uniform Cantor set, [20, Ex. 4.5])**.** *The construction of the uniform Cantor set F is the following. Let m be an integer greater than or equal to 2, and $0 < r < \frac{1}{m}$. Define F as the set obtained by replacing each basic interval I with m equally spaced subintervals of lengths $r|I|$, where the endpoints of I coincide with the endpoints of the extreme subintervals (see for example Figure 4.12). Then,* $\dim_{\mathrm{B}} F = \dim_{\mathrm{H}} F = \frac{\log m}{-\log r}$*, and* $0 < \mathcal{H}^{\frac{\log m}{-\log r}}(F) < \infty$.

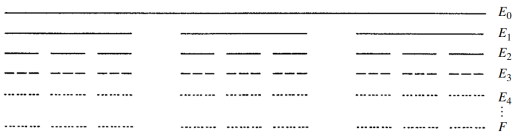

Figure 4.12: A uniform Cantor set F with $m = 3$ and $r = 4/15$.
Source: [20, p. 64]

Proof. For every positive integer k, the $n_k = m^k$ intervals of length $\delta_k = r^k$ in E_k form a cover of F. From Proposition 43 it follows that

$$\dim_{\mathrm{H}} F \leq \overline{\dim}_{\mathrm{B}} F \leq \overline{\lim_{k \to \infty}} \frac{\log m^k}{-\log r^k} = \frac{\log m}{-\log r}.$$

Moreover as $n_k \delta_k^{\log m/(-\log r)} = m^k r^{k \log m/(-\log r)} = 1$, from Proposition 43 it also follows that $\mathcal{H}^{\log m/(-\log r)}(F) < \infty$.

Now, consider μ as the natural mass distribution on F, where each of the m^k intervals of length r^k in E_k carries a mass of m^{-k}. If $r^{(k+1)} \leq |U| < r^k$ for some $k \geq 1$, then U can intersect at most two of the intervals in E_k. Thus,

$$\mu(U) \leq 2m^{-k} = 2mm^{-(k+1)} = 2mr^{(k+1)\log m/-\log r} \leq 2m|U|^{\log m/-\log r}.$$

According to the Mass distribution principle (see Proposition 38), we have $\mathcal{H}^{\frac{\log m}{-\log r}}(F) \geq \frac{\mu(F)}{2m} = \frac{1}{2m} > 0$, and $\dim_{\mathrm{H}} F \geq \frac{\log m}{-\log r}$. We thus conclude that $\dim_{\mathrm{H}} F = \dim_{\mathrm{B}} F = \frac{\log m}{-\log r}$ and $0 < \mathcal{H}^{\frac{\log m}{-\log r}}(F) < \infty$.

□

Example 38 (middle λ Cantor set)**.** *The middle λ Cantor set F is created by iteratively removing a fraction $0 < \lambda < 1$ from the middle of intervals, beginning with the unit interval. This process is a specific instance of a uniform Cantor set, where $m = 2$ and $r = \frac{1}{2}(1-\lambda)$. Consequently, from Example 37, $\dim_{\mathrm{H}} F = \dim_{\mathrm{B}} F = \frac{\log 2}{\log\left(\frac{2}{1-\lambda}\right)}$. The usual Cantor set F (see Example 2) is thus also called middle third Cantor set.*

Proposition 52 ([20, Exercise 4.9])**.** *There exists a compact subset $F \subset [0,1]$ such that $\dim_{\mathrm{H}} F = 1$ but $\mathcal{H}^1(F) = 0$.*

Proof. For every $0 < s < 1$, there exists a compact set $E_s \subset [0,1]$ such that its Hausdorff dimension equals s. For instance, by selecting $\lambda = 1 - 2^{1-1/s}$, in Example 38 of the middle λ Cantor set, we obtain a suitable set E_s. For each $n = 1, 2, \ldots$, let F_n denote a similar version of $E_{1-1/n}$, which is scaled and shifted so that $F_n \subset \left[\frac{1}{n+1}, \frac{1}{n}\right]$. Consequently, $\dim_{\mathrm{H}} F_n = 1 - 1/n$, and $\mathcal{H}^1(F_n) = 0$. Define

$$F = \{0\} \cup \bigcup_{n=1}^{\infty} F_n.$$

Thus, F is compact, by Proposition 29, $\dim_{\mathrm{H}} F = \sup_{1 \le n < \infty} \dim_{\mathrm{H}} F_n = 1$, and $\mathcal{H}^1(F) = \sum_{n=1}^{\infty} \mathcal{H}^1(F_n) = 0$, as desired. □

Example 39 ([20, Exercise 3.4])**.** *Consider the Cantor dust F (see Figure 3.10). Then $\dim_{\mathrm{B}} F = 1$.*

Proof. We denote by $N_\delta(F)$ the least number of squares of side δ that cover F. Then if $\delta_k = 4^{-k}$,

$$\dim_{\mathrm{B}} F = \lim_{k\to\infty} \frac{\log N_{\delta_k}(F)}{-\log \delta_k},$$

only if this limit exists.

From the construction of F outlined in Example 7 we have that $N_{\delta_k}(F) \le 4^k$. Therefore

$$\overline{\dim}_{\mathrm{B}} F = \overline{\lim_{k\to\infty}} \frac{\log N_{\delta_k}(F)}{-\log \delta_k} \le \overline{\lim_{k\to\infty}} \frac{\log 4^k}{\log 4^k} = 1$$

We note then that any square of side $\delta_k = 4^{-k}$ intersects at most two of the squares of side δ_k in E_k and F meets every one of the 4^k squares from E_k, so $N_{\delta_k}(F) \ge \frac{1}{2}4^k$, and

$$\begin{aligned} \underline{\dim}_{\mathrm{B}} F &= \underline{\lim_{k\to\infty}} \frac{\log N_{\delta_k}(F)}{-\log \delta_k} \ge \underline{\lim_{k\to\infty}} \frac{\log \frac{1}{2}4^k}{\log 4^k} \\ &= \underline{\lim_{k\to\infty}} \frac{k\log 4 - \log 2}{k \log 4} = 1. \end{aligned}$$

Hence $\dim_{\mathrm{H}} F = \dim_{\mathrm{B}} F = 1$. □

Example 40 ([20, Exercise 3.6]). *Consider the Sierpinksi triangle F (see Figure 3.8). Then* $\dim_{\mathrm{B}} F = \frac{\log 3}{\log 2}$.

Proof. We denote by $N_\delta(F)$ the least number of squares of side δ that cover F. Recall that the k-level interval E_k consists of 3^k squares of side 2^{-k} and they give a cover of F. In particular for $k = 1, 2, \ldots$, F can be covered by 3^k squares of side 2^{-k} Let $\delta_k = 2^{-k}$, then

$$\overline{\dim}_{\mathrm{B}} F = \overline{\lim_{k\to\infty}} \frac{\log N_{\delta_k}(F)}{-\log \delta_k} \leq \overline{\lim_{k\to\infty}} \frac{\log 3^k}{\log 2^k} = \frac{\log 3}{\log 2}$$

By using one of the equivalent definition, let now $N_\delta(F)$ be the greatest number of disjoint balls of radius δ with centres in F.

The top vertex of each of the 3^k triangles of E_k belongs to F and the balls of radius $\frac{1}{2^{k+1}}$ centered at these vertices are mutually disjoint. So, by taking $\delta_k = 2^{-(k+1)}$, we get

$$\underline{\dim}_{\mathrm{B}} F = \underline{\lim_{k\to\infty}} \frac{\log N_{\delta_k}(F)}{-\log \delta_k} \geq \underline{\lim_{k\to\infty}} \frac{\log 3^k}{\log 2^{k+1}} = \frac{\log 3}{\log 2}.$$

Hence $\dim_{\mathrm{H}} F = \dim_{\mathrm{B}} F = \frac{\log 3}{\log 2}$. □

Example 41 ([20, Exercise 3.5]). *Consider the Koch curve F (see Figure 3.3). Then* $\dim_{\mathrm{B}} F = \frac{\log 4}{\log 3}$.

Proof. Denote by $N_\delta(F)$ the smallest number of sets of diameter at most δ that cover F. For each line segment comprising E_k, consider taking a closed disk with a diameter of $\delta_k = 3^{-k}$, positioned at the midpoint of the line segment. There would be a total of 4^k such disks, covering F. Thus

$$\overline{\dim}_{\mathrm{B}} F = \overline{\lim_{k\to\infty}} \frac{\log N_{\delta_k}(F)}{-\log \delta_k} \leq \overline{\lim_{k\to\infty}} \frac{\log 4^k}{\log 3^k} = \frac{\log 4}{\log 3}$$

By using one of the equivalent definition, let now $N_\delta(F)$ denoting the largest number of disjoint balls of radius δ with centres in F.

The 4^k straight line segments that build up E_k have $4^k + 1$ distinct endpoints, each of which belongs to F.

The balls of radius $\frac{1}{3^{k+1}}$ centred at these endpoints are mutually disjoint. So, by taking $\delta_k = 3^{-(k+1)}$, we get

$$\begin{aligned}\underline{\dim}_{\mathrm{B}} F &= \underline{\lim_{k\to\infty}} \frac{\log N_{\delta_k}(F)}{-\log \delta_k} \geq \underline{\lim_{k\to\infty}} \frac{\log\left(4^k+1\right)}{\log 3^{k+1}} \\ &\geq \underline{\lim_{k\to\infty}} \frac{\log\left(4^k\right)}{\log 3^{k+1}} = \underline{\lim_{k\to\infty}} \frac{k\log 4}{(k+1)\log 3} = \frac{\log 4}{\log 3}\end{aligned}$$

Hence $\dim_{\mathrm{H}} F = \dim_{\mathrm{B}} F = \frac{\log 4}{\log 3}$. □

Example 42 ([20, Exercise 3.3])**.** *Consider the set F which comprises numbers within the interval $[0,1]$ that do not contain the digit 5 in their decimal expansions. Then* $\dim_{\mathrm{B}} F = \frac{\log 9}{\log 10}$.

Proof. Define E_k as the subset of numbers in the interval $[0,1]$ whose decimal expansions do not contain the digit 5 in the initial k decimal places. Then $F = \bigcap_{k=1}^{\infty} E_k$. Define $N_\delta(F)$ to be the smallest number of intervals of length δ that can cover F.

Define k as the integer such that $10^{-k} \leq \delta < 10^{-k-1}$. Because E_k can be seen as the union of 9^k intervals, each with a length of 10^{-k}, it follows that $N_\delta(F) \leq 9^k$. Then

$$\begin{aligned}\overline{\dim}_{\mathrm{B}} F &= \overline{\lim_{\delta\to 0}} \frac{\log N_\delta(F)}{-\log \delta} \leq \overline{\lim_{k\to\infty}} \frac{\log 9^k}{-\log 10^{-k-1}} \\ &\leq \overline{\lim_{k\to\infty}} \frac{k \log 9}{(k+1)\log 10} = \frac{\log 9}{\log 10}\end{aligned}$$

Now, consider $0 < \delta < 1$ and let k be the integer such that $10^{-k+1} \leq \delta < 10^{-k}$. As any set with a diameter of δ can intersect at most two of the constituent intervals of E_k, each with a length of 10^{-k}, and since each of these intervals contains points belonging to F, it follows that at least $\frac{1}{2}9^k$ intervals of length δ are required to cover F. Hence, $N_\delta(F) \geq \frac{1}{2}9^k$.

$$\begin{aligned}\underline{\dim}_{\mathrm{B}} F &= \underline{\lim_{\delta\to 0}} \frac{\log N_\delta(F)}{-\log \delta} \geq \underline{\lim_{k\to\infty}} \frac{\log \frac{1}{2}9^k}{-\log 10^{-k+1}} \\ &\geq \underline{\lim_{k\to\infty}} \frac{k\log 9 - \log 2}{(k-1)\log 10} = \frac{\log 9}{\log 10}\end{aligned}$$

Thus $\dim_{\mathrm{B}} F = \frac{\log 9}{\log 10}$. □

Example 43 ([20, Exercise 4.4])**.** *Let $0 < \lambda \leq \frac{1}{2}$, and define F to be the set of real numbers*

$$F = \left\{ \sum_{k=1}^{\infty} a_k \lambda^k : a_k = 0 \text{ or } 1 \text{ for } k = 1, 2, \ldots \right\}.$$

Then $\dim_{\mathrm{B}} F = \dim_{\mathrm{H}} F = \frac{-\log 2}{\log \lambda}$.

Proof. If $\lambda = \frac{1}{2}$, then $F = [0,1]$, so its Hausdorff dimension and box dimension are both 1. Now, suppose $0 < \lambda < \frac{1}{2}$. We observe that F lies within the interval $[0, \lambda/(1-\lambda)]$. Additionally, F consists of two similar copies of itself at scale λ, i.e. $F = (F \cap [0, \lambda^2/(1-\lambda)]) \cup (F \cap [\lambda, \lambda/(1-\lambda)])$. This self-similarity allows us to construct F iteratively, comparable to a Cantor set construction.

At each step, we replace intervals with two subintervals, each of length λ times that of the parent interval.

Let E_k denote the set of 2^k intervals of lengths $\lambda^{k+1}/(1-\lambda)$ generated at the k-th stage of this construction. Then F is the intersection of all such sets, $F = \bigcap_{k=0}^{\infty} E_k$. Each E_k forms a cover of F consisting of 2^k intervals. Hence, by Proposition 43, we have:

$$\begin{aligned}\overline{\dim}_{\mathrm{B}} F &\leq \overline{\lim_{k\to\infty}} \frac{\log 2^k}{-\log \lambda^{k+1}/(1-\lambda)} \\ &= \overline{\lim_{k\to\infty}} \frac{k \log 2}{-(1+k)\log\lambda + \log(1-\lambda)} = \frac{\log 2}{-\log \lambda}.\end{aligned}$$

Let μ represent the natural mass distribution on F, where each of the 2^k intervals of lengths $\lambda^{k+1}/(1-\lambda)$ in E_k carries a mass of 2^{-k}. If the size of a set U satisfies $\lambda^{k+1}(1-2\lambda)/(1-\lambda) \leq |U| < \lambda^k(1-2\lambda)/(1-\lambda)$ for some $k \geq 1$, then U can intersect at most one of the intervals in E_k. Thus, we have:

$$\mu(U) \leq 2^{-k} \leq \left(\lambda^k\right)^{-\frac{\log 2}{\log \lambda}} \leq \left(\frac{1-\lambda}{\lambda(1-2\lambda)}|U|\right)^{-\frac{\log 2}{\log \lambda}} = c|U|^{-\frac{\log 2}{\log \lambda}},$$

where $c > 0$ is independent of U. By the Mass distribution principle, it follows that $\dim_{\mathrm{H}} F \geq -\frac{\log 2}{\log \lambda}$. Finally, we deduce that $\dim_{\mathrm{H}} F = \dim_{\mathrm{B}} F = -\frac{\log 2}{\log \lambda}$. □

We construct now a specific example of a set E to demonstrate that $\underline{\dim}_{\mathrm{B}} E \neq \overline{\dim}_{\mathrm{B}} E$.

Example 44 (modified Cantor set, [20, Exercise 3.8])**.** *We modify the construction of the middle third Cantor set by removing the middle* $3/5$ *of intervals at certain scales instead of the middle* $1/3$*. Let* $k_n = 10^n$*, for* $n \in \mathbb{N}$*, and define* E *as the intersection of all sets* E_k*,* $E = \bigcap_{k=0}^{\infty} E_k$ *where* $E_0 = [0,1]$*, and:*

- *for* $k_{2n} < k \leq k_{2n+1}$ *for some* $n \in \mathbb{N}$*,* E_k *is obtained by deleting the middle* $1/3$ *of each interval in* E_{k-1}
- *for* $k_{2n-1} < k \leq k_{2n}$ *for some* $n \in \mathbb{N}_{>0}$*,* E_k *is obtained by deleting the middle* $3/5$ *of each interval in* E_{k-1}

We can evaluate the lower and upper box dimensions of E *by estimating* $N_\delta(E)$*, which represents the minimum number of closed intervals of length* δ *required to cover* E*. When* n *is even,* E_{k_n} *consists of* 2^{k_n} *intervals of length*

$$\delta_n = \left(\frac{1}{3}\right)^{k_1}\left(\frac{1}{5}\right)^{k_2-k_1}\cdots\left(\frac{1}{3}\right)^{k_{n-1}-k_{n-2}}\left(\frac{1}{5}\right)^{k_n-k_{n-1}} < \left(\frac{1}{5}\right)^{k_n-k_{n-1}}.$$

So, the length of every interval at this stage is smaller than $\left(\frac{1}{5}\right)^{k_n-k_{n-1}}$

Using these intervals as a covering set

$$\begin{aligned}\underline{\dim}_{\mathrm{B}}E &\leq \underline{\lim}_{n\to\infty}\frac{\log N_{\delta_n}(E)}{-\log\delta_n} \leq \underline{\lim}_{n\to\infty}\frac{\log 2^{k_n}}{\log 5^{k_n-k_{n-1}}}\\ &= \underline{\lim}_{n\to\infty}\frac{k_n\log 2}{(k_n-k_{n-1})\log 5} = \underline{\lim}_{n\to\infty}\frac{10k_{n-1}\log 2}{9k_{n-1}\log 5} = \frac{10\log 2}{9\log 5}\end{aligned}$$

Applying a comparable method, we can approximate the upper box-counting dimension. If n is odd, then E_{k_n} is made up of 2^{k_n} intervals of length

$$\begin{aligned}\delta_n &= \left(\frac{1}{3}\right)^{k_1}\left(\frac{1}{5}\right)^{k_2-k_1}\cdots\left(\frac{1}{5}\right)^{k_{n-1}-k_{n-2}}\left(\frac{1}{3}\right)^{k_n-k_{n-1}}\\ &> \left(\frac{1}{5}\right)^{k_{n-1}}\left(\frac{1}{3}\right)^{k_n-k_{n-1}}.\end{aligned}$$

Thus, the intervals at this stage have length $\left(\frac{1}{5}\right)^{k_{n-1}}\left(\frac{1}{3}\right)^{k_n-k_{n-1}}$ at least.

To cover E with intervals of length δ_n takes at least $2^{k_n}/2$ intervals, as every such interval can intersect at most two intervals of E_{k_n}. Also, since E has points in every interval in E_{k_n}, we get

$$\begin{aligned}\overline{\dim}_{\mathrm{B}}E &\geq \overline{\lim}_{n\to\infty}\frac{\log N_{\delta_n}(F)}{-\log\delta_n} \geq \overline{\lim}_{n\to\infty}\frac{\log\left(2^{k_n}/2\right)}{\log\left(5^{k_{n-1}}3^{k_n-k_{n-1}}\right)}\\ &= \overline{\lim}_{n\to\infty}\frac{k_n\log 2-\log 2}{k_{n-1}\log 5+(k_n-k_{n-1})\log 3}\\ &= \overline{\lim}_{n\to\infty}\frac{10k_{n-1}\log 2-\log 2}{k_{n-1}\log 5+9k_{n-1}\log 3}\\ &= \frac{10\log 2}{\log 5+9\log 3} \geq \frac{10\log 2}{11\log 3}\end{aligned}$$

In conclusion

$$\frac{10\log 2}{9\log 5} < \frac{10\log 2}{11\log 3}$$

Therefore

$$\underline{\dim}_{\mathrm{B}}E < \overline{\dim}_{\mathrm{B}}E.$$

We construct now a specific example of two sets F and E to demonstrate that $\underline{\dim}_{\mathrm{B}}(E\cup F) \neq \max\left\{\underline{\dim}_{\mathrm{B}}E, \underline{\dim}_{\mathrm{B}}F\right\}$.

Example 45 ([20, Exercise 3.10])**.** *Define the set E as in Example 44. We create the set F using an analogous method, but with intervals scaled in a complementary manner, and we position the set to be disjoint from E. Thus let $k_n = 10^n$, for $n \in \mathbb{N}$, and define F as the intersection of all sets F_k, $F = \bigcap_{k=0}^{\infty} F_k$ where $F_0 = [2,3]$, and:*

- *for $k_{2n} < k \leq k_{2n+1}$ for some $n \in \mathbb{N}$, E_k is obtained by deleting the middle $3/5$ of each interval in F_{k-1}*

- *for $k_{2n-1} < k \leq k_{2n}$ for some $n \in \mathbb{N}_{>0}$, E_k is obtained by deleting the middle $1/3$ of each interval in F_{k-1}*

In line with the solution to Exercise 44, we find that the lower box dimensions of E and F are both bounded above by $\frac{10\log 2}{9\log 5}$.

For every $k = 1, 2, \ldots$, define δ_k to be the length of the longest intervals in $E_k \cup F_k$. There are 2^k such intervals, each intersecting $E \cup F$. Since any other interval of length δ_k intersects at most two of these intervals, the minimum number of closed intervals of length δ_k covering $E \cup F$ is at least $2^k/2$. Now, $\delta_k \geq \left(\frac{1}{3}\right)^{k/2}\left(\frac{1}{5}\right)^{k/2}$ and $\delta_k \geq (1/5)\delta_{k-1}$. Hence, following the Remark 17, we have

$$\begin{aligned}\underline{\dim}_{\mathrm{B}} E \cup F = \underline{\lim}_{\delta_k \to 0} \frac{\log N_{\delta_k}(E \cup F)}{-\log \delta_k} &\geq \underline{\lim}_{k\to\infty} \frac{\log 2^k/2}{\log 5^{k/2} \log 3^{k/2}} \\ &= \underline{\lim}_{k\to\infty} \frac{k\log 2 - \log 2}{(k/2)\log 5 + (k/2)\log 3} = \frac{2\log 2}{\log 5 + \log 3}.\end{aligned}$$

Thus

$$\underline{\dim}_{\mathrm{B}} E \cup F \geq \frac{2\log 2}{\log 5 + \log 3} > \frac{10\log 2}{9\log 5} \geq \underline{\dim}_{\mathrm{B}} E, \underline{\dim}_{\mathrm{B}} F.$$

Example 46 ([20, Ex. 3.5])**.** *Consider the set $F = \left\{0, 1, \frac{1}{2}, \frac{1}{3}, \frac{1}{4}, \ldots\right\}$. Then $\dim_{\mathrm{B}} F = \frac{1}{2}$.*

Proof. Let $0 < \delta < \frac{1}{2}$. For a set U with $|U| < \delta$, let k such that

$$\frac{1}{k-1} - \frac{1}{k} = \frac{1}{k(k-1)} > \delta \geq \frac{1}{k(k+1)} = \frac{1}{k} - \frac{1}{k+1}.$$

Then U can cover at most one point of the set $\left\{1, \frac{1}{2}, \frac{1}{3}, \frac{1}{4}, \ldots, \frac{1}{k}\right\} \subset F$ and therefore $N_\delta(F) \geq k$, where $N_\delta(F)$ is the least number of sets of diameter at most δ that cover F, so

$$\frac{\log N_\delta(F)}{-\log \delta} \geq \frac{\log k}{\log k(k+1)}.$$

Letting $\delta \to 0$, so $k \to \infty$ we conclude, by l'Hôpital rule, $\underline{\dim}_{\mathrm{B}} F \geq \frac{1}{2}$.

For the other inequality, by taking the same k and δ as before, we note that $(k+1)$ intervals of length δ cover the interval $\left[0, \frac{1}{k}\right]$, leaving $(k-1)$ points of F out, which can be covered by another $(k-1)$ intervals. Thus,

$$\frac{\log N_\delta(F)}{-\log \delta} \leq \frac{\log((k+1)+(k-1))}{\log k(k-1)} \leq \frac{\log(2k)}{\log k(k-1)},$$

which gives $\underline{\dim}_{\mathrm{B}} F \leq \frac{1}{2}$. Thus $\dim_{\mathrm{B}} F = \frac{1}{2}$. □

This last example illustrates another scenario where the box dimension is shown to be unstable under countable operations. Despite having all but one of its points isolated and not being considered a fractal, the set still maintains a positive box dimension. This example should be compared with its analogous version of the Hausdorff dimension in Example 24.

Chapter 5

Iterated Function Systems

Previously mentioned, numerous fractals exhibit self-similarity, wherein they resemble themselves on smaller scales. These self-similar characteristics not only define fractals but also serve as a method for their identification and description. Hutchinson formally introduced the concept of self-similarity in 1981 [27], leading to a vast body of literature focused on representing self-similar sets and computing their dimensions and measures. This section introduces a specific approach for recognizing and depicting fractals prominently featuring such resemblances. Essentially, any collection of contracting maps generates a distinct fractal that remains invariant under these contractions. By iteratively applying these maps to a sufficiently large set, the fractal can be constructed. This assortment of maps forms an iterated function system, offering a concise method for determining the fractal's dimension. The section explores the direct association between iterated function systems and fractals, elucidating their interconnectedness and significance. The main source for this chapter is [20, chap. 9].

5.1 Introduction to IFS

Definition 42 (contraction, [20, p. 123])**.** *Let $D \subset \mathbb{R}^n$ be a closed subset. Then the map $S : D \to D$ is a contraction on D if $|S(x) - S(y)| \leq c|x - y|$ for all $x, y \in D$ and for some $0 < c < 1$. c is called the contraction ratio of S.*

Remark 18. *All contractions satisfy the Hölder condition with $\alpha = 1$.*

Proposition 53. *Let $|S(x)-S(y)| \leq c|x-y|$ be a contraction with contraction ratio c. Then S is continuous.*

Proof. Let $\epsilon > 0$. Then

$$|S(x) - S(y)| \leq c|x - y| < \epsilon$$

whenever $|x - y| < \delta$ where $\delta < \epsilon/c$. □

Definition 43 (contracting similarity, [20, p. 123])**.** *A contraction (see Def. 42) is called a (contracting) similarity if equality holds, i.e, when* $|S(x) - S(y)| = c|x-y|$*. In that case, the function* S *transforms sets into geometrically similar sets.*

This definition should be compared with Definition 16.

Definition 44 (Iterated function systems, [20, p. 123])**.** *A finite collections of contractions* $\{S_1, S_2, \ldots, S_m\}$*, with* $m \geq 2$*, is called an iterated function system, or more simply IFS.*

Definition 45 (attractor, [20, p. 123])**.** *Let* $\{S_1, S_2, \ldots, S_m\}$ *be an IFS. Then we call a non-empty compact subset* F *of* D *an attractor (or invariant set) for the IFS if*

$$F = \bigcup_{i=1}^{m} S_i(F)$$

Example 47 ([20, p. 123])**.** *Let* F *be the Cantor set. Clearly* F *is non-empty and compact (see Prop. 7). Then* $F = S_1(F) \cup S_2(F)$ *where* $S_1, S_2 : \mathbb{R} \to \mathbb{R}$ *are be given by*

$$S_1(x) = \frac{1}{3}x \quad S_2(x) = \frac{1}{3}x + \frac{2}{3}.$$

Hence F *is the attractor of the IFS consisting of the contractions* $\{S_1, S_2\}$*, these maps represent the self-similarities of the Cantor set. In fact in this specific case* S_1 *and* S_2 *are not only contractions but also similarities, each with contraction ratio* $\frac{1}{3}$*.*

To establish the foundational concept that an iterated function system (IFS) possesses a unique, non-empty and compact attractor, we introduce a metric distance, denoted as d, between subsets of D.

Definition 46 (Hausdorff distance, [20, p. 124])**.** *Let* $D \subset \mathbb{R}^n$ *and define* $\mathcal{S}$ *to be the set of all non-empty compact subsets of* D*. Let* $A, B \in \mathcal{S}$*. Define the Hausdorff metric on* $\mathcal{S}$ *as*

$$d(A, B) = \inf \{\delta : A \subset B_\delta \text{ and } B \subset A_\delta\}$$

Recall that A_δ *is the* δ*-neighbourhood of* A *(see Definition 5).*

Proposition 54 ([20, Exercise 9.1])**.** *The Hausdorff metric* d *satisfies the conditions for a metric.*

Proof. We cleary have $d(A, B) \geq 0$ and $d(A, A) = 0$. Now, let's assume that $d(A, B) = 0$. Considering an element $x \in B$, we observe that for every positive integer n, x must also belong to $B \subset A_{1/n}$. Consequently, there exists $x_n \in A$ such that $|x - x_n| \leq 1/n$. Thus, $x \in \bar{A} = A$, since A is compact and therefore closed. Consequently, $B \subset A$. Similarly, $A \subset B$, implying $A = B$, as needed.

The symmetry property follows by the definition.

We prove now the triangle inequality. We assume that $d(A, C) = \epsilon_1$ and $d(C, B) = \epsilon_2$. Then, for each $\delta_1 > \epsilon_1$ and each $\delta_2 > \epsilon_2$, we have:

$$\begin{aligned} A &\subset C_{\delta_1}, \\ C &\subset A_{\delta_1}, \\ C &\subset B_{\delta_2}, \\ B &\subset C_{\delta_2}. \end{aligned}$$

So,

$$\begin{aligned} &A \subset C_{\delta_1} \subset B_{\delta_1+\delta_2} \text{ and} \\ &B \subset C_{\delta_2} \subset A_{\delta_2+\delta_1}. \end{aligned}$$

Thus, $d(A, B) \leq \delta_1 + \delta_2$ for all δ_1, δ_2 with $\delta_1 > \epsilon_1$ and $\delta_2 > \epsilon_2$. Therefore, $d(A, B) \leq \epsilon_1 + \epsilon_2 = d(A, C) + d(C, B)$, as claimed. □

Before stating the main theorem for this section we have to recall the result of Banach's contraction mapping theorem.

Definition 47 (complete metric space)**.** *A metric space (X, d) is said to be complete, if every Cauchy sequence in X converges in X.*

Proposition 55 ([25])**.** *$(\mathcal{S}, d)$ is a complete metric space.*

Proof. Omitted. See [25]. □

Definition 48 (fixed point)**.** *A fixed point of a function f is a point x such that $f(x) = x$.*

Theorem 10 (Banach's contraction mapping theorem, [15, Thm 2.2.21])**.** *Let f be a contraction on a non-empty complete metric space (X, d). Then f admits a unique fixed point.*

Proof. Proof. First, we establish that there is at most one fixed point. Suppose x and y are both fixed points. Then, we have $d(x, y) = d(f(x), f(y)) \leq cd(x, y)$, where c is the contraction ratio. However, since $0 < c < 1$, this is impossible if $d(x, y) > 0$. Therefore, $d(x, y) = 0$, implying $x = y$.

Now, let x_0 be any point of X, recalling that X is nonempty. We define recursively

$$x_{n+1} = f(x_n) \text{ for } n \geq 0.$$

We claim that (x_n) is a Cauchy sequence. Let $a = d(x_0, x_1)$. By induction, we have $d(x_{n+1}, x_n) \leq ac^n$. Then, for $m < n$, we have

$$\begin{aligned} d(x_m, x_n) &\leq \sum_{j=m}^{n-1} d(x_{j+1}, x_j) \leq \sum_{j=m}^{n-1} ac^j \\ &= \frac{ac^m - ac^n}{1-c} = \frac{ar^m(1-c^{n-m})}{1-c} \\ &\leq \frac{ac^m}{1-c} \end{aligned}$$

Thus, if $\varepsilon > 0$ is given, we choose N large enough so that $ac^N/(1-c) < \varepsilon$. Then, for $n, m \geq N$, we have $d(x_m, x_n) < \varepsilon$.

Now, since X is complete and (x_n) is a Cauchy sequence, it converges. Let x be the limit. Since f is continuous, from $x_n \to x$, it follows that $f(x_n) \to f(x)$. But $f(x_n) = x_{n+1}$, so $f(x_n) \to x$. Therefore, the two limits are equal, $x = f(x)$, implying x is a fixed point. □

Theorem 11 ([20, Thm 9.1])**.** *Let $\{S_1, \ldots, S_m\}$ be an IFS on $D \subset \mathbb{R}^n$.*

$$|S_i(x) - S_i(y)| \leq c_i|x - y| \quad (x, y) \in D \tag{5.1}$$

with $c_i < 1$ for each i. Then there exists a unique attractor F such that

$$F = \bigcup_{i=1}^{m} S_i(F) \tag{5.2}$$

Moreover, if we define a transformation $S : \mathcal{S} \to \mathcal{S}$ by

$$S(E) = \bigcup_{i=1}^{m} S_i(E)$$

for $E \in \mathcal{S}$, and if we let S^k be the k-th iterate of S so that $S^0(E) = E$ and $S^k(E) = S\left(S^{k-1}(E)\right)$ for $k \geq 1$, then

$$F = \bigcap_{k=0}^{\infty} S^k(E) \tag{5.3}$$

for every set $E \in \mathcal{S}$ such that $S_i(E) \subset E$ for all i.

Proof. If $A, B \in \mathcal{S}$ then

$$d(S(A), S(B)) = d\left(\bigcup_{i=1}^{m} S_i(A), \bigcup_{i=1}^{m} S_i(B)\right) \leq \max_{1 \leq i \leq m} d(S_i(A), S_i(B))$$

by utilizing the definition of the metric d. It is observed that if the δ-neighborhood $(S_i(A))_\delta$ contains $S_i(B)$ for all i, then $\left(\bigcup_{i=1}^m S_i(A)\right)_\delta$ contains $\bigcup_{i=1}^m S_i(B)$, and vice versa. Based on equation (5.1),

$$d(S(A), S(B)) \leq \left(\max_{1 \leq i \leq m} c_i \right) d(A, B). \tag{5.4}$$

From Proposition 55 d is a complete metric space. From 5.4 and by the fact that $0 < \max_{1 \leq i \leq m} c_i < 1$ we conclude that S is a contraction on the complete metric space $(\mathcal{S}, d)$. By Theorem 10, S possesses a unique fixed point. This indicates that there exists a unique set $F \in \mathcal{S}$ such that $S(F) = F$, as described in equation (5.2). Additionally, $S^k(E) \to F$ as $k \to \infty$. Particularly, if $S_i(E) \subset E$ for all i, then $S(E) \subset E$, leading to $S^k(E)$ forming a decreasing sequence of non-empty compact sets containing F, with their intersection being $\bigcap_{k=0}^{\infty} S^k(E)$, which necessarily equals F. □

We conclude by noticing that the primary characteristic of an IFS is its ability to define a unique attractor, typically exhibiting fractal properties. Various categories of iterated function systems are of particular significance. When the functions $\{S_1, \ldots, S_m\}$ are similarities, the resulting attractor F is termed self-similar, if they are affine transformations, F is labeled as self-affine [19].

Example 48. *Let c denote any real number such that $0 < c < 1$. Then the interval $[0, 1]$ serves as the attractor for the similarity defined on $\mathbb{R}$ by $S_1(x) = cx$ and $S_2(x) = (1-c)x+c$, as $S_1([0,1]) \cup S_2([0,1]) = [0, c] \cup [c, 1] = [0, 1]$. It's evident that both S_1 and S_2 are contractions. Therefore, according to Theorem 11, $[0, 1]$ stands as the unique non-empty compact attractor for S_1 and S_2.*

Example 49. *It is easy to see that the Cantor dust F (see Figure 3.10) is the attractor of the four following similarities*

$$S_1(x, y) = \left(\tfrac{1}{4}x, \tfrac{1}{4}y + \tfrac{1}{2}\right), \qquad S_2(x, y) = \left(\tfrac{1}{4}x + \tfrac{1}{4}, \tfrac{1}{4}y\right),$$

$$S_3(x, y) = \left(\tfrac{1}{4}x + \tfrac{1}{2}, \tfrac{1}{4}y + \tfrac{3}{4}\right), \quad S_4(x, y) = \left(\tfrac{1}{4}x + \tfrac{3}{4}, \tfrac{1}{4}y + \tfrac{1}{4}\right)$$

so that $F = S_1(F) \cup S_2(F) \cup S_3(F) \cup S_4(F)$.

By Theorem 11, if we choose any compact set $E \in \mathcal{S}$ we get that the sets

$$S^k(E) = \bigcup_{\mathcal{I}_k} S_{i_1} \circ \cdots \circ S_{i_k}(E) = \bigcup_{\mathcal{I}_k} S_{i_1}\left(S_{i_2}\left(\cdots\left(S_{i_k}(E)\right)\cdots\right)\right)$$

give increasingly good approximations of F, where the union is over the set $\mathcal{I}_k$ of all k-term sequences $(i_1, \ldots, i_k)$ with $1 \leq i_j \leq m$. Thus, by plotting $S^k(E)$ we get an approximation of F.

Since (5.4) implies $d(S(E), F) = d(S(E), S(F)) \leq c d(E, F)$, we have $d\left(S^k(E), F\right) \leq c^k d(E, F)$, where $c = \max_{1 \leq i \leq m} c_i < 1$, therefore $d\left(S^k(E), F\right) \to 0$.

Moreover, if $S_i(E)$ is included in E for every i, and x is a point in F, then, according to (5.3), there exists a sequence $(i_1, i_2, \ldots)$ (which might not

be unique) such that x belongs to $S_{i_1} \circ \ldots \circ S_{i_k}(E)$ for all k. This sequence serves as a natural code for x, expressed as

$$x = x_{i_1,i_2,\ldots} = \bigcap_{k=1}^{\infty} S_{i_1} \circ \ldots \circ S_{i_k}(E),$$

thus F can be represented as $F = \bigcup \{x_{i_1,i_2,\ldots}\}$. This representation of $x_{i_1,i_2,\ldots}$ remains consistent regardless of the choice of E, as long as $S_i(E)$ is contained in E for all i. Note also that if the union in equation (5.2) is disjoint, then it follows that F must be totally disconnected, assuming the S_i are injections. This is because if $x_{i_1,i_2,\ldots} \neq x_{i'_1,i'_2,\ldots}$, we can find an index k such that $(i_1, \ldots, i_k) \neq (i'_1, \ldots, i'_k)$. Consequently, the disjoint closed sets $S_{i_1} \circ \ldots \circ S_{i_k}(F)$ and $S_{i'_1} \circ \ldots \circ S_{i'_k}(F)$ separate these two points.

If F is a fractal, the approximations $S^k(E)$ are sometimes called pre-fractals for F [19, p. 31]. The $S_{i_1} \circ \ldots \circ S_{i_k}(E)$ are called the level-k sets of the construction [20, p. 127].

The pre-fractals $S^k(E)$ provide the standard construction of many fractals for a suitably chosen initial set E. For example, if we take $E = [0,1] \times [0,1]$, in the previous example of the Cantor dust, then with this initial choice of the set E, we clearly see that $S^k(E) = E_k$ (compare to Example 7).

Example 50. *Consider $S_1(x) = \frac{1}{3}x, S_2(x) = \frac{1}{3}x + \frac{2}{3}$ from Example 47 for the Cantor set F. If $E = [0,1]$ then $S^k(E) = E_k$, the set of 2^k intervals of length 3^{-k} obtained at the k-th stage of the usual Cantor set construction (see Example 2).*

In the next example we find an IFS for the Koch curve.

Recall that the matrix which represents a rotation about the origin in the plane with angle θ is given by

$$\begin{pmatrix} \cos\theta & -\sin\theta \\ \sin\theta & \cos\theta \end{pmatrix}$$

Example 51 (Koch curve, [20, Exercise 9.4])**.** *First observe that the generator E_1 of the Koch curve (see Figure 3.3) has vertices $(0,0), \left(\frac{1}{3}, 0\right), \left(\frac{1}{2}, \frac{\sqrt{3}}{6}\right), \left(\frac{2}{3}, 0\right)$ and $(1,0)$. The contracting similarities maps are constructed with a composition of a rotation by $\pm\pi/3$, if needed, a scaling factor of $\frac{1}{3}$ and a translation. The IFS $\{S_1, S_2, S_3, S_4\}$ that produce as an attractor the Koch curve F is given*

by

$$
\begin{aligned}
S_1\begin{pmatrix} x \\ y \end{pmatrix} &= \frac{1}{3}\begin{pmatrix} x \\ y \end{pmatrix} \\
S_2\begin{pmatrix} x \\ y \end{pmatrix} &= \frac{1}{3}\begin{pmatrix} \frac{1}{2} & -\frac{\sqrt{3}}{2} \\ \frac{\sqrt{3}}{2} & \frac{1}{2} \end{pmatrix}\begin{pmatrix} x \\ y \end{pmatrix} + \begin{pmatrix} \frac{1}{3} \\ 0 \end{pmatrix} \\
S_3\begin{pmatrix} x \\ y \end{pmatrix} &= \frac{1}{3}\begin{pmatrix} \frac{1}{2} & \frac{\sqrt{3}}{2} \\ -\frac{\sqrt{3}}{2} & \frac{1}{2} \end{pmatrix}\begin{pmatrix} x \\ y \end{pmatrix} + \begin{pmatrix} \frac{1}{2} \\ \frac{\sqrt{3}}{6} \end{pmatrix} \\
S_4\begin{pmatrix} x \\ y \end{pmatrix} &= \frac{1}{3}\begin{pmatrix} x \\ y \end{pmatrix} + \begin{pmatrix} \frac{2}{3} \\ 0 \end{pmatrix}.
\end{aligned}
$$

Next examples illustrates the construction of an IFS for the Sierpinksi triangle.

Example 52 (Sierpinksi triangle, [41])**.** *The set E_1 (see Example 6) can be generated by resizing three copies of E_0, each by a factor of $\frac{1}{2}$, and then shifting two of the smaller triangles to arrange them as desired. If we visualize E_0 with its bottom side lying along the x-axis, with vertices at the origin and at the point $(1, 0)$, then we need to move two of the scaled triangles so that their lower left vertices are located at $(1/2, 0)$ and $(1/4, \sqrt{3}/4)$ respectively. The IFS $\{S_1, S_2, S_3\}$ that produce as an attractor the Sierpinksi triangle F is then given by*

$$
\begin{aligned}
S_1\begin{pmatrix} x \\ y \end{pmatrix} &= \begin{pmatrix} \frac{1}{2} & 0 \\ 0 & \frac{1}{2} \end{pmatrix}\begin{pmatrix} x \\ y \end{pmatrix} \\
S_2\begin{pmatrix} x \\ y \end{pmatrix} &= \begin{pmatrix} \frac{1}{2} & 0 \\ 0 & \frac{1}{2} \end{pmatrix}\begin{pmatrix} x \\ y \end{pmatrix} + \begin{pmatrix} \frac{1}{2} \\ 0 \end{pmatrix} \\
S_3\begin{pmatrix} x \\ y \end{pmatrix} &= \begin{pmatrix} \frac{1}{2} & 0 \\ 0 & \frac{1}{2} \end{pmatrix}\begin{pmatrix} x \\ y \end{pmatrix} + \begin{pmatrix} \frac{1}{4} \\ \frac{\sqrt{3}}{4} \end{pmatrix}
\end{aligned}
$$

Example 53 ([20, Exercise 9.5])**.** *Consider the fractal F depicted in Figure 5.1, constructed starting from a filled unit square. An IFS for F is given by*

$$
\begin{gathered}
S_1(x, y) = (x/4, y/4), \quad S_2(x, y) = (x/4 + 3/4, y/4), \\
S_3(x, y) = (x/4 + 3/4, y/4 + 3/4), \quad S_4(x, y) = (x/4, y/4 + 3/4) \\
S_5(x, y) = (x/2 + 1/4, y/2 + 1/4).
\end{gathered}
$$

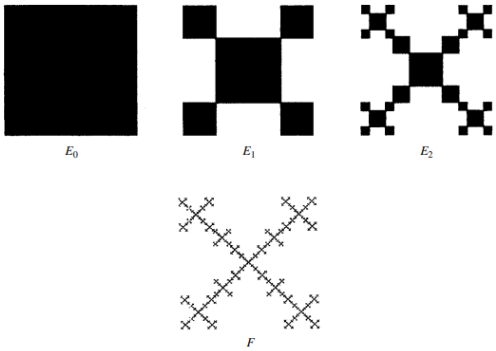

Figure 5.1: Self-similar fractal with two different similarity ratios.
Source: [20, p. xxi]

Example 54 (Sierpinski carpet, [41])**.** *Consider the Sierpinski carpet (see Example 16). Recall that F is made up of 8 copies of itself scaled by a scale factor of $\frac{1}{3}$. If we consider the original square E_0 to have a unit size with opposite corners at $(0,0)$ and $(1,1)$, then an iterative function system (IFS) describing the scaling by a factor of $c = \frac{1}{3}$ and the translations necessary to arrange the eight squares to form E_1 can be expressed through the following similarities*

$$
\begin{aligned}
S_1\begin{pmatrix} x \\ y \end{pmatrix} &= \begin{pmatrix} \frac{1}{3} & 0 \\ 0 & \frac{1}{3} \end{pmatrix}\begin{pmatrix} x \\ y \end{pmatrix} \\
S_2\begin{pmatrix} x \\ y \end{pmatrix} &= \begin{pmatrix} \frac{1}{3} & 0 \\ 0 & \frac{1}{3} \end{pmatrix}\begin{pmatrix} x \\ y \end{pmatrix} + \begin{pmatrix} 0 \\ \frac{1}{3} \end{pmatrix} \\
S_3\begin{pmatrix} x \\ y \end{pmatrix} &= \begin{pmatrix} \frac{1}{3} & 0 \\ 0 & \frac{1}{3} \end{pmatrix}\begin{pmatrix} x \\ y \end{pmatrix} + \begin{pmatrix} 0 \\ \frac{2}{3} \end{pmatrix} \\
S_4\begin{pmatrix} x \\ y \end{pmatrix} &= \begin{pmatrix} \frac{1}{3} & 0 \\ 0 & \frac{1}{3} \end{pmatrix}\begin{pmatrix} x \\ y \end{pmatrix} + \begin{pmatrix} \frac{1}{3} \\ 0 \end{pmatrix} \\
S_5\begin{pmatrix} x \\ y \end{pmatrix} &= \begin{pmatrix} \frac{1}{3} & 0 \\ 0 & \frac{1}{3} \end{pmatrix}\begin{pmatrix} x \\ y \end{pmatrix} + \begin{pmatrix} \frac{1}{3} \\ \frac{2}{3} \end{pmatrix} \\
S_6\begin{pmatrix} x \\ y \end{pmatrix} &= \begin{pmatrix} \frac{1}{3} & 0 \\ 0 & \frac{1}{3} \end{pmatrix}\begin{pmatrix} x \\ y \end{pmatrix} + \begin{pmatrix} \frac{2}{3} \\ 0 \end{pmatrix} \\
S_7\begin{pmatrix} x \\ y \end{pmatrix} &= \begin{pmatrix} \frac{1}{3} & 0 \\ 0 & \frac{1}{3} \end{pmatrix}\begin{pmatrix} x \\ y \end{pmatrix} + \begin{pmatrix} \frac{2}{3} \\ \frac{1}{3} \end{pmatrix} \\
S_8\begin{pmatrix} x \\ y \end{pmatrix} &= \begin{pmatrix} \frac{1}{3} & 0 \\ 0 & \frac{1}{3} \end{pmatrix}\begin{pmatrix} x \\ y \end{pmatrix} + \begin{pmatrix} \frac{2}{3} \\ \frac{2}{3} \end{pmatrix}
\end{aligned}
$$

Example 55 (Koch snowflake, [41])**.** *Here is an example of an iterated function system describing the Koch snowflake F (see Figures 3.7 and 4.6).*

$$
\begin{aligned}
S_1 \begin{pmatrix} x \\ y \end{pmatrix} &= \begin{pmatrix} \frac{1}{2} & -\frac{\sqrt{3}}{6} \\ \frac{\sqrt{3}}{6} & \frac{1}{2} \end{pmatrix} \begin{pmatrix} x \\ y \end{pmatrix} \\
S_2 \begin{pmatrix} x \\ y \end{pmatrix} &= \begin{pmatrix} \frac{1}{3} & 0 \\ 0 & \frac{1}{3} \end{pmatrix} \begin{pmatrix} x \\ y \end{pmatrix} + \begin{pmatrix} \frac{1}{\sqrt{3}} \\ \frac{1}{3} \end{pmatrix} \\
S_3 \begin{pmatrix} x \\ y \end{pmatrix} &= \begin{pmatrix} \frac{1}{3} & 0 \\ 0 & \frac{1}{3} \end{pmatrix} \begin{pmatrix} x \\ y \end{pmatrix} + \begin{pmatrix} 0 \\ \frac{2}{3} \end{pmatrix} \\
S_4 \begin{pmatrix} x \\ y \end{pmatrix} &= \begin{pmatrix} \frac{1}{3} & 0 \\ 0 & \frac{1}{3} \end{pmatrix} \begin{pmatrix} x \\ y \end{pmatrix} + \begin{pmatrix} -\frac{1}{\sqrt{3}} \\ \frac{1}{3} \end{pmatrix} \\
S_5 \begin{pmatrix} x \\ y \end{pmatrix} &= \begin{pmatrix} \frac{1}{3} & 0 \\ 0 & \frac{1}{3} \end{pmatrix} \begin{pmatrix} x \\ y \end{pmatrix} + \begin{pmatrix} -\frac{1}{\sqrt{3}} \\ -\frac{1}{3} \end{pmatrix} \\
S_6 \begin{pmatrix} x \\ y \end{pmatrix} &= \begin{pmatrix} \frac{1}{3} & 0 \\ 0 & \frac{1}{3} \end{pmatrix} \begin{pmatrix} x \\ y \end{pmatrix} + \begin{pmatrix} 0 \\ -\frac{2}{3} \end{pmatrix} \\
S_7 \begin{pmatrix} x \\ y \end{pmatrix} &= \begin{pmatrix} \frac{1}{3} & 0 \\ 0 & \frac{1}{3} \end{pmatrix} \begin{pmatrix} x \\ y \end{pmatrix} + \begin{pmatrix} \frac{1}{\sqrt{3}} \\ -\frac{1}{3} \end{pmatrix}
\end{aligned}
$$

Proof. This specific IFS is inspired by the following picture

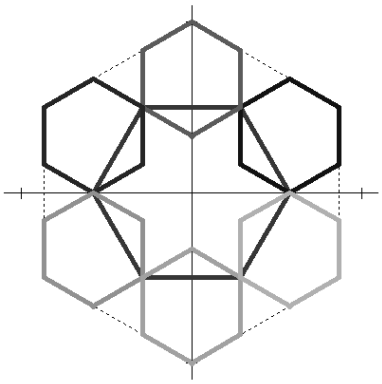

Figure 5.2: Construction of an IFS for the Koch snowflake.
Source: [41]

We start with an inscribed regular hexagon within a unit circle (depicted by dotted lines). The original hexagon accommodates six smaller hexagons when scaled down by a factor of 1/3. Utilizing the six points where these smaller hexagons intersect, generate another bigger hexagon. This hexagon's sides possess a length equivalent to $\sqrt{3}$ times the length of the smaller hexagons' sides, thus each side of the central hexagon is $\sqrt{3}\cdot(1/3) = 1/\sqrt{3}$. Consequently, the central hexagon has been scaled down by $1/\sqrt{3}$ and rotated by 30°.

Since the affine transformations for the six smaller hexagons entail solely scaling by 1/3 and translations, each vertex of the initial hexagon serves as a

fixed point for the transformation that relocates the scaled version back to that vertex. Assuming a particular vertex V for the corresponding transformation $f(\mathbf{x}) = (1/3)\mathbf{x} + b$, then

$$V = f(V) = \frac{1}{3}V + b \quad \Rightarrow \quad b = \frac{2}{3}V$$

Initiating with the vertex in the first quadrant, the vertices are situated at points $(\cos(30° + 60°k), \sin(30° + 60°k))$ for $k = 0, 1, 2, 3, 4, 5$. Consequently, the translation for the hexagon in the first quadrant, for instance, is

$$b = \frac{2}{3}\begin{pmatrix} \cos 30° \\ \sin 30° \end{pmatrix} = \frac{2}{3}\begin{pmatrix} \sqrt{3}/2 \\ 1/2 \end{pmatrix} = \begin{pmatrix} 1/\sqrt{3} \\ 1/3 \end{pmatrix}$$

The remaining translations can be derived in a similar manner. The central hexagon necessitates no translation post scaling and rotation. □

Example 56 (Barnsley Fern, [3])**.** *Barnsley [3] created the fern fractal F, a widely renowned fractal set, utilizing just four affine transformations. The IFS for F is given by*

$$S_i = \begin{pmatrix} r\cos\theta & -s\sin\phi \\ r\sin\theta & s\cos\phi \end{pmatrix}\begin{pmatrix} x \\ y \end{pmatrix} + \begin{pmatrix} e \\ f \end{pmatrix}$$

	r	s	θ	ϕ	e	f
S_1	0.85	0.85	−2.5	−2.5	0	1.6
S_2	0.3	0.34	49	49	0	1.6
S_3	0.3	0.37	120	−50	0	0.44
S_4	0	0.16	0	0	0	0

The angles are given in degrees. The initiator of the IFS is a rectangle.

Figure 5.3: The Barnsley Fern.
Source: [20, p. 146]

IFS pose two main challenges: representing a given set as the attractor of an IFS, and conversely, displaying the attractor of an IFS. While identifying

an IFS with a specific set as its unique attractor can often be done visually, especially if the set is self-similar or self-affine, it's not always feasible to find an exact match. However, it's typically possible to find an IFS with an attractor that closely approximates the desired set.

Understanding which objects can be represented or approximated by IFS attractors, as well as how to find contractions that lead to accurate representations, is crucial. The next theorem, called Collage Theorem, also known as Hutchinson-Barnsley Theorem, provides insight into the quality of approximation a set achieves as the attractor of an IFS.

Theorem 12 (Collage Theorem, [3, Thm 10.1])**.** *Let $\{S_1, S_2, \ldots, S_m\}$ be an iterated function system (IFS) defined on a subset $D \subset \mathbb{R}^n$, such that for each $i \in 1, \ldots, m$, we have:*

$$|S_i(x) - S_i(y)| \leq c|x - y|$$

for all $x, y \in D$, where $0 < c < 1$. Let $E \subset D$ be any non-empty compact set. Then, for the attractor F of the IFS, the following inequality holds:

$$d(E, F) \leq d\left(E, \bigcup_{i=1}^{m} S_i(E)\right) \frac{1}{1-c} \tag{5.5}$$

where F is the attractor for the IFS and d is the Hausdorff metric.

Proof. By the triangle inequality for the Hausdorff metric, the definition of attractor and (5.4)

$$\begin{aligned} d(E, F) &\leq d\left(E, \bigcup_{i=1}^{m} S_i(E)\right) + d\left(\bigcup_{i=1}^{m} S_i(E), F\right) \\ &= d\left(E, \bigcup_{i=1}^{m} S_i(E)\right) + d\left(\bigcup_{i=1}^{m} S_i(E), \bigcup_{i=1}^{m} S_i(F)\right) \\ &\leq d\left(E, \bigcup_{i=1}^{m} S_i(E)\right) + cd(E, F) \end{aligned}$$

Solving the inequality for $d(E, F)$ yields the result. □

Corollary 9 ([20, Cor. 9.14])**.** *For any non-empty compact subset $E \subset \mathbb{R}^n$ and a given $\delta > 0$, there exist contracting similarities $S_1, \ldots, S_m$ with attractor F such that the $d(E, F) < \delta$.*

Proof. Using the compactness of E, let $B_1, \ldots, B_m$ be a collection of balls that cover E with centres in E, each with radius at most $\frac{1}{4}\delta$. Then $E \subset \bigcup_{i=1}^{m} B_i \subset E_{\delta/4}$. For every i, define S_i be any contracting similarity of ratio less than $\frac{1}{2}$ that maps E into B_i. Then $S_i(E) \subset B_i \subset (S_i(E))_{\delta/2}$, thus $(\bigcup_{i=1}^{m} S_i(E)) \subset E_{\delta/4}$ and $E \subset \bigcup_{i=1}^{m} (S_i(E))_{\delta/2}$. By the Hausdorff metric, $d\left(E, \bigcup_{i=1}^{m} S_i(E)\right) \leq \frac{1}{2}\delta$. Therefore by (5.5) we conclude that $d(E, F) < \delta$ where F denotes the attractor. □

5.2 Fractal Dimension of Self-Similar Sets

Iterated function systems offer the advantage of facilitating the calculation or estimation of the dimension of the attractor, particularly when the defining contractions are relatively straightforward. In the scenario where the contractions are contracting similarities, both the box-counting and Hausdorff dimensions of these self-similar attractors can be elegantly formulated using the contraction ratios of the systems. This section presents the proof of the main theorem and then explores some examples demonstrating how this theorem can be applied to compute fractal dimensions.

Definition 49 (open set condition, [20, p. 129])**.** *Consider an iterated function system (IFS) denoted by $\{S_1, \ldots, S_m\}$. This system fulfills the open set condition if there exists a non-empty, bounded, and open set V such that*

$$\bigcup_{i=1}^{m} S_i(V) \subset V$$

and the sets $S_i(V)$ are pairwise disjoint.

Before we can demonstrate a formula for calculating the dimension of self-similar sets, it is essential to establish the following lemma.

Lemma 4 ([20, Lemma 9.2])**.** *Let $\{V_i\}$ be a collection of disjoint open subsets of $\mathbb{R}^n$ such that each V_i contains a ball of radius $a_1 r$ and is contained in a ball of radius $a_2 r$. Then any ball B of radius r intersects at most $(1 + 2a_2)^n a_1^{-n}$ of the closures $\overline{V_i}$.*

Proof. If $\overline{V_i}$ intersects B, then $\overline{V_i}$ is contained in a ball of radius

$$r + |V_i| \leq (1 + 2a_2)\, r$$

centered at the center of B. Assume that q of the sets $\overline{V_i}$ intersect B. A single ball with a radius of $(1 + 2a_2)\, r$ contains all q sets $\overline{V_i}$, and consequently includes q balls each with a radius of $a_1 r$. By summing the volumes of these q inner balls, we obtain

$$\begin{aligned} q\,(a_1 r)^n &\leq (1 + 2a_2)^n\, r^n \\ q &\leq (1 + 2a_2)^n\, a_1^{-n}. \end{aligned}$$

□

Theorem 13 ([20, Thm 9.13])**.** *Consider an IFS given by $\{S_1, \ldots, S_m\}$ consisting of contracting similarities on $\mathbb{R}^n$ with corresponding ratios $\{c_1, \ldots, c_m\}$ and attractor F.*

$$F = \bigcup_{i=1}^{m} S_i(F) \tag{5.6}$$

Assume that this system satisfies the open set condition and let s be the unique value such that

$$\sum_{i=1}^{m} c_i^s = 1. \tag{5.7}$$

Then

$$\dim_{\mathrm{S}}(F) = \dim_{\mathrm{H}}(F) = \dim_{\mathrm{B}}(F) = s.$$

Moreover, for this value of $s, 0 < \mathcal{H}^s(F) < \infty$.

In particular, if $c_1 = \ldots = c_m = c$ for some $0 < c < 1$, then $\dim_{\mathrm{S}}(F) = \dim_{\mathrm{H}}(F) = \dim_{\mathrm{B}}(F) = \frac{\log m}{\log(1/c)}$.

Proof. Define s in accordance to (5.7). Let $\mathcal{I}_k$ denote the set of all k-term sequences $(i_1, \ldots, i_k)$ with $1 \le i_j \le m$.

For any set A and a specified sequence $(i_1, \ldots, i_k)$ in $\mathcal{I}_k$, let $A_{i_1,\ldots,i_k} = S_{i_1} \circ \cdots \circ S_{i_k}(A)$. Given that F is a fixed point under the IFS, we can express it as the union over all sequences in $\mathcal{I}_k$ of the sets $F_{i_1,\ldots,i_k}$. This can be written as:

$$F = \bigcup_{\mathcal{I}_k} F_{i_1,\ldots,i_k}$$

Then the sets $\{F_{i_1,\ldots,i_k}\}$ cover F. We verify that these coverings of F offer an appropriate upper bound for the Hausdorff measure.

Observe that the composition $S_{i_1} \circ \cdots \circ S_{i_k}$ represents a contracting similarity, where the contraction ratio is given by $c_{i_1} \cdot \ldots \cdot c_{i_k}$.

Thus by (5.7)

$$\sum_{\mathcal{I}_k} |F_{i_1,\ldots,i_k}|^s = \sum_{\mathcal{I}_k} (c_{i_1} \cdots c_{i_k})^s |F|^s = \left(\sum_{i_1} c_{i_1}^s\right) \cdots \left(\sum_{i_k} c_{i_k}^s\right) |F|^s = |F|^s \tag{5.8}$$

For any given $\delta > 0$, we can select a sufficiently large k such that $(\max_i c_i)^k |F| \le \delta$. Since $|F_{i_1,\ldots,i_k}| \le (\max_i c_i)^k |F|$, the sets $\{F_{i_1,\ldots,i_k}\}$ cover F with $|F_{i_1,\ldots,i_k}| \le \delta$ for all sequences $(i_1, \ldots, i_k)$ in $\mathcal{I}_k$.

Consequently, by (5.8) $\mathcal{H}^s(F) \le \sum_{\mathcal{I}_k} |F_{i_1,\ldots,i_k}|^s = |F|^s$.

We proceed now with the lower bound. Let $\mathcal{I}$ be the set of all infinite sequences $(i_1, i_2 \ldots)$ with $1 \le i_j \le m$, and define $I_{i_1,\ldots,i_k}$ to be the subset of $\mathcal{I}$ consisting only of sequences that start with $i_1, \ldots, i_k$.

Then one may put a mass distribution μ on $\mathcal{I}$ such that $\mu(I_{i_1,\ldots,i_k}) = (c_{i_1} \cdots c_{i_k})^s$. μ is indeed a mass distribution on subsets of $\mathcal{I}$, as $(c_{i_1} \cdots c_{i_k})^s = \sum_{i=1}^{m} (c_{i_1} \cdots c_{i_k} c_i)^s$, then it follows directly from $\mu(I_{i_1,\ldots,i_k}) = \sum_{i=1}^{m} \mu(I_{i_1,\ldots,i_k,i})$ and also from (5.7) $\mu(\mathcal{I}) = 1$.

We transfer μ to a mass distribution $\tilde{\mu}$ on F in a natural way by defining for a subset A in F $\tilde{\mu}(A) = \mu(\{I_{i_1,\ldots,i_k} : x_{i_1,\ldots,i_k,\ldots} \in A\})$. where $x_{i_1,i_2,\ldots} =$

$\bigcap_{k=1}^{\infty} F_{i_1,\ldots,i_k}$. We check now that $\tilde{\mu}$ satisfies the conditions of the Mass distribution principle (Proposition 38).

Let V denote the open set ensured by the open set condition (Def. 49). Then $\bar{V} \supset S(\bar{V}) = \bigcup_{i=1}^{m} S_i(\bar{V})$ and the decreasing sequence of iterates $S^k(\bar{V})$ converges to F, see (5.3). Therefore $\bar{V} \supset F$ and $\bar{V}_{i_1,\ldots,i_k} \supset F_{i_1,\ldots,i_k}$ for every finite sequence $(i_1,\ldots,i_k)$.

Let B be any ball with a radius $r < 1$. To estimate $\tilde{\mu}(B)$, we focus on the sets $V_{i_1,\ldots,i_k}$ whose diameters are comparable to that of B and whose closures intersect $F \cap B$. We truncate each infinite sequence $(i_1, i_2, \ldots) \in \mathcal{I}$ after the initial term i_k for which

$$\left(\min_{1\le i\le m} c_i\right) r \le c_{i_1} c_{i_2} \cdots c_{i_k} \le r \tag{5.9}$$

and denote by $\mathcal{Q}$ the finite set comprising all (finite) sequences derived in this manner.

For every infinite sequence $(i_1, i_2, \ldots) \in \mathcal{I}$, there exists precisely one value of k such that $(i_1,\ldots,i_k) \in \mathcal{Q}$. Since $V_1,\ldots,V_m$ are disjoint, the sets $V_{i_1,\ldots,i_k,1},\ldots,V_{i_1,\ldots,i_k,m}$ for each $(i_1,\ldots,i_k)$ are also disjoint. By employing this nested property, we conclude that the collection of open sets $\{V_{i_1,\ldots,i_k} : (i_1,\ldots,i_k) \in \mathcal{Q}\}$ is disjoint.

Furthermore, we have:

$$F = \bigcup_{\mathcal{I}} F_{i_1,i_2,\ldots} \subset \bigcup_{\mathcal{Q}} F_{i_1,\ldots,i_k} \subset \bigcup_{\mathcal{Q}} \bar{V}_{i_1,\ldots,i_k}$$

We select values for a_1 and a_2 such that V contains a ball of radius a_1 and is contained in a ball of radius a_2. Then, for every $(i_1,\ldots,i_k) \in \mathcal{Q}$, the set $V_{i_1,\ldots,i_k}$ contains a ball of radius $c_{i_1}\cdots c_{i_k} a_1$, and consequently, one of radius $(\min_i c_i)\, a_1 r$. It is also contained in a ball of radius $c_{i_1}\cdots c_{i_k} a_2$, and thus within a ball of radius $a_2 r$. Let $\mathcal{Q}_1$ denote the sequences $(i_1,\ldots,i_k)$ in $\mathcal{Q}$ such that B intersects $\bar{V}_{i_1,\ldots,i_k}$. According to Lemma 4, there are at most $q = (1+2a_2)^n\, a_1^{-n}\, (\min_i c_i)^{-n}$ sequences in $\mathcal{Q}_1$.

Then

$$\begin{aligned}
\tilde{\mu}(B) &= \tilde{\mu}(F \cap B) \\
&= \mu\left(\{I_{i_1,\ldots,i_k} : x_{i_1,\ldots,i_k,\ldots} \in F \cap B\}\right) \\
&\le \mu\left(\left\{I_{i_1,\ldots,i_k} : x_{i_1,\ldots,i_k,\ldots} \in \left(\bigcup_{\mathcal{Q}} \bar{V}_{i_1,\ldots,i_k}\right) \cap B\right\}\right) \quad \le \mu\left\{\bigcup_{\mathcal{Q}_1} I_{i_1,\ldots,i_k}\right\}
\end{aligned}$$

Because, if $x_{i_1,i_2,\ldots} \in F \cap B \subset \bigcup_{\mathcal{Q}_1} \bar{V}_{i_1,\ldots,i_k}$, then there is an integer k such that $(i_1,\ldots,i_k) \in \mathcal{Q}_1$. Therefore

$$\begin{aligned}
\tilde{\mu}(B) &\le \sum_{\mathcal{Q}_1} \mu\left(I_{i_1,\ldots,i_k}\right) \\
&= \sum_{\mathcal{Q}_1} \left(c_{i_1}\cdots c_{i_k}\right)^s \le \sum_{\mathcal{Q}_1} r^s \le r^s q
\end{aligned}$$

Considering any set U contained in a ball of radius $|U|$, we obtain $\tilde{\mu}(U) \leq |U|^s q$. Thus, according to the Mass distribution principle, we have $\mathcal{H}^s(F) \geq q^{-1} > 0$, and therefore $\dim_{\mathrm{H}} F = s$.

If $\mathcal{Q}$ is any set of finite sequences such that for every $(i_1, i_2, \ldots) \in \mathcal{I}$, there exists exactly one integer k with $(i_1, \ldots, i_k) \in \mathcal{Q}$, then by induction from (5.7), we derive that $\sum_{\mathcal{Q}} (c_{i_1} c_{i_2} \cdots c_{i_k})^s = 1$. Consequently, if $\mathcal{Q}$ is chosen as in (5.9), it contains at most $(\min_i c_i)^{-s} r^{-s}$ sequences. For each sequence $(i_1, \ldots, i_k) \in \mathcal{Q}$, we have $\left|\bar{V}_{i_1,\ldots,i_k}\right| = c_{i_1} \cdots c_{i_k} |\bar{V}| \leq r|\bar{V}|$. Hence, F can be covered by $(\min_i c_i)^{-s} r^{-s}$ sets of diameter $r|\bar{V}|$ for each $r < 1$. It follows (by taking $N_\delta(F)$ as the smallest number of sets of diameter at most δ that cover F) that $\overline{\dim}_{\mathrm{B}} F \leq s$. Noting that $s = \dim_{\mathrm{H}} F \leq \underline{\dim}_{\mathrm{B}} F \leq \overline{\dim}_{\mathrm{B}} F \leq s$, we complete the proof.

□

The computations utilized in Theorem 13 can be adjusted to approximate the dimension of an attractor F of an IFS comprised of contractions that do not necessarily qualify as similarities.

Proposition 56 ([20, Prop. 9.6])**.** *Consider the attractor F of an iterated function system (IFS) comprising contractions $\{S_1, \ldots, S_m\}$, with corresponding ratios $\{c_1, \ldots, c_m\}$, defined on a closed subset $D \subset \mathbb{R}^n$.*

Then

$$\dim_{\mathrm{H}} F \leq s \text{ and } \overline{\dim}_{\mathrm{B}} F \leq s \text{ where } \sum_{i=1}^{m} c_i^s = 1.$$

Proof. The estimates provided are essentially reflections of the initial and final segments of the proof for Theorem 13, taking into account the inequality $|A_{i_1,\ldots,i_k}| \leq c_{i_1} \cdots c_{i_k} |A|$ for each set A, instead of equality. □

We establish now a useful lower bound for the dimension when the components $S_i(F)$ of F are disjoint.

Proposition 57 ([20, Prop. 9.7])**.** *Consider the iterated function system comprising contractions $\{S_1, \ldots, S_m\}$ defined on a closed subset D of $\mathbb{R}^n$ such that*

$$b_i |x - y| \leqslant |S_i(x) - S_i(y)| \quad (x, y \in D)$$

where $0 < b_i < 1$ for each i. Assume that the attractor F satisfies

$$F = \bigcup_{i=1}^{m} S_i(F)$$

with this union disjoint. Then F is totally disconnected, and the Hausdorff dimension of F satisfies $\dim_{\mathrm{H}} F \geq s$ where

$$\sum_{i=1}^{m} b_i^s = 1.$$

Proof. The proof of this proposition follows a similar procedure to that of Theorem 13, simpler due to the disjoint sets $S_1(F), \ldots, S_m(F)$. More details in [20, Prop. 9.7]. □

Computing the fractal dimension using IFS

Theorem 13 provides a significantly simplified method for determining the dimensions of self-similar fractals compared to the approaches we've encountered previously. Let's look at some examples.

Example 57 (Cantor set)**.** *From Example 47 the Cantor set F is the (unique) attractor of the IFS consisting of the similarities $S_1, S_2 : \mathbb{R} \to \mathbb{R}$ given by*

$$S_1(x) = \frac{1}{3}x \quad S_2(x) = \frac{1}{3}x + \frac{2}{3}.$$

each with contraction ratio $\frac{1}{3}$. Thus

$$F = \bigcup_{i=1}^{2} S_i(F).$$

The open set condition holds for $V = (0, 1)$, then $\dim_{\mathrm{S}} F = \dim_{\mathrm{H}} F = \dim_{\mathrm{B}} F = s$ where s is the solution of the equation $\sum_{i=1}^{2} (\frac{1}{3})^s = 1$. Thus

$$\dim_{\mathrm{S}} F = \dim_{\mathrm{H}} F = \dim_{\mathrm{B}} F = \frac{\log 2}{\log 3}.$$

Example 58 (Cantor set)**.** *To construct a different IFS that yields the Cantor set as its unique attractor, we can use the following four similarity transformations on $\mathbb{R}$ that map the interval $E_0 = [0, 1]$ onto the four intervals in E_2:*

$$S_1(x) = \frac{x}{9}, \quad S_2(x) = \frac{x}{9} + \frac{2}{9}, \quad S_3(x) = \frac{x}{9} + \frac{2}{3}, \quad S_4(x) = \frac{x}{9} + \frac{8}{9}.$$

The similarity ratios for these transformations are all $\frac{1}{9}$. Thus, the Cantor set F satisfies the following equation:

$$F = \bigcup_{i=1}^{4} S_i(F).$$

The open set condition holds for $V = (0, 1)$, then $\dim_{\mathrm{S}} F = \dim_{\mathrm{H}} F = \dim_{\mathrm{B}} F = s$ where s is the solution of the equation $\sum_{i=1}^{4} (\frac{1}{9})^s = 1$.

To solve for s, we write:

$$4\left(\frac{1}{9}\right)^s = 1.$$

Taking the logarithm of both sides, we get:

$$\log 4 + s \log\left(\frac{1}{9}\right) = 0,$$

$$s = \frac{\log 4}{\log 9}.$$

We can simplify further by recognizing that:

$$\log 4 = \log 2^2 = 2 \log 2,$$

$$\log 9 = \log 3^2 = 2 \log 3.$$

Thus,

$$s = \frac{2 \log 2}{2 \log 3} = \frac{\log 2}{\log 3}.$$

This confirms that the fractal dimension of the Cantor set remains the same under this different IFS construction.

Example 59 (Koch curve)**.** *An IFS* $\{S_1, S_2, S_3, S_4\}$ *that has the Koch curve as attractor is given by Example 51. Thus*

$$F = \bigcup_{i=1}^{4} S_i(F).$$

Each S_i *is a similarity with ratio of* $\frac{1}{3}$*. The open set condition holds by taking* V *to be the interior of the isosceles triangle with vertices* $(0,0), \left(\frac{1}{2}, \frac{\sqrt{3}}{6}\right)$ *and* $(1,0)$*. Then* $\dim_{\mathrm{S}} F = \dim_{\mathrm{H}} F = \dim_{\mathrm{B}} F = s$ *where* s *is the solution of the equation* $\sum_{i=1}^{4} (\frac{1}{3})^s = 1$*. Thus*

$$\dim_{\mathrm{S}} F = \dim_{\mathrm{H}} F = \dim_{\mathrm{B}} F = \frac{\log 4}{\log 3}.$$

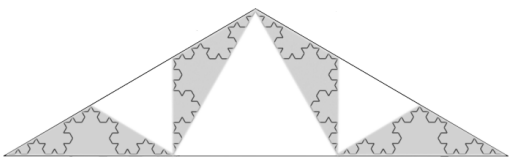

Figure 5.4: The open set condition for the Koch curve.
Source: [48]

Example 60 (Sierpinski triangle)**.** *An IFS* $\{S_1, S_2, S_3\}$ *that has the Sierpinski triangle as attractor is given by Example 52. Thus*

$$F = \bigcup_{i=1}^{3} S_i(F).$$

The IFS consists of three similarities each of ratio $\frac{1}{2}$*. The open set condition holds, by taking* V *as the interior of the initial triangle* E_0*. Then* $\dim_{\mathrm{S}} F = \dim_{\mathrm{H}} F = \dim_{\mathrm{B}} F = s$ *where* s *is the solution of the equation* $\sum_{i=1}^{3} (\frac{1}{2})^s = 1$*. Thus*

$$\dim_{\mathrm{S}} F = \dim_{\mathrm{H}} F = \dim_{\mathrm{B}} F = \frac{\log 3}{\log 2}.$$

Example 61 (Sierpinski carpet)**.** *An IFS* $\{S_1, S_2, S_3, S_4, S_5, S_6, S_7, S_8\}$ *that has the Sierpinski carpet as attractor is given by Example 54. Thus*

$$F = \bigcup_{i=1}^{8} S_i(F).$$

The IFS consists of eight similarities each of ratio $\frac{1}{3}$*. The open set condition holds, by taking* V *as the interior of the initial square* E_0*. Then* $\dim_{\mathrm{S}} F = \dim_{\mathrm{H}} F = \dim_{\mathrm{B}} F = s$ *where* s *is the solution of the equation* $\sum_{i=1}^{8} (\frac{1}{3})^s = 1$*. Thus*

$$\dim_{\mathrm{S}} F = \dim_{\mathrm{H}} F = \dim_{\mathrm{B}} F = \frac{\log 8}{\log 3}.$$

Example 62 ([20, Exercise 10.1])**.** *Let* F *be the set of numbers in* $[0, 1]$ *containing only even digits. We have already determined that* $\dim_{\mathrm{H}} F = \frac{\log 5}{\log 10}$ *(see Example 34). Now, we will explore an alternative approach using IFS and Theorem 13 to find the Hausdorff dimension. In particular* F *is the attractor of the IFS of similarities on* $\mathbb{R}$ $\{S_1, \ldots, S_5\}$ *where* $S_i = \frac{1}{10}x + \frac{i-1}{5} \quad (i = 1, \ldots, 5)$*. Moreover*

$$\bigcup_{i=1}^{5} S_i(0,1) = \bigcup_{i=1}^{5} S_i\left(\frac{i-1}{5}, \frac{i-1}{5} + \frac{1}{10}\right) \subset (0,1).$$

Therefore the open set condition holds by taking $V = (0, 1)$*, so by Theorem 13,* $\dim_{\mathrm{H}} F = s$*, where* $5 \cdot (1/10)^s = 1$ *and thus*

$$\dim_{\mathrm{H}} F = \dim_{\mathrm{B}} F = \dim_{\mathrm{S}} F = \frac{\log 5}{\log 10}.$$

Example 63. *The fractal* F *of Example 53 is the attractor of the IFS* $\{S_1, S_2, S_3, S_4, S_5\}$*. Thus*

$$F = \bigcup_{i=1}^{5} S_i(F).$$

The ratios of these similarities are $\frac{1}{4}, \frac{1}{4}, \frac{1}{4}, \frac{1}{4}, \frac{1}{2}$ *respectively. The open set condition holds, by taking* V *as the interior of the initial square* E_0*. Then* $\dim_{\mathrm{S}} F = \dim_{\mathrm{H}} F = \dim_{\mathrm{B}} F = s$ *where* s *is the solution of the equation* $4(\frac{1}{4})^s + (\frac{1}{2})^s$*. This can be solved by putting* $x = (\frac{1}{2})^s$ *so that*

$$4x^2 + x - 1 = 0$$

Thus

$$x = \frac{(-1 \pm \sqrt{17})}{8}.$$

As $x = (\frac{1}{2})^s > 0$*, it follows that* $(\frac{1}{2})^s = \frac{-1}{8} + \frac{\sqrt{17}}{8}$*. Then*

$$s = \frac{-\log(-1/8 + \sqrt{17}/8)}{\log 2}.$$

Chapter 6

Complex Dynamics

Julia sets, named after the French mathematician Gaston Julia, offer a captivating demonstration of how a seemingly straightforward procedure can produce highly complex sets with fractal characteristics. Julia sets are intricate fractal sets in the complex plane resulting from the iteration of functions of a complex variable. This field, arising from dynamical systems, is known as complex dynamics and explores the behavior of sequences $f^k(z)$ for various initial z. Similar to the Mandelbrot set, which focuses on specific quadratic functions iterated in the complex plane, Julia sets exhibit remarkable complexity and beauty, making them not only subjects of mathematical study but also sources of visually stunning fractal imagery. Prior to the emergence of the Mandelbrot set, exploration into the dynamics of complex mappings was pioneered by Pierre Fatou and Gaston Julia in the early 20th century [28][22]. The main source for this chapter is [20, chap. 14]. More general details on complex dynamics can be found in [37]. A comprehensive overview of complex analysis is available for example in [35].

6.1 Julia Sets

Let $f : \mathbb{C} \to \mathbb{C}$ be a polynomial of degree $n \geq 2$ with complex coefficients,

$$f(z) = a_0 + a_1 z + a_2 z^2 + \ldots + a_n z^n, \quad a_i \in \mathbb{C}, a_n \neq 0.$$

Let also $f^k(z) = f(f(\ldots f(z)\ldots))$ be the k-fold composition of f with itself. We introduce first some basic definitions. Recall from Def. 48 that if $f(w) = w$ for some $w \in \mathbb{C}$, we call w a fixed point of f.

Definition 50. *The sequence of iterates $\left\{f^k(w)\right\}_{k=1}^{\infty}$ is called the orbit of w under f.*

Definition 51. *If $f^p(w) = w$ for some $p \geq 1$, we call w a periodic point of f.*

Definition 52. *If w is a periodic point of f, the period p of w under f is defined as*

$$p = \min \{n \in \mathbb{N} \mid f^n(w) = w\}$$

Definition 53. *If w is a periodic point with period p, then $\{w, f(w), \ldots, f^{p-1}(w)\}$ is the period p orbit of w.*

Proposition 58. *If an orbit $z_n = f^n(z_0)$ converges to $z \in \mathbb{C}$, then z is a fixed point of f.*

Proof. $f(z) = f(\lim_{n\to\infty} z_n) = \lim_{n\to\infty} f(z_n) = \lim_{n\to\infty} z_{n+1} = z$, by the continuity of f at z. □

Definition 54 (classification of periodic points)**.** *Let w be a periodic point of period p, with $(f^p)'(w) = \lambda$, where the prime denotes complex differentiation. The point w is called attractive, meaning that nearby points tend to converge towards its orbit under iteration by f, if $0 \leq |\lambda| < 1$, and repelling if $|\lambda| > 1$, indicating that points close to its orbit diverge away under iteration by f.*

Remark 19. *In this chapter $|z|$ denotes the modulus of a complex number $z \in \mathbb{C}$.*

Proposition 59. *Consider an attractive fixed point z_0 so that $|f'(z_0)| < 1$. Then there exists $r > 0$ such that for every $z \in B_r(z_0)$, the orbit of z converges to z_0.*

Proof. By continuity of f', as $|f'(z_0)| < 1$, we get $|f'(z_0)| \leq c < 1$ in a small neighbourhood $B_r(z_0)$ of z_0. Then for any $z \in B_r(z_0)$,

$$|f(z) - f(z_0)| \leq c\,|z - z_0|,$$

so f is a contraction there, and by the contraction mapping theorem, any starting point z has its orbit converge to z_0. □

Similar conclusions apply for the case of attracting periodic points and for the real case.

Remark 20. *Following a similar approach to this proof, we can comprehend the notion of repelling. In such instances, the condition $|f(z) - f(z_0)| > C\,|z - z_0|$ near z_0 for some $C > 1$ holds, thereby hindering the convergence of any sequence originating close to z_0 towards z_0.*

Definition 55 (basin of attraction, [20, p. 221])**.** *If w is an attractive fixed point, we define the set*

$$A(w) = \left\{z \in \mathbb{C} : f^k(z) \to w \text{ as } k \to \infty\right\}$$

to be the basin of attraction for the point w.

$A(\infty)$, the basin of attraction of infinity, is defined in an analogous way. We can generalize the space so that $f : \mathbb{C}^* \to \mathbb{C}^*$, with $\mathbb{C}^* = \mathbb{C} \cup \{\infty\}$ being the Riemann sphere. We say that the fixed point $z = \infty$ is an attractive fixed point if $|\frac{1}{f'(z)}| < 1$ [37] and use the convention that $\frac{1}{\infty} = 0$.

Proposition 60 ([20, p. 222])**.** *Let w be a fixed point of f. Then the basin of attraction $A(w)$ is an open set.*

Proof. As w is an attracting point, there exists an open set V containing w within $A(w)$. If $w = \infty$, we can choose V as $\{z : |z| > r\}$, for a sufficiently large r. This assertion implies the openness of $A(w)$. To elaborate, consider any z belonging to $A(w)$ with $f^k(z) \in V$ for some k. It follows that $z \in f^{-k}(V)$, which is open as it is the preimage of an open set under a continuous function. Moreover, the arbitrary union of open sets is an open set. □

Definition 56 (filled-in Julia set, [20, p. 215])**.** *The filled-in Julia set of the polynomial f is defined as*

$$K(f) = \left\{ z \in \mathbb{C} : f^k(z) \not\to \infty \right\}.$$

We introduce now the main definition of the Julia set.

Definition 57 (Julia set, [20, p. 215])**.** *The Julia set of f is the boundary of the filled-in Julia set,*

$$J(f) = \partial K(f).$$

Remark 21. *Sometimes we just write K for $K(f)$ and J for $J(f)$ when the function is clear.*

Remark 22. *From the above definition, $z \in J(f)$ if in every neighbourhood of z there are points w and v with $f^k(w) \to \infty$ and $f^k(v) \not\to \infty$.*

Definition 58 (Fatou set, [20, p. 216])**.** *The complement of the Julia set is called the Fatou set.*

Julia sets, fundamental constructs in complex dynamics, exhibit very often a captivating fractal geometry.

Example 64. *Consider $f : \mathbb{C} \to \mathbb{C}, f(z) = z^2$, Then $J(z^2) = \{z \in \mathbb{C} : |z| = 1\}$ is the unit circle in the plane.*

Proof. We have $f^k(z) = z^{2^k}$. Then if $|z| < 1$ $f^k(z) \to 0$ as $k \to \infty$ and $f^k(z) \to \infty$ if $|z| > 1$. If $|z| = 1$ then $f^k(z)$ remains on the circle $|z| = 1$ for all k. Therefore, the filled-in Julia set $K(f)$ is the unit disc $|z| \leq 1$, and the Julia set J is its boundary, in particular is the boundary between the sets of points which iterate to 0 and ∞, which is the unit circle, $|z| = 1$. □

Note that in this particular case $J(f)$ is not a fractal.

Example 65. *Consider $f : \mathbb{C} \to \mathbb{C}, f(z) = z^2 + c$ where $|c|$ is small. Then one can prove that we still have $f^k(z) \to w$ if z is small, where w is the attractive fixed point of f close to 0, and that $f^k(z) \to \infty$ if z is large (see Example 67 for more details). $J(f)$, the Julia set, is the boundary between these two types of behaviour and in that case J is a fractal curve.*

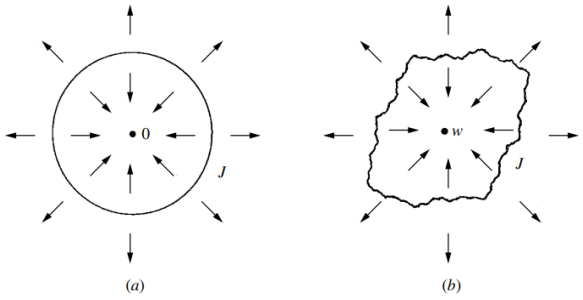

Figure 6.1: (a) The Julia set of $f(z) = z^2$ is the circle $|z| = 1$. (b) If f is perturbed to the function $f(z) = z^2 + c$, for a small $|c|$, the curve J becomes a fractal.

Source: [20, p. 216]

We would like now to see two equivalent definitions of the Julia set. To do so we need to develop first some results.

Proposition 61 ([20, Lemma 14.1])**.** *Let f be a polynomial, $f(z) = a_0 + a_1 z + a_2 z^2 + \ldots + a_n z^n$, with $a_n \neq 0$. Then there exists a real number r such that if $|z| \geq r$, then $|f(z)| \geq 2|z|$. If $|f^m(z)| \geq r$, for some $m \geq 0$, then $f^k(z) \to \infty$ as $k \to \infty$. So either $f^k(z) \to \infty$ or $\left\{f^k(z) : k \in \mathbb{N}\right\}$ is bounded.*

Proof. Take r sufficiently large to ensure that if $|z| \geq r$ then $\frac{1}{2}|a_n||z|^n \geq 2|z|$ and $(|a_{n-1}||z|^{n-1} + \cdots + |a_1||z| + |a_0|) \leq \frac{1}{2}|a_n||z|^n$. Then if $|z| \geq r$,

$$\begin{aligned} |f(z)| &\geq |a_n|\,|z|^n - \left(|a_{n-1}|\,|z|^{n-1} + \cdots + |a_1|\,|z| + |a_0|\right) \\ &\geq \frac{1}{2}\,|a_n|\,|z|^n \geq 2|z|. \end{aligned}$$

Additionally, if $|f^m(z)| \geq r$ for some m, then, by applying these steps inductively, we get $\left|f^{m+k}(z)\right| \geq 2^m \left|f^k(z)\right| \geq r$, so $f^k(z) \to \infty$. □

Proposition 62 ([20, Prop 14.4])**.** *$J\left(f^p\right) = J(f)$ for every positive integer p.*

Proof. Proposition 61 implies that $f^k(z) \to \infty$ if and only if $\left(f^p\right)^k(z) = f^{kp}(z) \to \infty$. Consequently, f and f^p share the same filled-in Julia sets, and thus have identical Julia sets. □

Definition 59 (normal family, [20, p. 218]). *Let U be an open subset of $\mathbb{C}$, and let $g_k : U \to \mathbb{C}$, $k = 1, 2, \ldots$ be a family of complex analytic functions. The family $\{g_k\}$ is said to be normal on U if every sequence of functions selected from $\{g_k\}$ has a subsequence which converges uniformly on every compact subset of U either to ∞ or to a bounded analytic function. The family is normal at a point in $w \in U$ if there is some open subset $V \subset U$ that contains w and such that $\{g_k\}$ is a normal family on V.*

Remark 23. *Analytics functions are differentiable functions on U in the complex sense.*

Theorem 14 (Montel, [20, Thm 14.5]). *Let $\{g_k\}$ be a family of complex analytic functions on an open domain U. If $\{g_k\}$ is not a normal family, then for all $z \in \mathbb{C}$ with at most one exception, we have $g_k(w) = z$ for some $w \in U$ and some k.*

Proof. Omitted. See [35, chap. 10]. □

Montel's theorem, an elegant and powerful result in complex analysis, provides us with an alternative formulation for characterizing Julia sets.

Proposition 63 ([20, Prop 14.6]).

$$J(f) = \left\{ z \in \mathbb{C} : \text{the family } \left\{ f^k \right\} \text{ is not normal at } z \right\}.$$

Proof. Assume first $z \in J$, then in every neighbourhood V of z there are points w such that $f^k(w) \to \infty$, whilst $f^k(z)$ remains bounded. Therefore no subsequence of $\left\{ f^k \right\}$ is uniformly convergent on V, so that $\left\{ f^k \right\}$ is not normal at z.

On the contrary, suppose $z \notin J$. In this case, there are two possibilities. Firstly, if z lies in the interior of K, we can select an open set V containing z such that $z \in V \subset \operatorname{int} K$. For all $w \in V$ and k, the sequence $f^k(w)$ remains within K. According to Montel's theorem contrapositive statement, $\left\{ f^k \right\}$ is normal at w. Alternatively, if $z \in \mathbb{C} \backslash K$, there exists some k such that $\left| f^k(z) \right| > r$ where r is given by Proposition 61. Consequently, for all w in a neighborhood V of z, $\left| f^k(w) \right| > r$. By Proposition 61, $f^k(w) \to \infty$ uniformly on V, indicating that $\left\{ f^k \right\}$ is again normal at w. □

Proposition 64 ([20, Thm 14.5]). *Let f be a polynomial, $w \in J(f)$ and U be any neighborhood of w. Then for each $j \in \{1, 2, \ldots\}$ the set $W \equiv \bigcup_{k=j}^{\infty} f^k(U) = \mathbb{C}$, except possibly for a single point. Any such exceptional point is not in $J(f)$, and does not depend on w or U.*

Proof. Given that $w \in J(f)$, for any $j \in 1, 2, \ldots$, the sequence $\left\{ f^k \right\}_{k=j}^{\infty}$ is not normal at w, as per Proposition 63. Therefore, by Montel's Theorem, for any $z \in \mathbb{C}$, there exists a function f^k such that $f^k(w) = z$, with at most one exception.

Let's consider $v \notin W$. If $f(z) = v$, then as $f(W) \subset W$, it implies that z is not in W. Since $\mathbb{C}\backslash W$ contains at most one point, we conclude that $z = v$. Hence, f is a polynomial of degree n such that the only solution of $f(z) - v = 0$ is v, indicating that $f(z) - v = c(z - v)^n$ for some constant c. For z sufficiently close to v, the sequence $f^k(z) - v$ tends to 0 as k goes to infinity, with convergence being uniform on, let's say, $\{z : |z - v| < \delta\}$. Consequently, $\left\{f^k\right\}$ is normal at v, implying that the exceptional point v does not belong to $J(f)$. It's evident that v is solely determined by the polynomial f. □

Proposition 65 ([20, Prop 14.3])**.** *The Julia set $J = J(f)$ of f is forward and backward invariant under f, so $J = f(J) = f^{-1}(J)$.*

Proof. Let $z \in J$. Then $f^k(z) \not\to \infty$, and we can find $w_n \to z$ with $f^k(w_n) \to \infty$ as $k \to \infty$ for all n. Consequently, $f^k(f(z)) \not\to \infty$ and $f^k(f(w_n)) \to \infty$, where due to the continuity of f, $f(w_n)$ can be chosen to be as close as we like to $f(z)$. Therefore, $f(z) \in J$, implying $f(J) \subset J$, which also implies $J \subset f^{-1}(f(J)) \subset f^{-1}(J)$.

Similarly, considering z and w_n as described above, if $f(z_0) = z$, then we can find $v_n \to z_0$ with $f(v_n) = w_n$, by the continuity of roots of a polynomial. Hence, $f^k(z_0) = f^{k-1}(z) \not\to \infty$, and $f^k(v_n) = f^{k-1}(w_n) \to \infty$ as $k \to \infty$, so $z_0 \in J$. Consequently, $f^{-1}(J) \subset J$, which implies $J = f(f^{-1}(J)) \subset f(J)$. □

We can now state the second equivalent definition of the Julia set which involves the basin of attraction of an attractive fixed point of f (see Def. 55).

Proposition 66 ([20, Lemma 14.11])**.** *Let w be an attractive fixed point of f. Then $\partial A(w) = J(f)$. The same holds if $w = \infty$.*

Proof. According to Theorem 65, if $z \in J(f)$, then $f^k(z) \in J(f)$ for all k, meaning it cannot converge to an attractive fixed point, and $z \notin A(w)$. However, for any neighborhood U of z, Proposition 64 implies that the set $f^k(U)$ contains points of $A(w)$ for some k. Therefore, there are points arbitrarily close to z that iterate to w. This implies $z \in \overline{A(w)}$ and thus $z \in \partial A(w)$.

Suppose $z \in \partial A(w)$ but $z \notin J(f)$. Then z has a connected open neighborhood V on which $\left\{f^k\right\}$ has a subsequence converging either to an analytic function or to ∞ (Proposition 63). This subsequence converges to w on $V \cap A(w)$, which is open and nonempty, and thus on V, since an analytic function is constant on a connected set if it is constant on any open subset. All points of V are mapped into $A(w)$ by iterates of f, so $V \subset A(w)$, contradicting that $z \in \partial A(w)$. □

Let's illustrate the two preceding examples of the Julia set utilizing this proposition.

Example 66. *Let $f : \mathbb{C}^* \to \mathbb{C}^*$, $f(z) = z^2$. Let us consider the fixed points of f.*

$$\begin{aligned} f(z) &= z \\ z^2 &= z \\ z(z-1) &= 0. \end{aligned}$$

So, we have two fixed points, $z_0 = 0$ and $z_1 = 1$. We also have to consider $z_\infty = \infty$, which we notice also satisfies $f(z) = z$, so we include it as a fixed point. Then,

$$\begin{aligned} f'(z) &= 2z \\ |f'(z_0)| &= 0 \\ |f'(z_1)| &= 2 \\ |(f'(z_\infty))^{-1}| &= 0 \end{aligned}$$

Therefore, z_0 and z_∞ are attractive fixed points, while $z_1 = 1$ is a repelling fixed point. Consequently, we expect points near 0 to approach closer to 0 under f, while points near 1 will move away from it. Then

$$J\left(z^2\right) = \partial A(z_0) = \partial A(z_\infty).$$

Example 67. *Let $f : \mathbb{C}^* \to \mathbb{C}^*$, $f(z) = z^2 + c$, where $c \in \mathbb{C}$. Let us consider the fixed points of f.*

$$\begin{aligned} f(z) &= z \\ z^2 + c &= z \\ z^2 - z + c &= 0. \end{aligned}$$

The solutions are

$$z_\pm = \frac{1}{2}(1 \pm \sqrt{1-4c})$$

We also consider the fixed point z_∞. Then

$$\begin{aligned} f'(z) &= 2z \\ |f'(z_+)| &= |1 + \sqrt{1-4c}| \\ |f'(z_-)| &= |1 - \sqrt{1-4c}| \\ |(f'(z_\infty))^{-1}| &= 0 \end{aligned}$$

When $|c|$ is sufficiently small, it is guaranteed that $|f'(z_+)| > 1$ and $|f'(z_-)| < 1$, meaning that our first fixed point will be repelling for such c, while our second one will be attracting. The point at infinity is attractive for all c.

Now, considering that there is an attracting fixed point near the origin for small $|c|$, and the only other attracting fixed point is at ∞, we observe two distinct types of behavior in the complex plane: some starting points will iterate towards z_-, while others will diverge to infinity.

Thus, the Julia set delineates the boundary between these two basins of attraction. Such curves are sometimes referred to as quasi-circles.

$$J\left(z^2+c\right) = \partial A\left(z_-\right) = \partial A\left(z_\infty\right).$$

Let's delve into additional interesting descriptions and proprieties of the Julia sets. With our emphasis on grasping the fractal dimension of $J(f)$ (as outlined in Theorem 19), rather than demonstrating these properties, we will move forward to explore our final fractal example, the Mandelbrot set. This set is closely intertwined with the Julia sets we've recently examined.

Proposition 67 ([20, Prop 14.2])**.** *Let $f(z)$ be a polynomial. Then the filled-in Julia set $K(f)$ and the Julia set $J(f)$ are non-empty and compact, with $J(f) \subset K(f)$. Additionally, $J(f)$ has an empty interior.*

Proof. Omitted. See [20, Prop 14.2]. □

Proposition 68 ([20, Cor. 14.8b])**.** *If $z \in J(f)$ then $J(f)$ is the closure of $\bigcup_{k=1}^{\infty} f^{-k}(z)$.*

Proof. Omitted. See [20, Cor. 14.8b]. □

Proposition 69 ([20, Prop. 14.9])**.** *$J(f)$ is a perfect set (closed and with no isolated points) and is therefore uncountable.*

Proof. Omitted. See [20, Prop. 14.9]. □

The following theorem presents a third approach to interpreting the definition of the Julia set.

Theorem 15 ([20, Thm 14.10])**.** *If f is a polynomial, $J(f)$ is the closure of the repelling periodic points of f.*

Proof. Omitted. See [20, Thm 14.10]. □

The following images beautifully showcase the intricate patterns of the Julia sets, vividly demonstrating their inherent fractal properties.

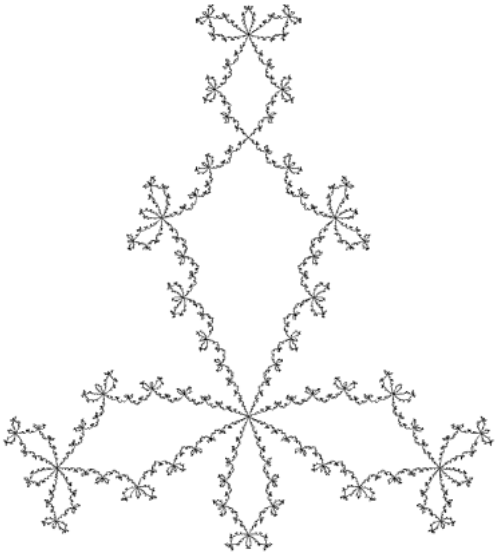

Figure 6.2: Julia set for $f(z) = z^3 + \frac{12}{25}z + \frac{116}{125}i$.
Source: [37, p. 3-7]

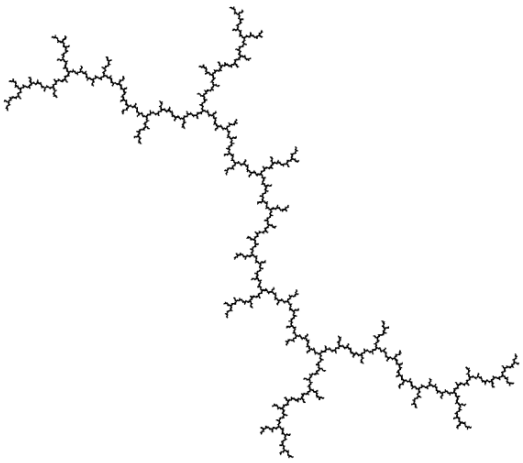

Figure 6.3: Julia set for $z \mapsto z^2 + i$.
Source: [37, p. 3-3]

Figure 6.4: Julia set for $z \mapsto z^2 + (-0.765 + 0.12i)$.
Source: [37, p. 3-2]

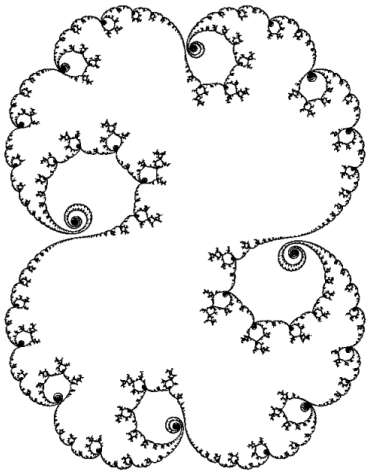

Figure 6.5: Julia set for $z \mapsto z^2 + (0.99 + 0.14i)z$.
Source: [37, p. 3-2]

See Appendix A.4 for a simple way to create in Python visualizations of general Julia sets based on the function $f(z) = z^2 + c$.

6.2 Mandelbrot Set

The Mandelbrot set is derived from quadratic functions that are iterated within the complex plane. It emerges from investigating Julia sets of functions expressed as $f_c(z) = z^2 + c$, which we briefly explored in the preceding section. This set was initially formulated and illustrated by Brooks and Matelski in 1978 [6]. Subsequently, it garnered significant attention through extensive examination by Mandelbrot [33], ultimately leading to its association with his name. Its widespread recognition beyond the confines of mathematics is largely attributed to the captivating visual representations of fractals, thanks in no small part to the contributions of Peitgen and Richter [40].

Definition 60 (quadratic family)**.** *The quadratic family is the family of quadratic polynomials of the form*

$$f_c(z) = z^2 + c$$

where c is a (complex) constant called the parameter.

Proposition 70 ([20, p. 223])**.** *Every quadratic polynomial is conjugate to some member of the quadratic family.*

Proof. Let $f_c : \mathbb{C} \to \mathbb{C}$ be the complex function defined as $f_c(z) = z^2 + c$. Suppose we have another complex function $h(z) = \alpha z + \beta$, where α, β are complex numbers with $\alpha \neq 0$. The inverse function of h is given by $h^{-1}(z) = \frac{z-\beta}{\alpha}$.

Using h, we can demonstrate that f_c is conjugate to another quadratic function f. Specifically, we have:

$$\begin{aligned} h^{-1}\left(f_c(h(z))\right) &= h^{-1}\left(f_c(\alpha z + \beta)\right) \\ &= h^{-1}\left((\alpha z + \beta)^2 + c\right) \\ &= h^{-1}\left(\alpha^2 z^2 + 2\alpha\beta z + \beta^2 + c\right) \\ &= \frac{\alpha^2 z^2 + 2\alpha\beta z + \beta^2 + c - \beta}{\alpha} \\ &= f(z) \end{aligned}$$

By selecting suitable values for α, β, and c, we can transform this expression into any quadratic function f of our choice. This transformation h is referred to as a conjugacy between f and f_c. Consequently, we have $h^{-1} \circ f_c \circ h = f$, implying $h^{-1} \circ f_c^k \circ h = f^k$ for all k. □

This observation implies that the sequence of iterates $\left\{f^k(z)\right\}$ of a point z under f is essentially the same as the image, under h^{-1}, of the sequence of iterates $\left\{f_c^k(h(z))\right\}$ of the point $h(z)$ under f_c. In essence, if $f^k(z)$ diverges to infinity, then $f_c^k(z)$ also diverges to infinity, and vice versa. Consequently, the Julia set of f is just the image, under h^{-1}, of the Julia set of f_c.

This proposition proves that the Julia set for any quadratic polynomial is similar to the Julia set for some member of the quadratic family. Therefore, by examining the Julia sets of f_c for $c \in \mathbb{C}$, we effectively explore the Julia sets of all quadratic polynomials. Hence, it is logical to focus our investigation of quadratic Julia sets within this family.

Example 68 ([20, Exercise 14.2])**.** *Let $f(z) = z^2 + 4z + 2$, then $J(f)$ is the unit circle.*

Proof. If $f(z) = \frac{\alpha^2 z^2 + 2\alpha\beta z + \beta^2 + c - \beta}{\alpha}$, then $J(f) = h^{-1}\left(J\left(f_c\right)\right)$, where $f_c(z) = z^2 + c$ and $h(z) = \alpha z + \beta$.

Given $f(z) = z^2 + 4z + 2$, we deduce that $\frac{\alpha^2}{\alpha} = 1$, $\frac{2\alpha\beta}{\alpha} = 4$, and $\frac{\beta^2 + c - \beta}{\alpha} = 2$. Hence, $\alpha = 1$, $\beta = 2$, and $c = 2 + \beta - \beta^2 = 0$. Consequently, $f_c(z) = z^2$, leading to $J\left(f_c\right)$ being the unit circle.

With $h^{-1}(z) = \frac{z-\beta}{\alpha} = z - 2$, we conclude that $J(f)$ is the circle with radius of 1 and center at -2. □

We give now the definition of the Mandelbrot set.

Definition 61 (Mandelbrot set, [20, p. 223])**.**

$$M = \{c \in \mathbb{C} : J(f_c) \text{ is connected } \}.$$

Remark 24. *The unit circle $J(z^2)$ is a connected set, and as a result, the point $c = 0$ is part of the set M. Thus, M is not empty.*

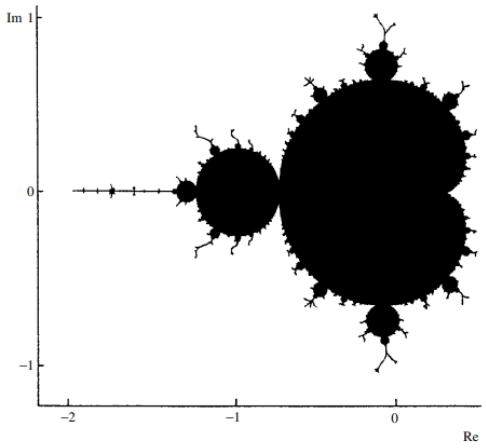

Figure 6.6: The Mandelbrot set M.
Source: [20, p. 224]

The Mandelbrot set's image depicts an immensely intricate structure. It prominently features a central cardioid shape with attached circular bulbs, each of which further extends into smaller buds. Additionally, delicate, branching 'hairs' emanate from these buds, carrying miniature replicas of the entire Mandelbrot set along their length. It is a connected set [13]. The conjecture that the Mandelbrot set is locally connected remains unresolved, constituting an open question in complex dynamics. This conjecture is commonly referred to as MLC, an abbreviation for Mandelbrot Locally Connected [26].

When magnified, the boundary of the Mandelbrot set reveals an infinitely complex pattern, showcasing increasingly detailed recursive intricacies. This boundary is renowned as a prime example of a fractal curve, displaying remarkable self-similar patterns at varying scales.

Theorem 16 ([46, Thm. A])**.**

$$\dim_{\mathrm{H}}(\partial M) = 2.$$

Moreover for any open set U which intersects ∂M, we have $\dim_{\mathrm{H}}(\partial M \cap U) = 2$.

Proof. Omitted. See [46]. □

According to this finding by Shishikura [46], the Hausdorff dimension of the boundary of the Mandelbrot set is determined to be 2. This result indicates that the boundary's fractal nature is exceptionally intricate, surpassing its topological dimension of 1 by a whole integer. In simpler terms, Shishikura's discovery suggests that the Mandelbrot set boundary is so densely and intricately structured that on a local level, it fills space as effectively as a two-dimensional plane.

The unresolved question of whether the boundary of the Mandelbrot set possesses positive area (area denotes the two-dimensional measure and is the sole Hausdorff measure that could theoretically be both non-zero and non-infinite in that case) remains an open topic, as indicated in [2], where it is described as *one of the important questions in complex dynamics which is still open.*

Proposition 71 ([20, Exercise 14.15])**.** *f_c has an attractive fixed point precisely when c lies inside the main cardioid of M given by $z = \frac{1}{2}e^{i\theta}\left(1 - \frac{1}{2}e^{i\theta}\right)$ for $0 \leq \theta \leq 2\pi$.*

Proof. If $f_c(z) = z^2 + c$, then the fixed points of f_c are the solutions of $z^2 + c = z$. As $f_c'(z) = 2z$, we deduce that $z = re^{i\theta}$ is an attractive fixed point of f_c if and only if $0 \leq r < 1/2, 0 \leq \theta < 2\pi$. Therefore

$$c = z - z^2 = z(1 - z) = re^{i\theta}\left(1 - re^{i\theta}\right).$$

Thus f_c has an attractive fixed point precisely when c lies inside the main cardioid of M. As already observed in Example 67, our expectation remains that the Julia sets of $f_c(z) = z^2 + c$ will exhibit quasi-circular characteristics for any c positioned within the main cardioid of the Mandelbrot set. □

In particular, has we have established in our prior discussions (Examples 66 and 67), when $c = 0$, the Julia set $J(f_c)$ forms the unit circle. For small values of $|c|$ and $|z|$, the iterates $f_c^k(z)$ converge to a point w as $k \to \infty$, where w is the attractive fixed point $\frac{1}{2}(1 - \sqrt{1 - 4c})$ in close proximity to 0. Conversely, if $|z|$ is large, $f_c^k(z)$ diverges to infinity. It's reasonable to anticipate that the unit circle undergoes a 'distortion' into a simple closed curve that delineates these two distinct behaviors as c deviates from 0.

Theorem 17 ([20, Thm 14.15])**.** *If c lies in the main cardioid of M, then $J(f_c)$ is a simple closed curve, so in particular $c \in M$.*

Proof. Omitted. See [20, Thm 14.15] and the extension of this result. □

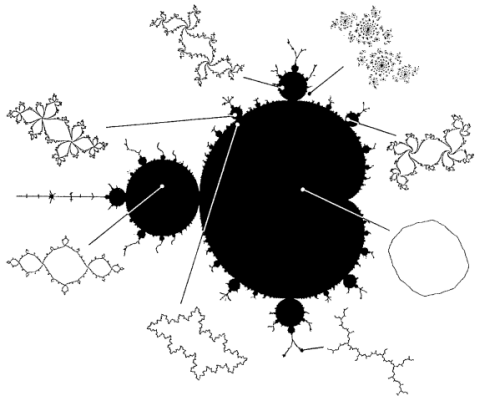

Figure 6.7: The Julia sets $J(f_c)$ for different values of c across M.
Source: [20, p. 233]

Proposition 72 ([20, Exercise 14.16])**.** *f_c has an attractive period-2 point precisely when c is contained in the main bulb of M given by $|c+1| < \frac{1}{4}$.*

Proof. Given $f_c(z) = z^2 + c$ and $f_c^2(z) = f_c(f_c(z))$, we have

$$\begin{aligned} f_c^2(z) - z &= \left(z^2 + c\right)^2 + c - z \\ &= z^4 + 2cz^2 - z + c^2 + c \\ &= \left(z^2 - z + c\right)\left(z^2 + z + c + 1\right). \end{aligned}$$

A point z is a periodic point of f_c of period 2 if and only if $f_c^2(z) = z$ and $f_c(z) \neq z$. Thus, we seek solutions to $f_c^2(z) - z = 0$ that are not solutions of $f_c(z) - z = z^2 - z + c = 0$. In other words, we are interested in the solutions of $z^2 + z + c + 1 = 0$. By the chain rule,

$$\left(f_c^2\right)'(z) = f_c'\left(f_c(z)\right) f_c'(z) = 2\left(z^2 + c\right) 2z$$

so z is an attractive fixed point of f_c^2 if and only if

$$\left|\left(z^2 + c\right) z\right| < 1/4 \text{ and } z^2 + z + c + 1 = 0.$$

Using the second condition to rewrite the first, we find that f_c^2 has an attractive fixed point if and only if

$$\left|\left(z^2 + c\right) z\right| = |(z+1)z| = \left|z^2 + z\right| = |c+1| < 1/4.$$

Thus, f_c^2 has an attractive fixed point precisely when c belongs to the main bud of the Mandelbrot set M, i.e., the filled circle with center at -1 and radius $1/4$ (see Figure 6.6). □

We would like now to see an equivalent and more intuitive definition of the Mandelbrot set. To achieve this purpose, we introduce first some definitions and a lemma.

Definition 62 (loop, [20, p. 223])**.** *A loop is a smooth, closed, simple curve in the complex plane.*

Definition 63 (figure of eight, [20, p. 223])**.** *A figure of eight is a smooth closed curve with a single point of self-intersection.*

Lemma 5 ([20, Lemma 14.13])**.** *Let C be a loop in the complex plane.*

a) If c is inside C then $f_c^{-1}(C)$ is a loop, with the inverse image of the interior of C as the interior of $f_c^{-1}(C)$.

b) If c lies on C then $f_c^{-1}(C)$ is a figure of eight with self-intersection at 0, such that the inverse image of the interior of C is the interior of the two loops.

Proof. a) Observe that $f_c^{-1}(z) = \pm(z-c)^{1/2}$ and $(f_c^{-1})'(z) = \pm\frac{1}{2}(z-c)^{-1/2}$, which remains finite and non-zero for $z \neq c$. Thus, if we choose one branch of f_c^{-1}, the set $f_c^{-1}(C)$ locally forms a smooth curve, assuming $c \notin C$. Suppose c lies inside C. Taking an initial point w on C and selecting one value for $f_c^{-1}(w)$, as z varies continuously along C, $f_c^{-1}(z)$ traces out a smooth curve. However, upon z returning to w, $f_c^{-1}(w)$ adopts its second value. As z traverses C again, $f_c^{-1}(z)$ continues smoothly until it closes upon reaching w for the second time. Since $c \notin C$, we have $0 \notin f_c^{-1}(C)$, ensuring $f_c'(z) \neq 0$ on $f_c^{-1}(C)$. Therefore, f_c locally forms a smooth bijective transformation near points on $f_c^{-1}(C)$, implying $z \in f_c^{-1}(C)$ cannot be a point of selfintersection of $f_c^{-1}(C)$, as it would result in $f_c(z)$ intersecting C. Thus, $f_c^{-1}(C)$ is a loop.

As f_c continuously maps the loop $f_c^{-1}(C)$ and no other points onto C, the polynomial f_c must map the interior and exterior of $f_c^{-1}(C)$ to the interior and exterior of C, respectively. Therefore, f_c^{-1} maps the interior of C to the interior of $f_c^{-1}(C)$.

b) This can be demonstrated similarly to part (a), where if C' represents a smooth segment of a curve passing through c, then $f_c^{-1}(C')$ comprises two smooth segments of curves passing through 0 and intersecting at right angles, thereby forming the self-intersection characteristic of the figure-eight shape.

□

Theorem 18 (Fundamental theorem of the Mandelbrot set, [20, Thm 14.14])**.**

$$M = \left\{ c \in \mathbb{C} : \left\{ f_c^k(0) \right\}_{k \geq 1} \text{ is bounded} \right\} = \left\{ c \in \mathbb{C} : f_c^k(0) \not\to \infty \text{ as } k \to \infty \right\}.$$

Proof. It is clear, by Lemma 61, that $f_c^k(0) \not\to \infty$ if and only if $\left\{ f_c^k(0) \right\}$ is bounded, so the two sets are in fact equal.

First, we demonstrate that if the sequence $\left\{f_c^k(0)\right\}$ is bounded, then the Julia set $J(f_c)$ is connected.

Consider a large circle C in the complex plane containing all points $\left\{f_c^k(0)\right\}$, with $f_c^{-1}(C)$ being interior to C and points outside C tending to ∞ under iteration by f_c^k. Since $c = f_c(0)$ lies inside C, Lemma 5(a) implies that $f_c^{-1}(C)$ forms a loop contained within C. Additionally, $f_c(c) = f_c^2(0)$ lies inside C, and f_c^{-1} maps the exterior of C onto the exterior of $f_c^{-1}(C)$, implying that c is inside $f_c^{-1}(C)$. Again applying Lemma 5(a), we find that $f_c^{-2}(C)$ forms a loop contained within the interior of $f_c^{-1}(C)$. Continuing this process, we observe that $\left\{f_c^{-k}(C)\right\}$ constitutes a sequence of loops, each enclosing the next within its interior.Let K represent the closed set comprising points lying on or within the loops $f_c^{-k}(C)$ for all k. If $z \in \mathbb{C}\backslash K$, then some iterate $f_c^k(z)$ lies outside C, leading $f_c^k(z)$ to tend to ∞. Thus, we have

$$A(\infty) = \left\{z : f_c^k(z) \to \infty \text{ as } k \to \infty\right\} = \mathbb{C}\backslash K$$

Therefore, K represents the filled Julia set of f_c. According to Proposition 66, $J(f_c)$ forms the boundary of $\mathbb{C}\backslash K$, which is equivalent to the boundary of K. Since K is the intersection of a decreasing sequence of closed simply connected sets, it follows from a topological argument that K is simply connected and thus possesses a connected boundary. Hence, $J(f_c)$ is connected.

We establish next the converse implication, namely, if $J(f_c)$ is connected, then $\left\{f_c^k(0)\right\}$ is bounded. This is done by contrapositive, aiming to show that an unbounded sequence $\left\{f_c^k(0)\right\}$ leads to the disconnection of $J(f_c)$.

We commence similarly to the previous argument. Let C denote a large circle in $\mathbb{C}$ such that $f_c^{-1}(C)$ lies inside C, and all points outside C diverge to ∞ under iteration. However, this time, the sequence $\left\{f_c^k(0)\right\}$ is unbounded. Hence, let p be such that $f_c^{p-1}(c) = f_c^p(0) \in C$, with $f_c^k(0)$ positioned either inside or outside C contingent upon whether k exceeds p. We proceed to construct a sequence of loops $\left\{f_c^{-k}(C)\right\}$ where each loop contains the subsequent one. Yet, upon reaching the loop $f_c^{-(p-1)}(C)$, we encounter a divergence: since $c \in f_c^{-(p-1)}(C)$, Lemma 5(a) no longer applies. Nonetheless, we can introduce a figure-eight shape E obtained from Lemma 5(b), lying within $f_c^{-(p-1)}(C)$. E possesses the property that f_c maps the interior of both halves of E onto the interior of $f_c^{-(p-1)}(C)$. The Julia set $J(f_c)$ must reside within the interior of the loops comprising E, as other points will diverge to ∞. Given that $J(f_c)$ remains invariant under the action of f_c^{-1}, we must locate parts of it within each loop of E. Consequently, E partitions $J(f_c)$, leading to its disconnection. □

Corollary 10 (escape criterion, [20, Exercise 14.11])**.** *Let $f_c(z) = z^2 + c$, then if $|c| > 2$, $c \notin M$.*

Proof. We claim that if $\varepsilon > 0$ and if $|z| \geq \max(2 + \varepsilon, |c|)$ then $|f_c(z)| \geq |z|(1 + \varepsilon)$.

We have

$$|f_c(z)| = \left|z^2 + c\right| \geq |z|^2 - |c| = |z| \left(|z| - \frac{|c|}{|z|} \right) \geq |z|(2 + \epsilon - 1)$$
$$\geq |z|(1 + \epsilon),$$

assuming that $|z| \geq \max\{2 + \epsilon, |c|\}$. If $|c| > 2$, we can select $\epsilon > 0$ such that $|c| > 2 + \epsilon$. Therefore, observing $f_c(0) = c$ and applying the above estimate iteratively, we find

$$\left|f_c^k(0)\right| \geq (1 + \epsilon)^k |c| \to \infty$$

Therefore by Theorem 18 $c \notin M$. □

Corollary 11 ([20, Exercise 14.12])**.** $M^c = \left\{c : \left|f_c^k(0)\right| > 2 \text{ for some } k\right\}$.

Proof. If c is such that $\left|f_c^k(0)\right| > 2$ for some k, then either:

a) $|c| > 2$, which implies $c \notin M$ by Corollary 10.

b) $|c| \leq 2$, and we can select $\epsilon > 0$ such that $\left|f_c^k(0)\right| > 2 + \epsilon > |c|$. Subsequently, applying the first part of Corollary 10 iteratively to $z = f_c^k(0)$ and its iterates under f_c, we obtain:

$$\left|f_c^{k+n}(0)\right| = \left|f_c^n\left(f_c^k(0)\right)\right| \geq (1 + \epsilon)^n \left|f_c^k(0)\right| \to \infty$$

This implies that $c \notin M$. Conversely, if $c \notin M$, then $\left|f_c^k(0)\right| \to \infty$, thus $\left|f_c^k(0)\right| > 2$ for some k. □

The equivalent definition outlined in Theorem 18 and the following corollaries forms the fundamental approach for creating computer visualizations of the Mandelbrot set. The process involves a computer iterating through various values of c and determining whether the magnitude of its iterates surpasses a certain threshold, typically $r = 2$ (Corollary 6.2). If the magnitude exceeds r, then $c \notin M$; otherwise, $c \in M$ (see for an example Appendix A.5). Many visual representations of the Mandelbrot set incorporate diverse colors. In such images, points corresponding to $c \notin M$ are colored based on the speed at which their iterates approach infinity.

Corollary 12. *M is a compact set.*

Proof. From escape criterion M is a bounded set. Consider now the set $M_k = \left\{c \in \mathbb{C} : \left|f_c^k(0)\right| \leq 2\right\}$. Let $\{c_j\} \subset M_k$ be a sequence in M_k, and $c_j \to c$. Then $\left|f_{c_j}^k(0)\right| \to \left|f_c^k(0)\right|$. Since $\left|f_{c_j}^k(0)\right| \leq 2, \left|f_c^k(0)\right| \leq 2$, so for each k, M_k is a closed set. Then by Corollary 11,

$$M = \bigcap_{k=1}^{\infty} M_k$$

Thus M is the arbitrary intersection of closed sets and thus is closed. □

To conclude this chapter we revisit the discussion on Hausdorff dimension, which serves as a core point of our research. As previously discussed, the boundary of the Mandelbrot set exhibits a Hausdorff dimension of 2. However, when examining the Julia sets defined by the function $z \to z^2 + c$, obtaining an exact solution for their Hausdorff dimension proves elusive. Only in exceedingly rare cases has an exact value been determined, leaving the majority of Julia sets with their Hausdorff dimension yet to be precisely characterized. Now, we turn our attention to some results that provide insight into the Hausdorff dimension in specific cases.

Theorem 19 ([20, Thm 14.15])**.** *Assume* $|c| > \frac{1}{4}(5 + 2\sqrt{6}) \simeq 2.475$*. Then* $J(f_c)$ *is totally disconnected, and is the attractor (see Definition 45) of the contractions given by the two branches of* $f_c^{-1}(z) = \pm(z - c)^{1/2}$ *for* z *near* J*. Then*

$$\frac{2\log 2}{\log 4\left(|c| + |2c|^{1/2}\right)} \leq \dim_{\mathrm{H}} J(f_c) \leq \frac{2\log 2}{\log 4\left(|c| - |2c|^{1/2}\right)}$$

Proof. The proof begins with Lemma 5, which sets the foundation for the subsequent arguments. Let C denote the circle $|z| = |c|$, and D its interior $|z| < |c|$. The inverse image of C under f_c is given by:

$$f_c^{-1}(C) = \left\{ \left(c\mathrm{e}^{i\theta} - c\right)^{1/2} : 0 \leq \theta \leq 4\pi \right\}$$

This set forms a figure of eight with a self-intersection at 0, with the loops lying on either side of a straight line passing through the origin. Since $|c| > 2$, it follows that $f_c^{-1}(C) \subset D$, as for $|z| > |c|$, $|f_c(z)| \geq |z^2| - |c| \geq |c|^2 - |c| > |c|$. Each interior of the loops of $f_c^{-1}(C)$ is mapped bijectively by f_c onto D. Denote by $S_1, S_2 : D \to D$ the branches of $f_c^{-1}(z)$ inside each loop, with $S_1(D)$ and $S_2(D)$ representing the interiors of the two loops.

Let V be the disk $\left\{z : |z| < |2c|^{1/2}\right\}$. The radius of V is chosen such that V contains $f_c^{-1}(C)$, thus $S_1(D), S_2(D) \subset V \subset D$. Consequently, $S_1(V)$ and $S_2(V)$ are also contained within V, with $S_1(\bar{V})$ and $S_2(\bar{V})$ being disjoint. For $i = 1, 2$, we have:

$$|S_i(z_1) - S_i(z_2)| = \left|(z_1 - c)^{1/2} - (z_2 - c)^{1/2}\right| = \frac{|z_1 - z_2|}{\left|(z_1 - c)^{1/2} + (z_2 - c)^{1/2}\right|}$$

Therefore, if $z_1, z_2 \in \bar{V}$, considering the least and greatest values, we have:

$$\frac{1}{2}\left(|c| + |2c|^{1/2}\right)^{-1/2} \leq \frac{|S_i(z_1) - S_i(z_2)|}{|z_1 - z_2|} \leq \frac{1}{2}\left(|c| - |2c|^{1/2}\right)^{-1/2} \tag{6.1}$$

The upper bound is less than 1 if $|c| > \frac{1}{4}(5 + 2\sqrt{6})$, in which case S_1 and S_2 are contractions on the disc $\bar{V}$. According to Theorem 11, there exists a unique attractor $F \subset \bar{V}$ satisfying:

$$S_1(F) \cup S_2(F) = F$$

Since $S_1(\bar{V})$ and $S_2(\bar{V})$ are disjoint, it follows that $S_1(F)$ and $S_2(F)$ are also disjoint, implying that F is totally disconnected.

We claim that F corresponds to the Julia set $J = J(f_c)$. To observe this note first that since $\bar{V}$ contains at least one point z of J (for instance, a repelling fixed point of f_c), we have by Proposition 68 $J = \text{closure}\left(\bigcup_{k=1}^{\infty} f_c^{-k}(z)\right) \subset \bar{V}$, since $f_c^{-k}(\bar{V}) \subset \bar{V}$. Also, by Proposition 67 J is a non-empty compact subset of $\bar{V}$ satisfying, by Proposition 65 $J = f_c^{-1}(J)$ or, equivalently, $J = S_1(J) \cup S_2(J)$. Therefore, $J = F$.

To estimate the dimension of $J(f_c) = F$, we can utilize Propositions 56 and 57 along with (6.1). These propositions provide lower and upper bounds for the Hausdorff dimension $\dim_{\mathrm{H}} J(f_c)$, given by the solutions of:

$$2\left(\frac{1}{2}\left(|c| \pm |2c|^{1/2}\right)^{-1/2}\right)^{s} = 1$$

That is, by $s = \frac{2\log 2}{\log 4\left(|c| \pm |2c|^{1/2}\right)}$, which yields the estimate as stated. □

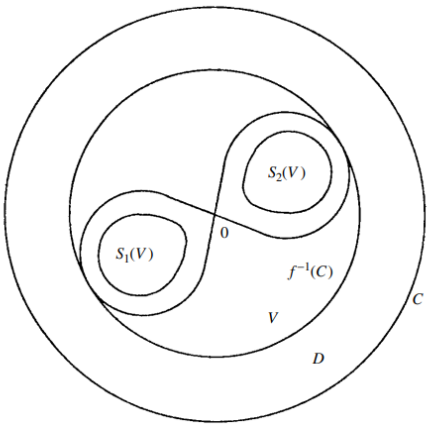

Figure 6.8: The proof of Theorem 19.
Source: [20, p. 229]

Example 69 ([20, Exercise 14.14]). *Let $f(z) = z^3 + c$. Then*

$$\frac{\log 3}{\log 3 + (2/3)\log\left(|c| + |2c|^{1/3}\right)} \leq \dim_{\mathrm{H}} J(f) \leq \frac{\log 3}{\log 3 + (2/3)\log\left(|c| - |2c|^{1/3}\right)}$$

when $|c|$ is large.

Proof. The approach parallels the proof of Theorem 19. Suppose $|c| > \sqrt{2}$. Let C be the circle $|z| = |c|$ and D be its interior $|z| < |c|$. If we define $S_1, S_2, S_3 : D \to D$ as the branches of f^{-1}, then $S_1(D), S_2(D)$, and $S_3(D)$ are the interiors of the three loops of the curve $f^{-1}(C)$. Let V be the disc $\left\{z : |z| < |2c|^{1/3}\right\}$, such that V just contains $f^{-1}(C)$. Note that if $|c| > \sqrt{2}$,

then $\bar{V} \subset D$, and thus the sets $S_1(V), S_2(V)$, and $S_3(V)$ are all in V, while the sets $S_1(\bar{V}), S_2(\bar{V})$, and $S_3(\bar{V})$ are disjoint. For $i = 1, 2, 3$, we have

$$|S_i'(z)| = \frac{1}{3}|z - c|^{-2/3}$$

and thus, if $z \in \bar{V}$,

$$\frac{1}{3}\left(|c| + |2c|^{1/3}\right)^{-2/3} \leq |S_i'(z)| \leq \frac{1}{3}\left(|c| - |2c|^{1/3}\right)^{-2/3}$$

From the complex mean-value theorem it follows that

$$\frac{1}{3}\left(|c| + |2c|^{1/3}\right)^{-2/3} \leq \frac{|S_i(z_1) - S_i(z_2)|}{|z_1 - z_2|} \leq \frac{1}{3}\left(|c| - |2c|^{1/3}\right)^{-2/3}$$

for $i = 1, 2, 3$, and $z_1, z_2 \in \bar{V}$. If $|c| > 2$ (for instance), the upper bound is less than 1 , implying S_1, S_2, and S_3 are contractions on the disc $\bar{V}$. Consequently, by Theorem 11, there exists a unique non-empty compact invariant set $F \subset \bar{V}$ satisfying:

$$S_1(F) \cup S_2(F) \cup S_3(F) = F$$

Propositions 56 and 57 provide lower and upper bounds for $\dim_{\mathrm{H}} F$, which are given by solutions of:

$$3\left(\frac{1}{3}\left(|c| \pm |2c|^{1/3}\right)^{-2/3}\right)^{s} = 1$$

Thus, $s = \frac{\log 3}{\log 3 + (2/3)\log\left(|c| \pm |2c|^{1/3}\right)}$. We claim that $F = J(f)$. If $|c| > \sqrt{2}$ and $|z| \notin \bar{V}$, then

$$|f(z)| = \left|z^3 + c\right| \geq |z|^3 - |c| \geq |z|^3 - \frac{1}{2}|z|^3 = \frac{1}{2}|z|^3 = |z|\frac{1}{2}|z|^2 \geq |z|\frac{1}{2}|2c|^{2/3} = \lambda|z|$$

where $\lambda = \frac{1}{2}|2c|^{2/3} > \frac{1}{2}|2|^{2/3}|2|^{1/3} = 1$. Iterating, it follows that $\left|f^k(z)\right| \geq \lambda^k|z| \to \infty$, so $z \notin J(f)$. Thus $J(f) \subset K(f) \subset \bar{V}$. From Propositions 67 and 68, $J(f)$ is the non-empty compact subset of $\bar{V}$ satisfying $J(f) = f^{-1}(J(f))$, i.e., $J(f) = S_1(J(f)) \cup S_2(J(f)) \cup S_3(J(f))$, and hence $J(f) = F$ as claimed. □

Next, let's consider the scenario when $|c|$ is small. As already mentioned earlier, for small values of $|c|$, the Julia sets of these quadratic polynomials are often described as quasi-circles (see for example Figure 6.9). There exists a formula similar to the one mentioned above for small $|c|$, as established by Bowen [5] and Ruelle [43]. However, proving this formula in this scenario is considerably more challenging, as we cannot rely on the properties of contractions as in the previous case.

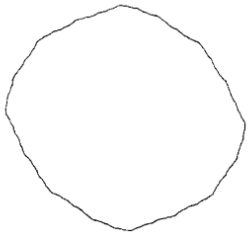

Figure 6.9: Julia set for $z \mapsto z^2 + (-0.1 + 0.1i)$
Source: [20, p. 234]

Theorem 20 (Ruelle Theorem, [43])**.** *For small values of $|c|$, the Hausdorff dimension of the Julia set $J_c(f)$ of the map $f_c : z \to z^2 + c$ is given by*

$$\dim_{\mathrm{H}} J\left(f_c\right) = 1 + \frac{|c|^2}{4 \log 2} + \text{ terms in } |c|^3 \text{ and higher powers.}$$

Proof. Omitted. See [43]. □

To conclude, we mention a last result by Shishikura [46], that provides the Hausdorff dimension of a Julia set given by the map f_c where $c \in \partial M$.

Theorem 21 ([46, Thm. B])**.** *For a generic $c \in \partial M$, we have*

$$\dim_{\mathrm{H}} J\left(f_c\right) = 2$$

Proof. Omitted. See [46]. □

Appendix A

Python Scripts

A.1 Visualizing the Construction of the Cantor Set

Below, we present a Python script for an animation of the construction of the Cantor set.

```
import numpy as np
import matplotlib.pyplot as plt
from matplotlib.animation import FuncAnimation

# Function to generate the Cantor set
def cantor_set(x_start, x_end, depth):
    if depth == 0:
        return [(x_start, x_end)]
    else:
        interval_length = (x_end - x_start) / 3
        new_intervals = cantor_set(x_start, x_start +
           interval_length, depth - 1) + \
                        cantor_set(x_end -
                           interval_length, x_end, depth
                           - 1)
        return new_intervals

# Animation function
def animate(frame):
    plt.cla()  # Clear the current axes
    plt.xlim(0, 1)
    plt.ylim(0, 1)
    plt.gca().set_aspect('equal', adjustable='box')
    plt.axis('off')  # Turn off the axes

```

```
    # Plot the unit blue segment
    plt.plot([0, 1], [0.5, 0.5], color='blue')

    y_offset = 0.1  # Start the vertical offset for
       iteration 1
    for i in range(1, frame + 1):
        intervals = cantor_set(0, 1, i)
        for interval in intervals:
            plt.plot([interval[0], interval[1]], [0.5 -
               y_offset, 0.5 - y_offset], color='blue')
        y_offset += 0.1  # Adjust the vertical offset
           between each iteration

    plt.title(f"Cantor set (Iteration {frame})")
    if frame == frames - 1:
        ani.event_source.stop()  # Stop the animation
           after the last frame

# Set up the animation
frames = 6
ani = FuncAnimation(plt.gcf(), animate, frames=frames,
    interval=1000)  # Added a pause of 1 second between
    each iteration

plt.show()
```

Listing A.1: Python code the Cantor set.

A.2 Visualizing the Construction of the Koch Curve

Below, we present a Python script for an animation of the construction of the Koch curve.

```
import numpy as np
import matplotlib.pyplot as plt
from matplotlib.animation import FuncAnimation

# Function to generate Koch curve points
def koch_curve(start, end, n):
    if n == 0:
        return [start, end]
    # Calculate intermediate points
    p1 = start + (end - start) / 3
```

```
    p3 = end - (end - start) / 3
    p2 = p1 + np.exp(1j * np.pi / 3) * (p3 - p1)
    # Recursively calculate points
    points = koch_curve(start, p1, n - 1)[:-1]
    points.extend(koch_curve(p1, p2, n - 1)[:-1])
    points.extend(koch_curve(p2, p3, n - 1)[:-1])
    points.extend(koch_curve(p3, end, n - 1))
    return points

# Function to animate construction of Koch curve
def animate(i):
    plt.cla()
    points = koch_curve(complex(0, 0), complex(1, 0), i)
    x = [p.real for p in points]
    y = [p.imag for p in points]
    plt.plot(x, y, color='blue')
    plt.title(f'Koch Curve (Iteration {i})')
    plt.axis('equal')
    plt.axis('off')

# Create animation
fig = plt.figure(figsize=(6, 6))
ani = FuncAnimation(fig, animate, frames=range(0, 6),
    interval=1000, repeat=False)

plt.show()
```

Listing A.2: Python code the Koch curve.

A.3 Visualizing the Construction of the Sierpinski Triangle

Below, we present a Python script for an animation of the construction of the Sierpinski triangle.

```
import numpy as np
import matplotlib.pyplot as plt
from matplotlib.animation import FuncAnimation

# Function to generate midpoint of two points
def midpoint(p1, p2):
    return (p1[0] + p2[0]) / 2, (p1[1] + p2[1]) / 2

# Function to generate Sierpinski triangle points
```

```
def sierpinski_triangle(points, depth):
    if depth == 0:
        return [points]
    else:
        new_points = []
        for p1, p2, p3 in points:
            m1 = midpoint(p1, p2)
            m2 = midpoint(p2, p3)
            m3 = midpoint(p1, p3)
            new_points.extend([
                (p1, m1, m3),
                (m1, p2, m2),
                (m3, m2, p3)
            ])
        return sierpinski_triangle(new_points, depth - 1)

# Number of iterations
iterations = 6

# Initial triangle vertices
triangle_vertices = [(0, 0), (1, 0), (0.5, np.sqrt(3) /
    2)]
triangle = [triangle_vertices]

# Create the figure and axis
fig, ax = plt.subplots()
ax.set_aspect('equal')
ax.axis('off')

# Function to update the plot
def update(frame):
    ax.clear()
    ax.set_xlim(-0.1, 1.1)
    ax.set_ylim(-0.1, 1)
    ax.set_title(f"Sierpinski Triangle (Iteration {frame
        })")

    # Fill in the triangle with blue color
    ax.fill(*zip(*triangle_vertices), color='white')

    for triangle_points in sierpinski_triangle(triangle,
        frame):
        for p1, p2, p3 in triangle_points:
            # Draw the triangles
            ax.plot([p1[0], p2[0], p3[0], p1[0]], [p1[1],
                p2[1], p3[1], p1[1]], color='blue')
```

```
            # Remove the middle triangle and fill it with
                white
            ax.fill(*zip(p1, p2, p3), color='blue')
    ax.axis('off')

# Custom function to insert delay between frames
def animate_with_delay(frame):
    update(frame)
    plt.pause(1)  # Adjust the pause duration as needed
        (1 second in this case)

# Create the animation
ani = FuncAnimation(fig, animate_with_delay, frames=
    iterations, repeat=False)

plt.show()
```

Listing A.3: Python code the Sierpinski triangle.

A.4 Visualizing Julia Sets

Below, we present a Python script for visualizing Julia sets.

```
import numpy as np
import matplotlib.pyplot as plt

def julia(c, max_iter, width, height):
    # Create an array to store the escape time for each
        point
    escape_time = np.zeros((width, height))

    # Define the range of the complex plane
    x_min, x_max = -1.5, 1.5
    y_min, y_max = -1.5, 1.5

    # Generate evenly spaced points in the complex plane
    x_vals = np.linspace(x_min, x_max, width)
    y_vals = np.linspace(y_min, y_max, height)

    # Iterate over each point in the complex plane
    for i in range(width):
        for j in range(height):
            z = complex(x_vals[i], y_vals[j])
            n = 0
            while abs(z) <= 2 and n < max_iter:
```

```
22                 z = z*z + c
23                 n += 1
24             escape_time[i, j] = n
25
26     return escape_time
27
28 def plot_julia(c, max_iter, width, height):
29     julia_set = julia(c, max_iter, width, height)
30     plt.imshow(julia_set.T, extent=(-1.5, 1.5, -1.5, 1.5)
           , cmap='hot', origin='lower')
31     plt.xlabel('Re')
32     plt.ylabel('Im')
33     plt.title('Julia Set for c = {}'.format(c))
34     plt.show()
35
36 # Define the parameter c for the Julia set
37 c = complex(-0.8, 0.156)
38 # Define the maximum number of iterations
39 max_iter = 1000
40 # Define the width and height of the plot
41 width, height = 1000, 1000
42
43 # Plot the Julia set
44 plot_julia(c, max_iter, width, height)
```

Listing A.4: Python code for plotting Julia sets.

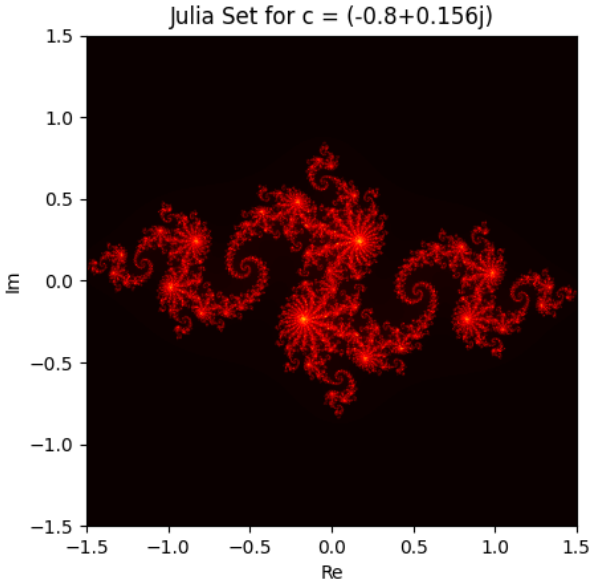

Figure A.1: An example of a Julia set produced by the code A.4.

A.5 Visualizing the Mandelbrot Set

Below, we present a Python script for visualizing the Mandelbrot set.

```
import numpy as np
import matplotlib.pyplot as plt

def mandelbrot(c, max_iter):
    z = 0
    n = 0
    while abs(z) <= 2 and n < max_iter:
        z = z*z + c
        n += 1
    return n

def mandelbrot_set(xmin, xmax, ymin, ymax, width, height, max_iter):
    x = np.linspace(xmin, xmax, width)
    y = np.linspace(ymin, ymax, height)
    mandelbrot_grid = np.zeros((width, height))
    for i in range(width):
        for j in range(height):
            mandelbrot_grid[i,j] = mandelbrot(complex(x[i], y[j]), max_iter)
    return mandelbrot_grid

def plot_mandelbrot(xmin, xmax, ymin, ymax, width, height, max_iter):
    mandelbrot_grid = mandelbrot_set(xmin, xmax, ymin, ymax, width, height, max_iter)
    plt.imshow(mandelbrot_grid.T, extent=(xmin, xmax, ymin, ymax), cmap='hot', origin='lower')
    plt.xlabel('Re')
    plt.ylabel('Im')
    plt.title('Mandelbrot Set')
    plt.show()



# Define the region and parameters
xmin, xmax = -2, 2
ymin, ymax = -2, 2
width, height = 1000, 1000
max_iter = 100


```

```
38 # Plot the Mandelbrot set
39 plot_mandelbrot(xmin, xmax, ymin, ymax, width, height,
       max_iter)
```

Listing A.5: Python code for plotting the Mandelbrot set.

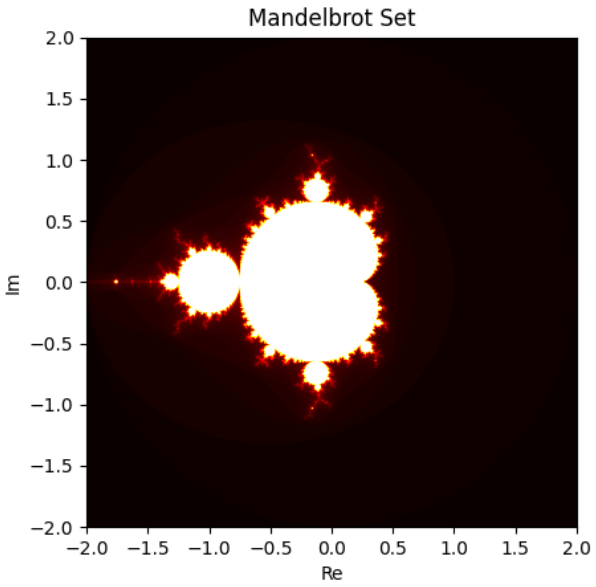

Figure A.2: The Mandelbrot set produced by the code A.5.

Bibliography

[1] H. Amman and J. Escher. *Analysis I*. 2nd ed. Basel: Birkäuser, 2006.

[2] M. Astorg et al. "Collet, Eckmann and the bifurcation measure." In: *Inventiones mathematica* 217 (2019), pp. 749–797.

[3] M. F. Barnsley. *Fractals Everywhere*. 2nd ed. Boston: Academic Press, 1993.

[4] A. S. Besicovitch. "On Linear Sets of Points of Fractional Dimensions." In: *Mathematische Annalen* 101 (1929), pp. 161–193.

[5] R. Bowen. "Hausdorff dimension of quasi-circles." In: *Publications Mathmatiques de l'IHS* 50 (1979), pp. 11–26.

[6] R. Brooks and J. P. Matelski. "The Dynamics of 2-Generator Subgroups of PSL(2, $\mathbb{C}$)." In: *Riemann Surfaces Related Topics (AM-97), Volume 97*. Ed. by I. Kra. Princeton: Princeton University Press, 1981, pp. 65–72.

[7] A. Burns. "Fractal Tilings." In: *The Mathematical Gazette* 78.482 (1994), pp. 193–196.

[8] G. Cantor. "Über unendliche, lineare Punkimannigfaltigkeiten." In: *Mathematischen Annalen* 21 (1883), pp. 545–591.

[9] C. Carathéodory. "Über das lineare Mass von Punktmengen–eine Verallgemeinerung das Längenbegriffs." In: *Nachrichten von der Gesellschaft der Wissenschaften zu Göttingen* 1914 (1914), pp. 406–426.

[10] D. L. Cohn. *Measure Theory*. 2nd ed. Boston: Birkhäuser, 2013. Chap. 1.

[11] R. M. Crownover. *Introduction to Fractals and Chaos*. London: Jones and Bartlett Publishers, 1995.

[12] Y. Demichel. *Who invented von Koch's Snowflake Curve?* 2023. arXiv: `2308.15093 [math.HO]`.

[13] A. Douady and J. H. Hubbard. "Itération des polynômes quadratiques complexes." In: *Comptes Rendus Acad. Sci. Paris* 294 (1982), pp. 123–126.

[14] G. Edgar. *Integral, Probability, and Fractal Measures*. New York: Springer, 1998.

[15] G. Edgar. *Measure, Topology, and Fractal Geometry*. 2nd ed. New York: Springer, 2007.

[16] R. Engelking. *Dimension Theory*. Amsterdam: North-Holland Publishing Company, 1978.

[17] L. C. Evans and R. F. Gariepy. *Measure Theory and Fine Properties of Functions*. Champaign, Illinois: CRC Press, 1992.

[18] K. Falconer. *The Geometry of Fractal Sets*. Cambridge: Cambridge University Press, 1985.

[19] K. Falconer. *Techniques in Fractal Geometry*. Chichester, England: John Wiley & Sons, 1997.

[20] K. Falconer. *Fractal Geometry: Mathematical Foundations and Applications*. 2nd ed. Chichester, England: John Wiley & Sons, 2003.

[21] K. Falconer. *Fractals. A Very Short Introduction*. Oxford: Oxford University Press, 2013.

[22] P. Fatou. "Sur les substitutions rationnelles." In: *Comptes Rendus de l'Académie des Sciences de Paris* 164 and 165 (1917), 806-808 and 992–995.

[23] O. Forster. *Maß- und Integrationstheorie, Integralsätze im $\mathbb{R}^n$ und Anwendungen*. 8th ed. Munich, Germany: Springer Spektrum, 2017. Chap. 1-3.

[24] F. Hausdorff. "Dimension und ausseres Mass." In: *Mathematische Annalen* 79 (1919), pp. 157–179.

[25] J. Henrikson. "Completeness and total boundedness of the Hausdorff metric." In: *MIT Undergraduate Journal of Mathematics* (1999), pp. 69–80.

[26] J. H. Hubbard. "Local connectivity of Julia sets and bifurcation loci: three theorems of J.-C. Yoccoz." In: *Topological methods in modern mathematics* (1993), pp. 467–511.

[27] J. E. Hutchinson. "Fractals and self-similarity." In: *Indiana University Mathematics Journal* 30 (1981), pp. 713–747.

[28] G. Julia. "Mémoire sur l'iteration des fonctions rationnelles." In: *Journal de Mathématiques Pures et Appliquées* 8 (1918), pp. 47–245.

[29] H. von Koch. "Sur une courbe continue sans tangente, obtenue par une construction géometrique élémentaire." In: *Arkiv för Matematik* 1 (1904), pp. 681–704.

[30] E. Lucas. "Théorie des Fonctions Numériques Simplement Périodiques." In: *American Journal of Mathematics* 1 (1878), pp. 184–196.

[31] B. B. Mandelbrot. "How Long Is the Coast of Britain? Statistical Self-Similarity and Fractional Dimension." In: *Science, New Series* 156.3775 (1967), pp. 636–638.

[32] B. B. Mandelbrot. *Les objets fractals, forme, hasard et dimension*. Paris: Flammarion, 1975.

[33] B. B. Mandelbrot. "Fractal aspects of the iteration of $z \mapsto \lambda z(1-z)$ for complex λ, z." In: *Annals of the New York Academy of Sciences* 357.1 (1980), pp. 249–259.

[34] B. B. Mandelbrot. *The Fractal Geometry of Nature*. San Francisco: Freeman, 1982.

[35] D. Marshall. *Complex Analysis*. Cambridge: Cambridge University Press, 2019.

[36] P. Mattila. *Geometry of Sets and Measures in Euclidean Spaces*. Cambdrige: Cambridge University Press, 1995.

[37] J. Milnor. *Dynamics in one complex variable: introductory lectures*. 1990. arXiv: `math/9201272 [math.DS]`.

[38] H-O. Peitgen, H. Jürgens, and D. Saupe. *Fractals for the Classroom*. Vol. 1. New York: Springer-Verlag, 1992.

[39] H-O. Peitgen, H. Jürgens, and D. Saupe. *Chaos and Fractals*. 2nd ed. New York: Springer-Verlag, 2004.

[40] H-O. Peitgen and R. Peter. *The Beauty of Fractals*. Heidelberg, Germany: Springer-Verlag, 1986.

[41] L. Riddle. *Classic Iterated Function Systems*. [Accessed 13-April-2024]. URL: `https://larryriddle.agnesscott.org/ifs/ifs.htm`.

[42] C. A. Rogers. *Hausdorff measures*. 2nd ed. Cambridge: Cambridge University Press, 1998.

[43] D. Ruelle. "Repellers for real analytic maps." In: *Ergodic Theory and Dynamical Systems* 2 (1982), pp. 99–108.

[44] J. T. Sandefur. "Using Self-Similarity to Find Length, Area, and Dimension." In: *The American Mathematical Monthly* 103.2 (1996), pp. 107–120.

[45] W. Shen. "Hausdorff dimension of the graphs of the classical Weierstrass functions." In: *Mathematische Zeitschrift* 289.223-266 (2018).

[46] M. Shishikura. "The Hausdorff Dimension of the Boundary of the Mandelbrot Set and Julia Sets." In: *Annals of Mathematics* 174.2 (1998), pp. 225–267.

[47] W. Sierpinski. "Sur une courbe dont tout point est un point de ramification." In: *Comptes Rendus de l'Académie des Sciences* 160 (1915), pp. 302–305.

[48] D. Da Silva. "Caratérisation de la nature multi-échelles des plantes par des outils de géométrie fractale, influence sur l'interception de la lumière". PhD thesis. Université Montpellier, 2008.

[49] I. Stewart. *How to Cut a Cake: And other mathematical conundrums.* Oxford: Oxford University Press, 2006.

[50] S. Ungar. "The Koch Curve: A Geometric Proof." In: *The American Mathematical Monthly* 114.1 (2007), pp. 61–66.

[51] K. Weierstrass. "Über continuirliche functionen eines reellen arguments, die für keinen werth des letzeren einen bestimmten differentialquotienten besitzen." In: *Royal Prussian Academy of Sciences* (1872).

[52] Wikimedia. *Pascal's Triangle with even numbers shaded.svg.* [Accessed 7-April-2024]. URL: https://commons.wikimedia.org/w/index.php?title=File:Pascal%27s_Triangle_with_even_numbers_shaded.svg&oldid=688466947.

[53] Wikipedia. *Minkowski–Bouligand dimension.* [Accessed 13-03-2024]. URL: https://en.wikipedia.org/wiki/Minkowski%E2%80%93Bouligand_dimension.

[54] Wikipedia. *Romanesco broccoli.* [Accessed 18-03-2024]. URL: https://en.wikipedia.org/wiki/Romanesco_broccoli#.

[55] M. Yamagauti, M. Hata, and J. Kigami. *Mathematics of Fractals.* Providence, Rhode Island: American Mathematical Society, 1993.